

Advancing 3D Point Cloud Understanding through Deep Transfer Learning: A Comprehensive Survey

Shahab Saquib Sohail^a, Yassine Himeur^{b,*}, Hamza Kheddar^c, Abbes Amira^{d,e}, Fodil Fadli^f, Shadi Atalla^b, Abigail Copiaco^b and Wathiq Mansoor^b

^aSchool of Computing Science and Engineering, VIT Bhopal University, Sehore, MP 466114, India

^bCollege of Engineering and Information Technology, University of Dubai, Dubai, UAE

^cLSEA Laboratory, Department of Electrical Engineering, University of Medea, 26000, Algeria

^dDepartment of Computer Science, University of Sharjah, UAE

^eInstitute of Artificial Intelligence, De Montfort University, Leicester, United Kingdom

^fDepartment of Architecture & Urban Planning, Qatar University, Doha, 2713, Qatar

ARTICLE INFO

Keywords:

3D point cloud
Deep transfer learning
Domain adaption
Fine-tuning
Classification
Segmentation and registration

ABSTRACT

The 3D point cloud (3DPC) has significantly evolved and benefited from the advance of deep learning (DL). However, the latter faces various issues, including the lack of data or annotated data, the existence of a significant gap between training data and test data, and the requirement for high computational resources. To that end, deep transfer learning (DTL), which decreases dependency and costs by utilizing knowledge gained from a source data/task in training a target data/task, has been widely investigated. Numerous DTL frameworks have been suggested for aligning point clouds obtained from several scans of the same scene. Additionally, DA, which is a subset of DTL, has been modified to enhance the point cloud data's quality by dealing with noise and missing points. Ultimately, fine-tuning and DA approaches have demonstrated their effectiveness in addressing the distinct difficulties inherent in point cloud data. This paper presents the first review shedding light on this aspect. It provides a comprehensive overview of the latest techniques for understanding 3DPC using DTL and domain adaptation (DA). Accordingly, DTL's background is first presented along with the datasets and evaluation metrics. A well-defined taxonomy is introduced, and detailed comparisons are presented, considering different aspects such as different knowledge transfer strategies, and performance. The paper covers various applications, such as 3DPC object detection, semantic labeling, segmentation, classification, registration, downsampling/upsampling, and denoising. Furthermore, the article discusses the advantages and limitations of the presented frameworks, identifies open challenges, and suggests potential research directions.

1. Introduction

1.1. Preliminary

Computer vision (CV) continues to attract significant interest as a growing branch of machine learning (ML), which targets different problems in smart cities, medicine, autonomous driving, medicine, video surveillance, scene understanding, safety, and security [1, 2]. With the rapid development of sensor technology, 3D sensors have recently been widely adopted, which increased the interest of the CV research community in developing 3D sensor data processing methodologies [3, 4]. Additionally, with the use of augmented reality and virtual reality (AR/VR), 3D vision problems become more important since they provide much richer information than 2D [5, 6]. Typically, numerous 3D sensors for acquiring 3D data have been used, including depth-sensing cameras (such as Apple Depth, RealSense, and Kinect cameras), light detection and ranging (LiDAR), which is used for mobile mapping terrestrial laser scanning, aerial LiDAR [7]. Moreover, generative adversarial networks (GANs) can be used to augment data when data scarcity problem occurs. In this context, 3D data can provide rich scale, shape, and geometric information to be complemented with 2D images for better representing the surrounding environment [8, 9].

While there are different approaches to representing 3D data, such as volumetric grids, meshes, and depth images, the 3D point clouds (3DPCs) are the most used. Typically, a 3DPC representation conserves the original geometric information in 3D space [10]. Besides, a 3DPC is an ensemble of data points representing an object's surfaces in 3D

 yhimeur@ud.ac.ae (Y. Himeur)

ORCID(s):

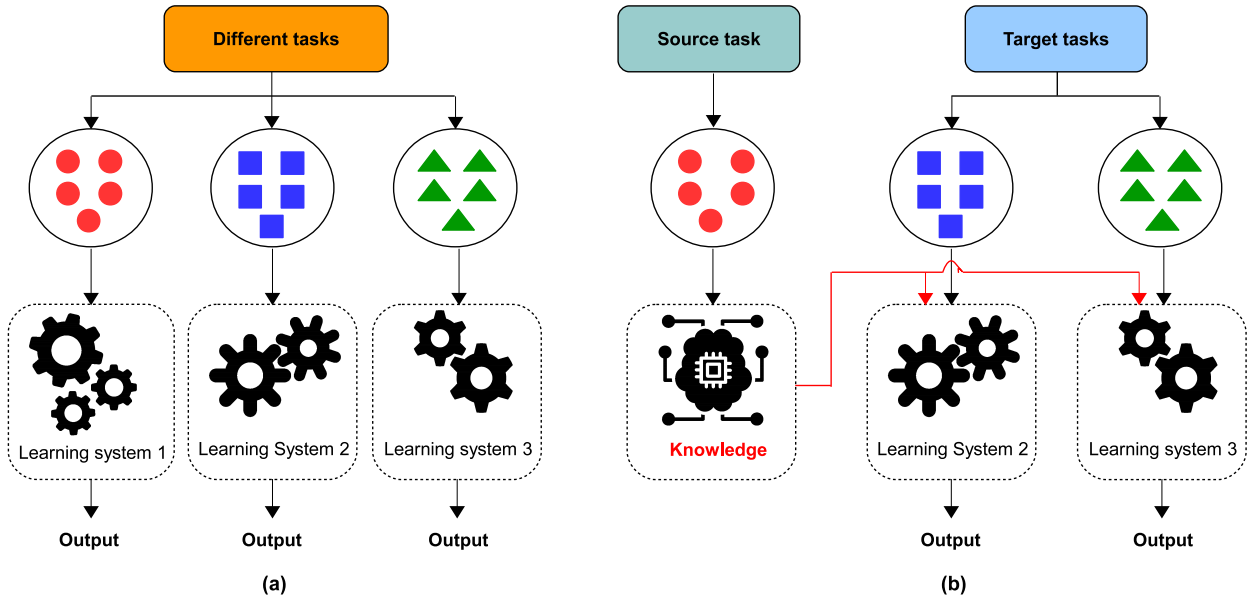


Figure 1: Difference between conventional ML and DTL techniques for multiple tasks: (a) conventional ML and (b) DTL.

coordinates. In this regard, spatial coordinates are used to represent data points, surface normals, and color information and format (e.g., RGB, HSV, and others) [11].

Additionally, although 3DPC can be considered as non-Euclidean geometric data, in practice, delineated as small Euclidean subgroups with a standard coordinates system and global parametrization [12]. The success of this representation is due to its invariability to transformations and attacks, including rotation, scaling, translation, etc., which makes it robust to extracting objects' features. Moreover, using deep learnings (DLs) techniques to extract 3DPC data and perform complex tasks such as detection, classification, recognition, and retrieval has expanded their adoption in many research and development areas [13]. Typically, 3DPCs are widely adopted to CV tasks, such as object recognition, semantic segmentation, and scene understanding [14, 15]. Additionally, they are used to create detailed models of environments for navigation and localization, detailed maps and models of buildings, landscapes, and other structures, as well as detailed models of buildings and other structures for design and planning [16]. Moreover, they can be utilized to inspect and maintain industrial equipment, infrastructure, and other assets [17, 18]. Besides, the 3DPC technology helps implement realistic and immersive experiences in AR and VR applications.

The traditional ML approaches and, recently, DL methods witnessed rapid growth and have attracted researchers because of their applicability in many real-life applications, including smart healthcare [19], disease diagnosis and medical image classifications [4], business and marketing [20], recommender systems [21], energy [22], agriculture [23], robotics [24], and more. The primary advantage of these learning algorithms is that they train a model that learns the hidden pattern and can be exploited for any specific purpose with high accuracy. However, with time, some issues have been raised by the research communities. First, these learning algorithms require extensive training datasets, especially DL algorithms [1]. Second, most DL models are based on supervised learning and then require huge amounts of ground-truth data. Third, it is a common assumption that the data that is trained and the future data to be processed must have the same distribution and be in the same feature space [25]. It becomes difficult and sometimes impossible to maintain the aforementioned assumption in several real-life scenarios. For example, when performing specific tasks, such as classification in a particular domain; however, we may have the requisite trained data in another domain, where both datasets may not have the same distribution or same feature space.

Furthermore, an essential factor for ensuring accurate performance of ML algorithms is consistency in the distribution and feature space of the datasets used for training and testing. If the distribution of data changes, it becomes necessary to rebuild the model from scratch by collecting new training data [26]. However, this process is not only costly but also often impractical due to the challenges associated with re-collecting training data. Therefore, there

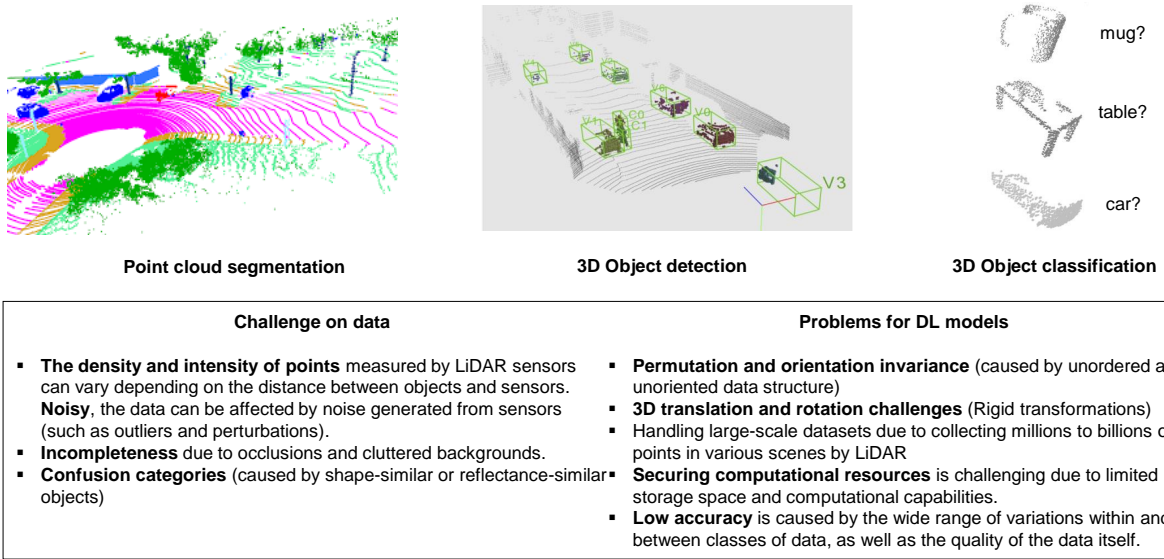


Figure 2: Tasks and challenges related to data and DL/DTL-based applications on 3DPCs.

is a need for a mechanism that can reduce the expenses associated with re-collecting training data, minimize the cost of data labeling, and still achieve high performance without requiring extensive amounts of training data. To that end, knowledge transfer has been suggested, which would fit the above constraints and can significantly improve performance. This knowledge transfer mechanism is termed *deep transfer learning (DTL)* [1, 26, 27]. Fig. 1 explains briefly the difference between conventional ML and DTL techniques.

On the one hand, employing DL for 3DPC poses a rather complex challenges because of: (i) the variability in point density and reflective intensity, influenced by the distance between objects and LiDAR sensors, (ii) existence of noise originated from sensors (e.g., perturbations and outliers), (iii) data incompleteness caused by occlusion between objects and cluttered background, and (iv) confusion categories caused by shape-similar or reflectance-similar objects. On the other hand, challenges of DL/DTL models include (i) permutation and orientation invariance, (ii) 3D translation and rotation challenges, (iii) difficulty of handling large-scale datasets, (iv) securing computational resources, and (v) low performance. Fig. 2 summarizes the tasks and challenges related to data and DL/DTL-based applications on 3DPCs.

1.2. Our contributions

Arguably, one of the top success stories of DL is DTL. Accordingly, the finding that pretraining a DL network on a rich source set (e.g., ImageNet) can help boost performance once fine-tuned on a usually much smaller target set has been instrumental to many applications in language and CV. Likewise, several studies have explored the potential of DTL in 3DPC applications to address the aforementioned challenges. This offers an opportunity to present the first review article that comprehensively examines the contributions of DTL-based approaches in advancing our understanding of 3D scenes, such as 3DPC segmentation, 3D object detection, 3D object classification, 3DPC registration, and more. For instance, DTL has been shown to be effective in various ways, including (i) leveraging knowledge learned from synthetic data to improve semantic segmentation in real LiDAR 3DPC, (ii) enabling accurate classification of 3DPCs even with limited training data, (iii) mitigating the issue of overfitting in 3DPC classification, and (iv) reducing the labor-intensive process of annotating 3DPC datasets, among other benefits. In this respect, this paper first presents a background of DTL, where a well-defined taxonomy is conducted. Moving on, datasets and evaluation metrics used to evaluate existing DTL-based 3DPCs techniques are discussed. Next, existing studies are overviewed based on different aspects, and their pros and cons are identified. After that, the challenges encountered when using DTL for 3DPCs are identified before deriving future research directions. To summarize, the main contributions of this review can be stated as follows:

Table 1
Research questions covered in this review.

No.	Question	Objective
RQ1	What are the key principles and theoretical foundations of DTL and 3DPC?	Provide a foundational understanding of the key principles and theories behind DTL and 3DPC. This will aid readers in grasping the basic tenets upon which the field of study is built and support comprehension of more complex concepts discussed later in the review.
RQ2	Why the application of DTL in 3DPC is receiving increasing attention?	Examine and explain why DTL is increasingly being used for 3DPC. This will help highlight the unique benefits and opportunities offered by DTL in handling 3D data, indicating its growing importance in the field.
RQ3	How the different 3DPC tasks can be implemented using DTL?	Present a comprehensive overview of how DTL can be utilized in various 3DPC tasks. This objective aims to showcase the versatility and wide-ranging applicability of DTL in 3DPC tasks, providing practical insights for researchers and practitioners.
RQ4	What are the DTL mechanisms and settings for performing the 3DPC tasks and optimizing their performance?	Delve into the specific mechanisms and settings of DTL that optimize performance in 3DPC tasks. The objective here is to provide a clear understanding of the operational details of DTL, which can serve as a guide for those intending to implement DTL in their own 3DPC tasks.
RQ5	Which DTL models are better appropriate for 3DPC tasks?	Evaluate and suggest DTL models that are most suitable for 3DPC tasks. By doing this, the review will provide practical advice for readers looking to apply DTL in 3DPC, assisting them in model selection.
RQ6	What are the issues in implementing DTL for performing the above tasks, and how to tackle these challenges?	Identify the key challenges associated with implementing DTL for 3DPC tasks and to propose potential solutions to these challenges. This will help improve the application of DTL in 3DPC by addressing problems head-on, promoting a robust and reliable usage of these techniques.
RQ7	What are the future research directions for improving DTL in 3DPC?	Forecast future research directions for DTL in 3DPC. This objective aims to stimulate new research initiatives by identifying promising avenues for further exploration, driving innovation and development in the field.

- Presenting, to the best of the authors’ knowledge, the first review article on using DTL and domain adaptation (DA) for 3DPC applications;
- Discussing existing datasets and evaluation metrics used for assessing the performance of 3DPC frameworks based in DTL;
- Introducing a well-defined taxonomy to overview existing DTL-based 3DPC studies;
- Identifying the current challenges encountered when using DTL for 3DPC understanding tasks; and
- Deriving future research directions that can attract significant research interest in the near future.

1.3. Methodology of the survey

The present review study is based on the protocols and procedure suggested in [28], which has recently been adopted widely in many studies such as [29]. This study is motivated by the recent developments in 3DPC technology. There are some reviews available on the theme which has exploited ML [30], DL [31], and reinforcement learning [32]; however, to the best of our search and efforts, we could not find a review exclusively exploring DTL for different 3DPC tasks. The proliferation of DTL techniques has influenced researchers by virtue of which the span of related techniques has been expanding and has covered much recent AI-driven research. Our study gives the readers an insight into how DTL is being implemented for performing many 3DPC tasks. This review aims at finding the answer to research questions presented in Table 1.

The bibliometric research is performed in the context of a narrative review. The recent works related to the 3DPC involving DTL techniques for performing their respective tasks have been searched. We searched the relevant keywords, like, "3D point cloud", "3D point cloud segmentation", "3D point cloud classification", "3D object detection", "deep transfer learning", and "domain adaptation", with different combinations on Scopus database in titles, abstracts, and keywords. The adopted search procedure is explained in Figs. 3(a) and 3(b). Typically, in response to the relevant queries, 176 articles were retrieved, with 149 of them being non-duplicates. These articles underwent further scrutiny to determine their relevance to the theme of the present study. Ultimately, 108 papers were selected for inclusion in this study.

The paper is organized as follows: Section 2 introduces background related to DTL definitions and terms, pre-trained models, useful datasets, and metrics used in 3DPC. Section 3 reviews relevant literature and work related to DTL and DA. Section 4 outlines state-of-the-art proposed applications based on DTL. Section 5 discusses open challenges. Section 6 suggests recent future research directions. Finally, Section 7 concludes the survey. Fig. 4 illustrates the survey’s structure, enhancing readability, and offering guidance to readers.

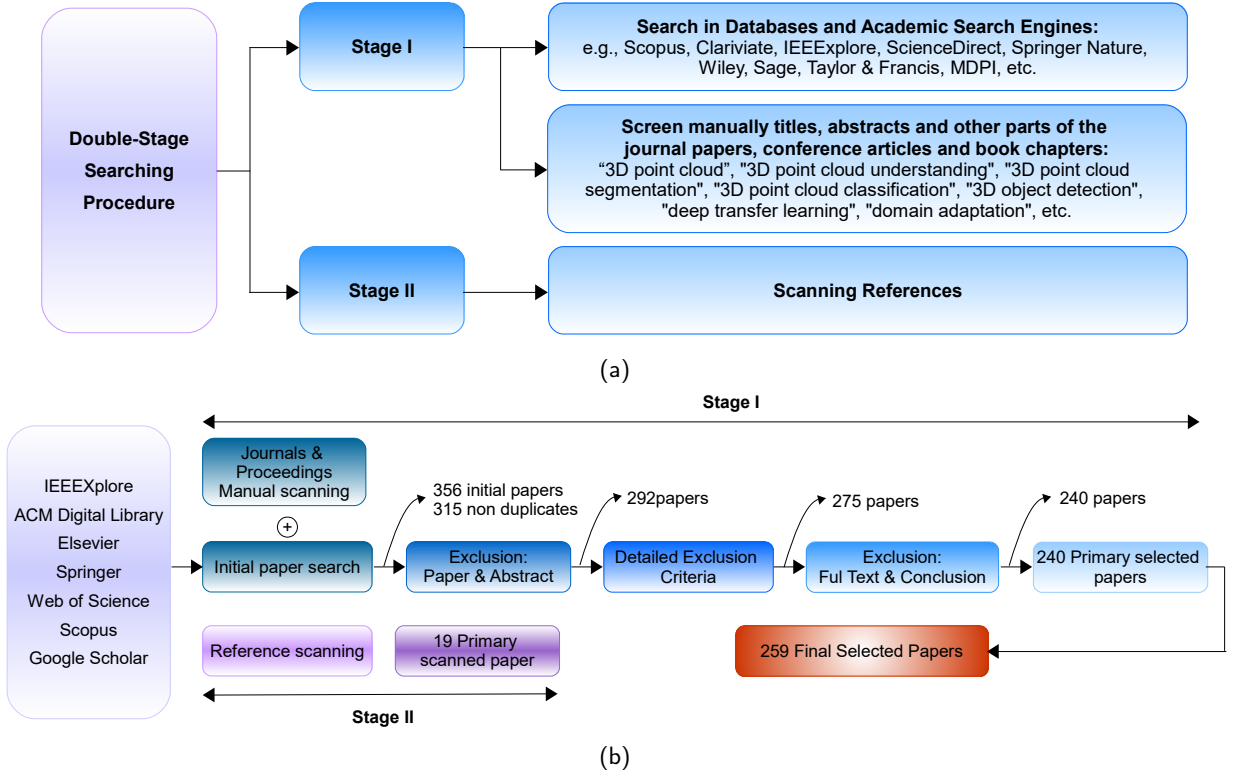


Figure 3: Summary of the approach used to search and select articles included in the review: (a) The adopted search procedure and (b) The selection criteria.

2. Background

2.1. 3D Point Cloud

A 3DPC is a collection of data points in a three-dimensional coordinate system. Each point in the point cloud is represented as:

$$P = \{p_1, p_2, \dots, p_n\}$$

where each point p_i is a vector in \mathbb{R}^3 :

$$p_i = (x_i, y_i, z_i)$$

2.1.1. Operations and Transformations

Common operations and transformations applied to 3DPCs include:

- **Translation:** Moving the point cloud by adding a constant vector $\mathbf{t} = (t_x, t_y, t_z)$ to each point:

$$p'_i = p_i + \mathbf{t}$$

- **Rotation:** Rotating the point cloud using a rotation matrix \mathbf{R} . The rotation matrix is a 3x3 matrix:

$$p'_i = \mathbf{R}p_i$$

Rotation matrices can be derived from Euler angles, axis-angle, or quaternion representations.

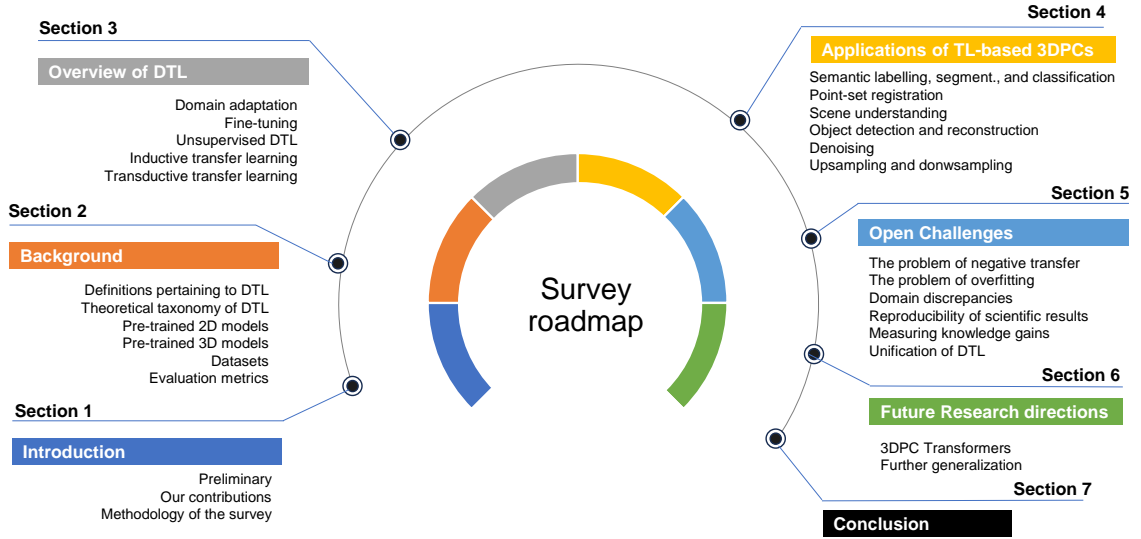


Figure 4: Survey structure with sections and sub-sections distribution.

- **Scaling:** Changing the size by scaling each point by a scalar s or different scalars for each axis:

$$p'_i = s \cdot p_i \text{ or } p'_i = (s_x x_i, s_y y_i, s_z z_i)$$

- **Transformation:** A combination of translation, rotation, and scaling, represented as matrix multiplication in homogeneous coordinates:

$$p'_i = \mathbf{T} \begin{bmatrix} x_i \\ y_i \\ z_i \\ 1 \end{bmatrix}$$

where \mathbf{T} is a 4x4 transformation matrix:

$$\mathbf{T} = \begin{bmatrix} \mathbf{R} & \mathbf{t} \\ 0 & 1 \end{bmatrix}$$

2.2. Definitions pertaining to DTL

This section presents the main definitions used in DTL-based 3DPC applications.

Def. 1 - Domain: Consider a dataset X consisting of n observations, x_1, \dots, x_n , in a feature space χ . The marginal probability distribution of X is represented by $P(X)$. A domain, denoted as \mathbb{D} , is defined as the set containing X and $P(X)$. In the field of DTL, the domain containing the initial knowledge is referred to as the source domain (SD), represented by \mathbb{D}_S , while the domain containing the unknown knowledge to be learned is called the target domain (TD) and represented by \mathbb{D}_T .

Def. 2 - Task: The dataset X contains n observations, x_1, \dots, x_n , in a feature space χ , and it is associated with a set of labels Y, y_1, \dots, y_n , in a label space γ . A task can be defined as a set containing the labels Y and a learning objective predictive function $\mathbb{F}(X)$, represented by $\mathbb{T} = \{Y, \mathbb{F}(X)\}$. This function is also denoted as the conditional distribution $P(Y|X)$. In accordance with this definition of task, the label spaces of the SD and TD are represented as γ_S and γ_T respectively [33].

One way to classify DTL methods is based on their approach to transferring knowledge, which can be broken down into *what*, *when*, and *how* knowledge is transferred.

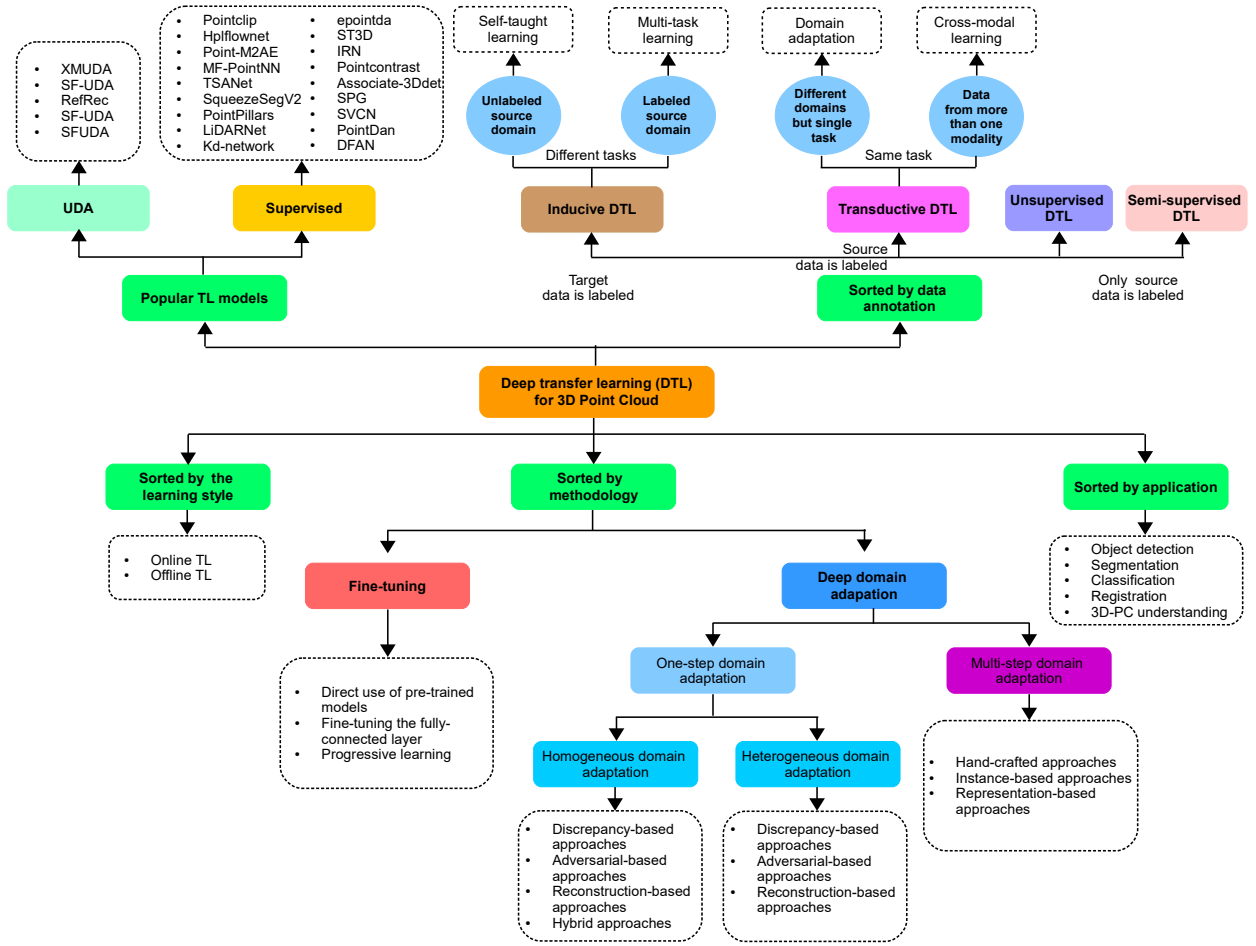


Figure 5: Proposed taxonomy of existing DTL algorithms for 3DPCs.

(a) **What knowledge is transferred:** The classification of DTL methods based on "what knowledge is transferred" examines the specific characteristics of knowledge that can be transferred across domains or tasks. Some information is unique to a particular domain or task, while other knowledge is general and can improve the performance of the TD or task. Based on this criterion, DTL methods can be categorized as model-based, relation-based, instance-based, and feature-based [34].

(b) **How knowledge is transferred:** The classification of DTL methods based on this question focuses on the specific algorithms or techniques used to transfer knowledge across domains or tasks.

(c) **When knowledge is transferred:** inquires as to when and under what circumstances knowledge should or should not be transferred.

2.3. Theoretical taxonomy of DTL

In this section, a clear categorization of DTL methodologies used for 3DPCs is presented. The proposed classification, shown in Fig. 5, is arranged based on the following criteria: (i) learning style, (ii) methodology, (iii) DTL type, (iv) data annotation, and (v) widely used DTL models. DTL techniques can generally be divided into different groups depending on whether the source and TDs and tasks are alike or not. The mathematical descriptions of the different DTL groups and their distinctions are presented in Fig. 6. While this information is discussed in the literature review, aiming to simplify it and present it in a more reader-friendly manner in this study.

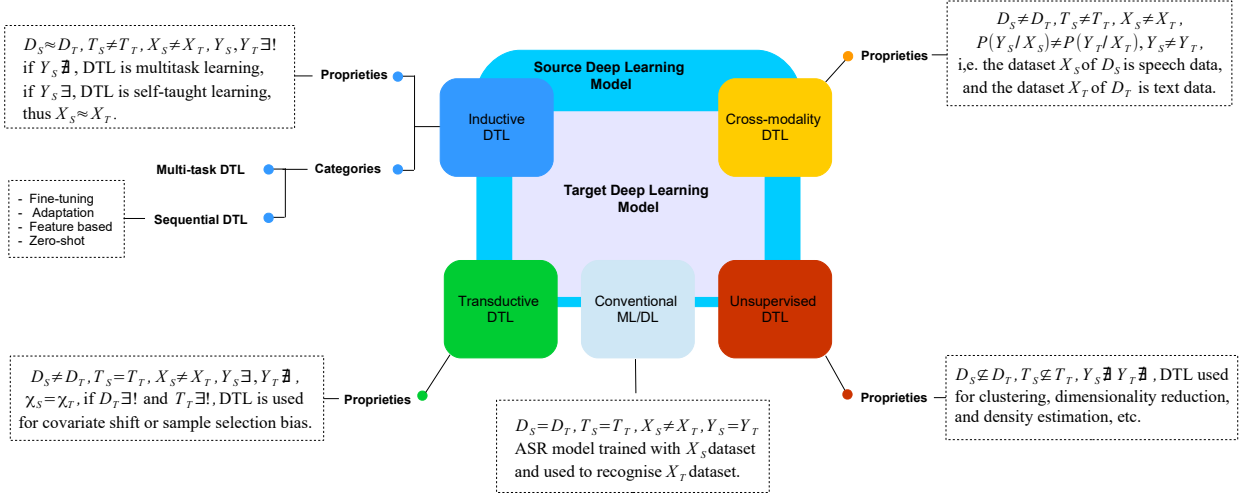


Figure 6: The DTL classification is determined by how similar the source and TDs and tasks are. The symbol (\nsubseteq) is used to indicate that the domains/tasks are distinct yet related. The symbol ($\exists!$) indicates the presence of a single unique domain/task. While (\approx) denotes that the domains, tasks, or spaces do not match.

2.3.1. Inductive DTL

The goal of inductive DTL is to improve the target prediction function \mathbb{F}_T in the TDs when compared to classical ML. This is achieved even when the target tasks \mathbb{T}_T are different from the source tasks \mathbb{T}_S . However, the SD \mathbb{D}_S and TD \mathbb{D}_T may not always be identical (as shown in Fig. 6). Inductive DTL can take two forms, depending on the availability of labeled or unlabeled data:

(a) **Multi-task DTL:** This approach is used when the SDs has a large labeled dataset (X_S labeled with Y_S). This is a specific form of multi-task learning where multiple tasks (T_1, T_2, \dots, T_n) are learned simultaneously (in parallel), including both the source and target tasks[35].

(b) **Sequential learning:** also known as self-taught learning, is a method used when the dataset in the SD is unlabeled. It relies on (i) transferring the feature representation learned from a large collection of unlabeled datasets, and (ii) applying the learned representation to labeled data for classification tasks. This DTL method involves sequentially learning multiple tasks where the gaps between the SDs and TDs may differ. For instance, assume we have a pre-trained model (PTM) M and we apply DTL to several tasks (T_1, T_2, \dots, T_n). In this approach, a specific task \mathbb{T}_T is learned at each time step t and it is slower than multi-task learning, however, when not all the tasks are present at the time of training, it may be advantageous. Sequential learning can be further classified into different types [36].

- 1- **Fine-tuning:** involves training a new function, \mathbb{F}_T , that adapts the parameters of a PTM M from a source task, \mathbb{T}_S , to a target task, \mathbb{T}_T , by translating the weights of the source task, W_S , to the weights of the target task, W_T . This can be done across all layers or just a subset of them, and the learning rate for each layer can be adjusted independently (known as discriminative fine-tuning). Additionally, new parameters, K , can be added to the model to improve its performance on the target task [37].

$$\mathbb{F}_T(W_T, K) = W_S \times K \quad (1)$$

- 2- **Adapter modules:** they are designed to take a PTM, M_S , and adapt its weights, W_S , to a target task, \mathbb{T}_T . The adapter module achieves this by introducing a new set of parameters, K , that are smaller in size compared to W_S , i.e. $K \ll W_S$. Both K and W_S are decomposed into smaller, more compact modules, such that $W_S = w_n$ and $K = k_n$. This allows the adapter module to learn a new function, \mathbb{F}_T , which adapts the model to the target task.

$$\mathbb{F}_T(K, W_S) = k'_1 \times w_1 \times \dots \times k'_n \times w_n \quad (2)$$

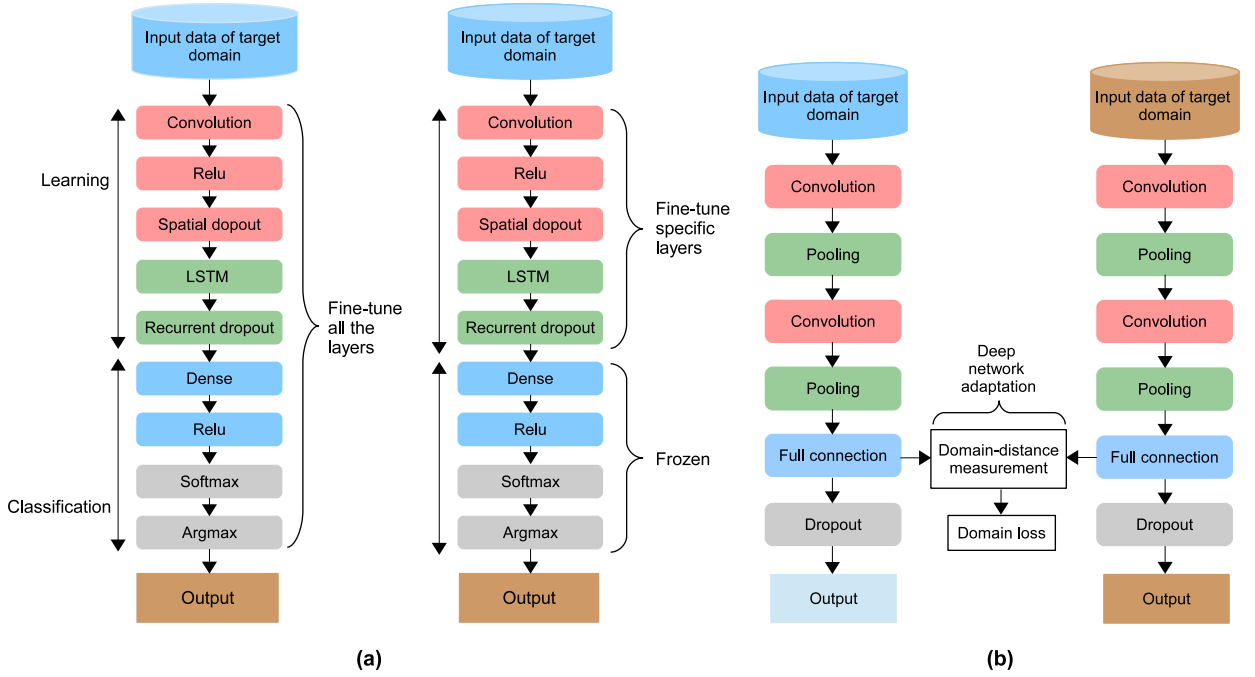


Figure 7: Example of DTL models used in 3DPCs: (a) fine-tuning, and (b) deep DA.

The equation (2) illustrates the procedure of adapting a model to a new task by dynamic weight adjustment, original weights $W_S = w_n$ remain unchanged, whereas the set of weights K are updated to $K' = k'_n$. This principle of Dynamic DA is illustrated in Fig. 7.

- 3- **Feature based:** it focuses on learning concepts and representations at various levels of an image, such as corners or interest points, blobs or regions of interest points, ridges, or edges E . In this approach, the collection of E obtained from a PTM M is kept unchanged and only W' is fine-tuned, such that the function \mathbb{F}_T can be represented as $E \times W'$. The idea is that E are the feature learned from PTM and fine-tuning only the last layer W' to adapt to the new task.
- 4- **Zero-shot:** is the simplest approach among all the others. It does not involve modifying or adding new parameters to a PTM by assuming that the existing parameters, denoted as W_S , cannot be changed. Essentially, zero-shot does not require any training to optimize or learn new parameters."

2.3.2. Transductive DTL

In comparison to traditional ML, which can be used as a benchmark for DA and DTL, DTL addresses the scenario where the TD data, denoted as $\mathbb{D}T$, differs from the SDs data, denoted as $\mathbb{D}S$. While the SDs has annotated data (X_S paired with Y_S), the TD has no labeled data. The source and target tasks are similar as outlined in Fig. 6. Transductive DTL aims at constructing a target prediction function \mathbb{F}_T using the knowledge from both the SD and TD. Additionally, transductive DTL can be further categorized into two groups based on the relationship between the SD and TD, as described in [38].

(a) Deep domain adaptation (DDA): refers to the situation where the feature spaces of the SD, denoted as χ_S , and the TDs, denoted as χ_T , are the same. However, the probability distributions of the input data are different, with $P(Y_S/X_S) \neq P(Y_T/X_T)$ as described in [39]. DDA is particularly useful when the target task has a unique distribution or limited labeled data, as highlighted in [40].

(b) Cross-modality DTL: most DTL techniques require some form of relationship between feature spaces (or label spaces) of the source and TDs, i.e., $\mathbb{D}S$ and $\mathbb{D}T$. This means that DTL can only be applied when the source and target have the same modality, such as text, speech, or video. In contrast, cross-modality DTL is one of the most challenging

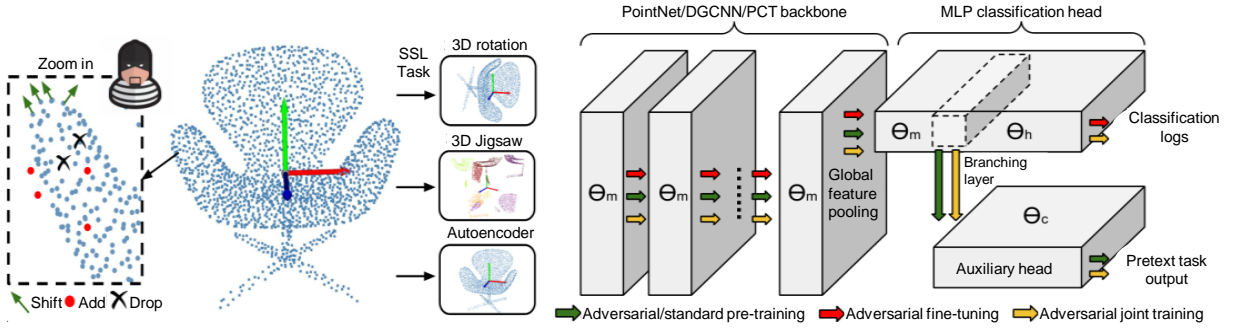


Figure 8: Flowchart of the adversarial TL-based 3DPC classification approach proposed in [51].

areas of DTL, as it assumes that the feature spaces of the source and TDs are completely different ($\chi_S \neq \chi_T$), such as speech-to-image, image-to-text, and text-to-speech. Additionally, the label spaces of the source Y_S and target Y_T domains may also differ ($Y_S \neq Y_T$) as described in [41].

(c) Unsupervised DTL: is a method of improving the learning of the target prediction function $\mathbb{F}T$ in the TD $\mathbb{D}T$ by using knowledge from the SDs $\mathbb{D}S$ and the source task $\mathbb{T}S$, even when the labels Y_S and Y_T are not present. It is important to note that the source and target tasks, $\mathbb{T}S$ and $\mathbb{T}T$, are related but distinct. Such kind of approach is useful when labels are not available for TD data, as stated in [42].

2.3.3. Adversarial DTL

Adversarial learning, as introduced in [43], is a method that helps to learn more transferable and discriminative representations. The first method using this approach, the domain-adversarial neural network (DANN) was presented in [44]. Unlike traditional methods that use predefined distance functions, DANN utilizes a domain-adversarial loss within the network. This approach has shown to improve the network's ability to learn discriminative data and has been used in many visual surveillance studies [45–48]. However, prior works in DANN have not considered the different effects of marginal and conditional distributions. An alternative approach, dynamic distribution alignment, was proposed in [49] that dynamically evaluates the importance of each distribution, thus providing a more nuanced approach." Another approach called the adversarial scoring network (ASNet) was introduced in [50] to bridge the gap between domains at different levels of granularity. This approach uses adversarial learning to align the SDs with the TD in the global and local feature space during the coarse-grained stage. The transferability of source attributes is then evaluated in fine-grained stage by comparing the similarity between the source and target samples at multiple levels, utilizing the generative probability obtained in the coarse stage. The transferable elements are then selectively used to assist the DTL adaptation process. This coarse-to-fine architecture effectively reduces the problem of domain disparity. Specifically, photographs are encoded into density maps by a generator, and then classified as SDs or TD using a dual-discriminator. Adversarial training is employed between the dual-discriminator and generator to bring the domains' distributions closer together. The dual-discriminator also generates four different scores which are used as a signal to optimize the density of the SDs during adaptation for fine-grained transfer as stated in [50].

In [51], the authors studied the adversarial robustness in 3DPC recognition using three different architectures: multi-layer perceptron (MLP) network (PointNet), convolutional network (DGCNN), and transformer-based network. They employed two methods: adversarial pretraining for fine-tuning, where self-supervised learning (SSL) tasks are utilized for pretraining, and adversarial joint training, where the self-supervised task is trained alongside the recognition task, as illustrated in Fig. 8.

2.4. Popular DL-based PC models

The development of DL-based 3DPC approaches is characterized by a rich diversity of deep learning models each aimed at overcoming specific challenges related to point cloud data processing. While these models offer significant improvements in processing speed, accuracy, and applicability, they also underscore the ongoing need for models that can generalize across different environments and handle the inherent complexities of 3D point data more effectively.

2.4.1. Feature Extraction and Geometric Detail Enhancement Models

Models such as PointNet [52] and PointNet++ [53] spearheaded the direct processing of point clouds by respecting permutation invariance and enhancing the capture of hierarchical structures, respectively. They are pivotal in tasks like object classification and segmentation, though they struggle with local detail due to uniform point processing. PointVGG [54] and PointPAVGG [55] extend these capabilities by adapting image-based convolutional and attention mechanisms to point clouds, striving to bridge gaps in capturing intricate geometric details but facing challenges in computational efficiency. SpiderCNN [56] and PointCNN [57] further innovate by adapting traditional CNN transformations to unordered point data, enhancing the models' ability to learn from complex datasets.

2.4.2. Segmentation and Object Detection Models

Models like SplatNet [58], SGPN [59], and FoldingNet [60] represent advances in segmentation and unsupervised learning. SplatNet leverages sparse bilateral convolutional layers for processing high-dimensional lattices in point clouds, suitable for segmentation but hampered by scaling issues. SGPN focuses on instance segmentation by predicting semantic classes and point groupings, which becomes complex in cluttered environments. FoldingNet explores unsupervised learning with a folding-based decoder that may not generalize across all point cloud types.

2.4.3. Data Integration and Upsampling Models

PU-Net [61] and PointGrid [62] focus on upsampling and integrating grid-based approaches with point processing. PU-Net enhances point cloud density using multi-level feature integration, while PointGrid blends point and grid-based methods for recognizing 3D models, though it struggles with sparse point clouds.

2.4.4. Specialized Application Models

Models such as Hand PointNet [63] and PointNetVLAD [64] are tailored for specific applications like 3D hand pose estimation and global descriptor extraction, critical for place recognition. However, these models often face limitations when applied outside their intended scope, such as dynamic environments or varying object types.

2.4.5. Innovative Approaches in Object Detection and Registration

Emerging models like PREDATOR [65] and 3DIOUMatch [66] showcase the potential of deep learning in object detection and registration. PREDATOR addresses low-overlap point cloud registration with a deep attention mechanism, suited for benchmark scenarios but limited in broader applications. 3DIOUMatch leverages a semi-supervised learning approach to enhance 3D object detection, showing dependency on initial label quality for performance efficacy. Table 2 summarizes the most popular 3DPC models proposed in the literature.

Table 2: Summary of popular DL-based 3DPC understanding models.

Ref.	Model Name	Contribution Description	Dataset	Application	Limitation
[52]	PointNet	Introduced a neural network that processes point clouds directly, respecting permutation invariance.	Various 3D benchmarks	Object classification, part segmentation, semantic parsing	Does not capture local structural details.
[67]	ScanNet	Developed an RGB-D video dataset with extensive annotations for deep learning applications.	ScanNet dataset	3D object classification, semantic voxel labeling, CAD model retrieval	Limited diversity in scene views and semantic annotations.
[68]	OctNet	Proposed a sparse 3D data representation that allows for deep, high-resolution 3D convolutional networks.	Not specified	3D object classification, orientation estimation, point cloud labeling	Focus on sparse data might not generalize to denser datasets.
[53]	PointNet++	Extended PointNet to capture local structures using a hierarchical neural network.	Challenging benchmarks of 3DPCs	Enhanced 3D recognition tasks	Performance drops with non-uniform point densities.
[54]	PointVGG	Introduced point convolution and pooling methods to adapt image-based techniques for point clouds.	Challenging benchmarks of 3DPCs	Object classification, part segmentation	May not fully capture intricate geometric details.
[55]	PointPAVGG	A VGG-based network that incorporates a point attention mechanism for feature extraction from point clouds.	ShapeNet, ModelNet	Point cloud classification, segmentation	Increased computational demand due to complex feature integration.
[58]	SplatNet	Utilized sparse bilateral convolutional layers for processing point clouds in a high-dimensional lattice.	Not specified	3D segmentation	Scaling issues with memory and computational cost in larger lattices.

Advancing 3D Point Cloud Understanding through Deep Transfer Learning

Ref.	Model Name	Contribution Description	Dataset	Application	Limitation
[60]	FoldingNet	Developed a deep auto-encoder with a folding-based decoder for unsupervised learning on point clouds.	Not specified	Unsupervised learning, 3D object reconstruction	Generic decoder structure may not work for all point cloud types.
[61]	PU-Net	Presented a method for upsampling 3DPCs using multi-level features.	Synthesis and scan data	Point cloud upsampling	Focus on upsampling may not improve other manipulations.
[69]	SO-Net	Built a permutation invariant architecture using Self-Organizing Maps for point cloud processing.	Not specified	Point cloud reconstruction, classification, segmentation, shape retrieval	Requires tuning of the network's receptive field.
[70]	PIXOR	Developed a real-time 3D object detection system from point clouds using BEV, optimized for autonomous driving.	KITTI, large-scale 3D vehicle detection benchmark	Real-time 3D object detection in autonomous driving	Primarily optimized for vehicle detection, may not generalize to other object types.
[59]	SGPN	Introduced a network for 3D instance segmentation by predicting point groupings and semantic classes.	Various 3D scenes	3D instance segmentation, object detection, semantic segmentation	May struggle with highly cluttered or complex environments.
[71]	VoxelNet	Unified feature extraction and bounding box prediction for 3DPCs into a single deep network.	KITTI	3D detection of cars, pedestrians, and cyclists	High computational cost due to dense voxelization of point clouds.
[63]	Hand PointNet	Developed a hand pose regression network using 3DPCs to capture complex hand structures.	Three challenging hand pose datasets	3D hand pose estimation	Focuses on hand pose, limiting its applicability to other forms of point cloud processing.
[64]	PointNetVLAD	Proposed a network for global descriptor extraction from point clouds for place recognition.	Created benchmark datasets for point cloud based retrieval	Place recognition from point clouds	May not be as effective in highly dynamic environments.
[72]	PPFNet	Introduced a network for learning globally informed 3D local feature descriptors from point clouds.	Not specified	Finding correspondences in unorganized point clouds	Dependency on the quality of local features and global context understanding.
[62]	PointGrid	Combined point and grid-based approaches to recognize 3D models from point clouds.	Popular shape recognition benchmarks	3D model recognition, classification, and segmentation	Might not handle extremely sparse or irregular point clouds effectively.
[73]	PointFusion	Leverages image and point cloud data for 3D object detection without dataset-specific tuning.	KITTI, SUN-RGBD	Generic 3D object detection across diverse environments	The fusion process can be complex and computationally intensive.
[74]	Frustum PointNets	Operates on raw point clouds for 3D object detection, combining 2D and 3D detection methods.	KITTI, SUN RGB-D	3D object detection in both indoor and outdoor scenes	Might encounter difficulties with very sparse point clouds or heavy occlusions.
[75]	3DFeat-Net	Learns 3D feature detectors and descriptors for point cloud matching using weak supervision.	Outdoor Lidar datasets	Point cloud matching for localization and mapping	Performance highly dependent on the effectiveness of weak supervision learning mechanisms.
[56]	SpiderCNN	Developed SpiderConv units to handle 3DPCs	ModelNet40	3DPC classification and segmentation	May struggle with very large or noisy datasets
[57]	PointCNN	Introduced a X-transformation to handle unordered point clouds for CNNs	Multiple challenging benchmark datasets	Feature learning from point clouds	Dependent on the effectiveness of the X-transformation
[76]	SqueezeSeg	Created a CNN pipeline for semantic segmentation of LiDAR data	KITTI, GTA-V (simulated)	Semantic segmentation in autonomous driving	Reliance on synthetic data for improved accuracy
[77]	2DPASS	Boosted point cloud learning via 2D image fusion during training	SemanticKITTI, NuScenes	Semantic segmentation of point clouds	Requires multi-modal data during training, complex implementation
[65]	PREDATOR	Focused on low-overlap point cloud registration with deep attention	3DMatch benchmark	Point cloud registration	Limited to pairwise registration, may not generalize beyond benchmark scenarios
[66]	3DIoUMatch	Implemented a semi-supervised 3D object detection with teacher-student learning	ScanNet, SUN-RGBD, KITTI	3D object detection	High task complexity and dependency on initial label quality
[78]	PointPoseNet	Developed a pipeline for 6D object pose estimation from point clouds	LINEMOD, Occlusion LINEMOD	6D pose estimation	Limited to known objects in complex scenes, sensitivity to occlusions
[79]	ASAP-Net	Enhanced spatio-temporal modeling of point clouds	Synthia, SemanticKITTI	Point cloud sequence segmentation	Requires specific attention and structure-aware algorithms for optimal performance
[80]	MUSCLE	Proposed a compression algorithm for LiDAR data using spatio-temporal relationships	UrbanCity, SemanticKITTI	LiDAR data compression	Efficiency depends on the variability of the input data

Ref.	Model Name	Contribution Description	Dataset	Application	Limitation
[81]	PC-RGNN	Addressed sparse and partial point clouds for 3D detection using GNNs	KITTI	3D object detection	Highly dependent on the quality of initial point cloud data

2.5. Pre-trained 2D models

Xu et al. [82] demonstrate how pretrained 2D image models can be adapted for 3DPC understanding with minimal modification. By extending 2D ConvNets and vision transformers to handle 3D data, the method involves inflating 2D filters to 3D and only finetuning specific layers like the input, output, and normalization layers. This approach leverages the deep feature representations learned from large-scale 2D image datasets, enabling the models to perform competitively on 3DPC tasks such as classification and segmentation, while significantly reducing the training time and data requirements compared to training from scratch. The transferability is facilitated by the similarity in feature representation between the 2D and 3D tasks, despite their differences in data modality.

Besides, shape classification and part segmentation pose significant challenges in CV. While trained convolutional neural networks (CNNs) have shown impressive performance on regular grid data like images, accurately capturing shape information and geometric representation from irregular and disordered point clouds is problematic. To address this, [54] proposes point convolution (Pconv) and point pooling (Ppool) techniques inspired by convolution and pooling in image processing, specifically designed for point clouds to learn high-level features. Pconv gradually magnifies receptive fields to capture local geometric information, while Ppool tackles the disorder of point clouds using a symmetric function that aggregates points progressively for a more detailed local geometric representation. Our novel network, named PointVGG, incorporates Pconv, Ppool, and a graph structure for feature learning in point clouds, and is applied to object classification and part segmentation tasks. Experimental results demonstrate that PointVGG achieves state-of-the-art performance on challenging benchmarks of 3DPC. Moreover, extracting high-level features from disordered point cloud data using pre-trained 2D CNN remains challenging. To address this, [55] proposes a VGG-based network called point positional attention VGG (PointPAVGG), inspired by the classical VGG network. Our approach combines global and local features by extracting local geometric information from every sphere domain and analyzing the global position score using our point attention (PA) module. PointPAVGG, with its graph structure point cloud feature extraction and PA, is applied to point cloud classification and segmentation tasks. Through comprehensive experiments on ShapeNet and ModelNet, our method demonstrates superior performance, achieving state-of-the-art results in classification and segmentation tasks.

The work in [83] presents a method for automatic detection of manhole covers from mobile mapping point cloud data, which are large-scale spatial databases used for various purposes. The method uses a fully CNN with DTL and a simplified class activation mapping (CAM) location algorithm to accurately determine the position of manhole covers. Different source model architectures, such as AlexNet, VGG-16, Inception-v3, and ResNet-101, are assessed. Results showed that VGG-16 achieved the best detection performance among others, with recall, precision, and F2-score of 0.973 each. The approach also achieves a horizontal 95% confidence interval of 16.5 cm for location performance using VGG-16 architecture. The study highlights the importance of incorporating geometric information channels in the ground image for improved detection and location accuracy. Aerial imaging using drones, an efficient timely data collection after natural hazards for post-event management, provides detailed site characterization with minimal ground support, but results in large amounts of 2D orthomosaic images and 3DPC. Effective data processing workflows are needed to identify structural damage states. Liao et al. [84] introduce two DL models, based on 2D and 3D CNNs, for post-windstorm classification. DTL from AlexNet and VGGNet is used for the 2D CNNs, while a 3D fully convolutional network (3DFCN) with skip connections is developed and trained for point cloud data. The models are compared using quantitative performance measures, and the 3DFCN shows greater robustness in detecting different damage classes. This highlights the importance of 3D datasets, particularly depth information, in distinguishing between different damage states in structures.

In [85], a DL-based approach is proposed, which involves projecting 3DPC into 2D rendering views and then feeding them into a CNN for quality score prediction. DTL is employed to leverage the capabilities of VGG-16 trained on the ImageNet database. The performance of the proposed model is evaluated on two benchmark databases, IICIP2020 and SJTU, and the results show a strong correlation between the predicted and subjective quality scores, outperforming state-of-the-art point cloud quality assessment models. [86] addresses the problem of learning outdoor 3DPC from monocular data using a sparse ground-truth dataset. A DL-based approach called Pix2Point is proposed,

which uses a 2D-3D hybrid neural network architecture and a supervised end-to-end minimization of an optimal transport divergence between point clouds. The proposed approach outperformed efficient monocular depth methods when trained on sparse point clouds. The paper highlights the potential of DL for monocular 3DPC prediction and its ability to handle complete and challenging outdoor scenes. The encoding block, in the target model, consists of convolution, pooling, and normalization layers to extract feature descriptions from the RGB image. These features are then processed by a fully connected layer to obtain a preliminary set of 3D point coordinates. Several source models, based on VGG, DenseNet, and ResNet architectures, are explored and compared, which are referred to as backbones.

Balado et al. [87] propose in 2020, a method that minimizes the use of point cloud samples for training CNNs by converting point clouds to images (pc-images). This enables the generation of multiple samples per object through multi-view, and the combination of pc-images with images from online datasets such as ImageNet and Google Images. Results suggest keeping some point cloud images in training; even 10% can lead to high classification accuracy. The work presented in [88] showcases a prototypical implementation of a service-oriented architecture for classifying indoor point cloud scenes in office environments. This approach utilizes multi-view techniques for semantic enrichment of captured scans and subsequent classification. The approach is tested using a pretrained CNN model, Inception V3, to classify common office furniture objects such as chairs, sofas, and desks in 3DPC scans. The results show that the approach can achieve acceptable accuracy in classifying common office furniture, based on RGB cubemap images of the octree partitioned areas of the 3DPC scan. Additional methods for web-based 3D visualization, editing, and annotation of point clouds are also discussed.

The authors in [89] propose a visual recognition and location method for object detection in soft robotic manipulation using RGB-D information fusion. The method involves scanning and reconstructing the environment using ORB-SLAM2, constructing an object feature database, matching point clouds using the iterative closest point (ICP) algorithm, identifying regions of interest, and using the inception-v3 model and DTL for object recognition. The position of the object relative to the camera is obtained through correspondence between color information and point cloud data. The method showed that objects belonging to the same object have much lower matching error compared to those not belonging to the same object, and successful object identification and location were achieved through color recognition. Moving on, the authors in [90] adopt the ResNet50 [91] pretrained on the ImageNet data set to extract deep features from each feature image and obtain five multi-scale and multi-view (MSMV) deep features per point.

Table 3 presents a summary of DTL-based 3DPC models.

Table 3: Summary of DTL-based 3DPC models.

Category	Model	Highlights	Limitations
Point-based methods	AtlasNet [12]	In AtlasNet, a surface representation is inferred by regarding a 3D shape as a collection of parametric surface elements.	The reiterated many times largely determines the reconstruction.
	MSN [92]	A sampling algorithm combines a set of parametric surface elements, which MSN predicts, with the partial input.	Fine-grained details of object shape aren't generated successfully.
	ASHF-Net [93]	A hierarchical folding decoder with the gated skip-attention and multi-resolution completion target to exploit the local structure details of the incomplete inputs is proposed by ASHF-Net.	The decoder [113] obtains unstructured predictions, and the surface of the results doesn't remain smooth.
Point-based methods	PCN [94]	The coarse-to-fine completion is performed by PCN, which combines the fully connected network and FoldingNet.	The synthesis of shape details is not achievable.
	SA-Net [95]	Hierarchical folding in the multi-stage points generation decoder is proposed by SA-Net.	The implicit representation of the target shape from the intermediate layer, which helps refine the shape in the local region, is difficult to interpret and constrain.
	FoldingNet [60]	It is commonly assumed in a two-stage generation process that a 2D-manifold can recover 3D objects.	Explicitly constraining the implicit intermediate is challenging.
Point-based methods	SK-PCN [96]	The global structure is acquired by predicting the 3D skeleton with SK-PCN, and the surface completion is achieved by learning the displacements of skeletal points.	The overall shapes are the sole focus of the meso-skeleton.
	GRNet [97]	Unordered point clouds are regularized by GRNet, which introduces 3D grids as intermediate representations.	The resolution still governs it. A significant computational cost is incurred when a higher resolution is used.
	VE-PCN [98]	The structure information is incorporated into the shape completion by VE-PCN through the utilization of edge generation.	High frequency components are the sole focus of the edges.
	Point-PEFT [99]	Introduces a Parameter-Efficient Fine-Tuning method for 3D models, minimizing adaptation costs for downstream tasks with minimal trainable parameters.	While effective, the specialized method's broader applicability and long-term adaptability across diverse domains remain unproven.

Table 3 (Continue)

Category	Model	Highlights	Limitations
	DAPT [100]	Implement a Dynamic Adapter for point cloud analysis, offering efficient parameter use and reducing training resources significantly.	Although reducing trainable parameters, the adaptability and effectiveness in extremely diverse environments is yet to be fully assessed.
	AgileGAN3D [101]	A novel framework for 3D artistic portrait stylization using unpaired 2D exemplars and advanced 3D GAN models.	The dependency on the quality and diversity of the 2D exemplars might limit the model's versatility in less controlled scenarios.
	3D-TRAM [102]	Combines transfer learning with a memory component to enhance 3D reconstruction from 2D images, leveraging CAD models for better accuracy.	The method's performance can vary significantly with the complexity of the scene and the quality of the available CAD models.

2.6. Pre-trained 3D models

Implementing a standardized approach to 3DPC neural network design has the potential to yield comparable advancements seen in the extensive research conducted on pre-training visual models, especially in the image domain. However, compared to the 2D domain, the design of neural networks for point cloud data is less mature, as evidenced by the numerous new architectures proposed recently. This is due to several factors, including the challenge of processing unordered sets [103], the choice of neighborhood aggregation mechanism, which could be hierarchical [53, 104, 105], spatial CNN-like [56, 57, 106, 107], spectral [108, 109], or graph-based [110, 111], and the fact that points are discrete samples of an underlying surface, which has led to the consideration of continuous convolutions [112, 113].

While pre-training image models have been successful in achieving high levels of prosperity, pre-training 3D models is still in the developmental stage. To address this issue, numerous researchers have explored various SSL mechanisms that utilize different pretext tasks, such as solving jigsaw puzzles [114], estimating orientation [115], and reconstructing deformations [116]. Drawing inspiration from pre-training strategies in the image domain, several approaches have been proposed in the 3D domain, including point contrast [117], which uses a contrastive learning principle, and OcCo [118], Point-BERT [119], and Point-M2AE [120], which introduce reconstruction pretext tasks to facilitate better representation learning. However, the lack of available data in the 3D domain remains a significant obstacle in developing more effective pre-training strategies.

In this respect, Choy et al. proposed the Minkowski Engine [121], which is an extension of sub-manifold sparse convolutional networks [122] to higher dimensions. By facilitating the adoption of common deep architectures from 2D vision, sparse convolutional networks could help standardize DL for point cloud. In [117], the authors use a unified UNet [123] architecture built with Minkowski Engine as the backbone network in all our experiments and show that it can seamlessly transfer between tasks and datasets. [120] The paper proposes Point-M2AE scheme, a multi-scale masked autoencoder (MAE) pre-training framework for SSL of 3DPC. Unlike standard auto-encoder (AE)-based transformers, Point-M2AE modifies the encoder and decoder into pyramid architectures to model spatial geometries and capture fine-grained and high-level semantics of 3D shapes. The encoder uses a multi-scale masking strategy for consistent visible regions across scales and a local spatial self-attention [124] mechanism during fine-tuning. The lightweight decoder gradually upsamples point tokens with skip connections from the encoder, promoting reconstruction from a global-to-local perspective. Point-M2AE achieves 92.9% accuracy on ModelNet40 using a linear SVM. Fine-tuning enhances performance to 86.43% on ScanObjectNN and provides benefits in various tasks, such as few-shot classification, part segmentation, and 3D object detection.

The reference [125] introduces the PointCLIP method, which encodes point clouds by projecting them into multi-view depth maps and aggregates view-wise zero-shot predictions for knowledge transfer from 2D to 3D. An inter-view adapter is designed to extract global features and adaptively fuse few-shot knowledge from 3D into CLIP pre-trained in 2D. Fine-tuning the lightweight adapter in few-shot settings significantly improves PointCLIP's performance. PointCLIP also exhibits complementary properties with classical 3D-supervised networks, and ensembling with baseline models further boosts performance, surpassing state-of-the-art models. PointCLIP is a promising alternative for effective 3DPC understanding with low resource cost and data regime, as demonstrated through experiments on ModelNet10, ModelNet40, and ScanObjectNN datasets. Huang et al. [126] proposes a method called MF-PointNN for surrogate modeling of melt pool in metallic additive manufacturing. Melt pool modeling is important for uncertainty quantification and quality control in metal additive manufacturing, but finite element simulation for thermal modeling can be time-consuming. MF-PointNN is a multi-fidelity approach that combines low-fidelity analytical models and

high-fidelity finite element simulation data using DTL. A basic PointNN is first trained with low-fidelity data to establish correlation between inputs and thermal field of analytical models. Then, the basic PointNN is updated and fine-tuned using a small amount of high-fidelity data to build the MF-PointNN. This latter efficiently maps input variables and spatial positions to thermal histories, allowing for efficient prediction of the three-dimensional melt pool. Results of melt pool modeling for Ti-6Al-4V in electron beam additive manufacturing under uncertainty show the effectiveness of the proposed approach.

2.7. Evaluation metrics

Several metrics have been reported to evaluate the performance of different DTL approaches for various 3DPC tasks. F1 measures and overall accuracy (OA), are the most frequently used measures to assess the performance of algorithms over benchmark datasets. These metrics are used for many purposes, including segmentation, classification, and registration. F1 measures give an idea about the behavior of the precision and recall curve, whereas OA conveys the mean accuracy for instances of the test. Besides, intersection over union (IoU) and mean IoU have been extensively used, especially for object detection and segmentation purpose. For instance, in [127], authors have used mean IoU between point-wise ground truth and prediction. In [128], authors have computed IoU for different shapes. It is calculated as the average of IoUs of all parts in a shape. Furthermore, for some particular categories, mean IoUs (mIoUs) are obtained by finding out the average of all IoUs shapes. Other metrics, instance mIoU (Ins. mIoU) and category mIoU (Cat. mIoU) are also introduced and computed by calculating the average of all shapes and the average of mIoUs for all categories, respectively.

Metrics such as OA and mIoU provide a holistic view of the model's performance across different categories. Additionally, the frame per second (FPS) metric evaluates the efficiency and speed of real-time applications, while root mean squared error (RMSE) and mean absolute percentage error (MAPE) are used for precision in measurement tasks. Moving on, consistency rate (CR), consistency proportion (CP), and weight coverage (WCov) are advanced evaluation metrics used to assess the quality of 3D point cloud reconstructions. CR measures the rate at which a reconstructed scene maintains geometric consistency across different views or instances. CP evaluates the proportion of consistent data points within the entire dataset, providing a sense of how uniformly the model performs. WCov assesses the coverage of the weighted areas in the point cloud, indicating how well the model captures the essential features and structures of the scene.

To evaluate the performance or semantic segmentation, authors in [129] have used errors of commission and errors of omission metrics over the CMP façade dataset. Frame per second (FPS) metric is used by [130] on the ouster LiDAR-64 dataset. In addition to this, Zong et al. [131] have used average precision (mPrec) and average recall (mRec) to test their segmentation method. Moreover, the best performance for OA on the Shapenet dataset is 94.5% [132]. However, the highest precision (85.99%) is achieved on CMP facade dataset [129]. The F1 score has been calculated on different datasets, viz. CMP facade, ISPRS, Semantic 3D dataset, ModelNet4, and other. The best performance has been reported by [133] on ModelNet40. The aforementioned metrics are not only applicable to 3DPC tasks but also to other artificial intelligence-related tasks such as classification, segmentation, and other. However, subsequent subsections thoroughly elaborate on specific metrics relevant to 3DPC tasks.

2.7.1. Distance metrics

Distance metrics play a pivotal role in the processing of point clouds for tasks such as nearest-neighbor search, clustering, and segmentation. They provide a measure of similarity or dissimilarity between points in space, influencing the outcomes of many algorithms.

2.7.2. Euclidean Distance

Defined as the square root of the sum of the squared differences between the coordinates of two points:

$$d(\mathbf{p}, \mathbf{q}) = \sqrt{(p_1 - q_1)^2 + (p_2 - q_2)^2 + \dots + (p_n - q_n)^2}$$

where $\mathbf{p} = (p_1, p_2, \dots, p_n)$ and $\mathbf{q} = (q_1, q_2, \dots, q_n)$ represent the coordinates of two points in an n -dimensional space. The Euclidean distance $d(\mathbf{p}, \mathbf{q})$ calculates the "as-the-crow-flies" distance between the two points, effectively measuring the length of the straight line segment that connects them.

2.7.3. Manhattan Distance

Also known as taxicab or city block distance, it is the sum of the absolute differences of their coordinates:

$$d(\mathbf{p}, \mathbf{q}) = |p_1 - q_1| + |p_2 - q_2| + \dots + |p_n - q_n|$$

This metric is ideal for grid-based and urban environments where travel paths are constrained to grid layouts.

2.7.4. Mahalanobis Distance

Takes into account the correlations of the dataset and is scale-invariant, defined as:

$$d(\mathbf{x}, \mu) = \sqrt{(\mathbf{x} - \mu)^T \mathbf{S}^{-1} (\mathbf{x} - \mu)}$$

where:

- \mathbf{x} is the vector representing the point whose distance from the distribution is being measured.
- μ is the mean vector of the distribution, representing the central tendency.
- \mathbf{S}^{-1} is the inverse of the covariance matrix \mathbf{S} of the distribution, which adjusts the distance measure to account for the spread and orientation of the data points.

This formulation accounts for the shape of the data distribution, correcting distances based on how data spreads and correlates across dimensions, thus providing a more nuanced measure of distance.

2.7.5. Hausdorff distance

Let us assume that there are two point clouds S_1 and S_2 in R^3 with N_1 and N_2 points in each cloud, respectively. In order to compare these point sets, one of the earliest methods that was proposed is the Hausdorff distance (D_H), which is based on finding the minimum distance from a point to a set [134]:

$$d(x, y) = \|x - y\|_2 \quad (3)$$

$$D(x, S) = \min_{y \in S} d(x, y) \quad (4)$$

and calculates a symmetric max min distance [135]:

$$D_H(S_1, S_2) = \max \left\{ \max_{a \in S_1} D(a, S_2), \max_{b \in S_2} D(b, S_1) \right\} \quad (5)$$

2.7.6. Chamfer distance

The Chamfer distance (CD) is a metric used to evaluate the similarity between two sets of points in space. It considers the distance between each point in both sets and finds the nearest point in the other set, then sums the square of these distances. CD is commonly used in the ShapeNet's shape reconstruction challenge. The CD between two point clouds, S_1 and S_2 , is defined as [136]:

$$D_{CD}(S_1, S_2) = \frac{1}{|S_1|} \sum_{x \in S_1} \min_{y \in S_2} \|x - y\|_2^2 + \frac{1}{|S_2|} \sum_{y \in S_2} \min_{x \in S_1} \|x - y\|_2^2 \quad (6)$$

2.7.7. Earth mover's distance

In contrast to the Hausdorff distance and its derivative methods that involve identifying the closest neighboring point for each point, the Earth mover's distance (EMD) or the Wasserstein distance operates by establishing a one-to-one correspondence (i.e., bijection represented by ζ) between the two sets of points. The objective is to minimize the total distance between the corresponding points in the two sets [134].

$$D_{EMD}(S_1, S_2) = \min_{\zeta: S_1 \rightarrow S_2} \sum_{a \in S_1} \|a - \zeta(a)\|_2 \quad (7)$$

2.8. Datasets

There is a considerable number of datasets available for performing various 3DPC tasks using state-of-the-art techniques. A detail about datasets on which DL has been implemented is reported in [31]. However, in our study, we have considered the datasets for which DTL has been incorporated to carry out 3DPC tasks. These include widely used benchmarks like, PointNet [137], ShapeNet [117], ModelNet [128], ScanNet [117], ISPRS [138], KITTI 3D object detection [130], Campus3D [139] and semantic 3D dataset [140]. Apart from these well-known benchmarks, in this study, newly introduced datasets are also included. These comprises of Scaffolds dataset [140], CMP façade dataset [129], DFC [138], Ouster LiDAR-64 [130], Santa Monica point cloud data [141], UTD-MHAD [142], PointDA-10 [143], NYU [144], SHREC2018 [145], and EndoSLAM dataset [146].

These datasets are used for 3DPC segmentation (semantic, panoptic, and instance), classification, and object detection and tracking and contain features beneficial for carrying out related tasks. For instance, datasets like ModelNet 40, ShapeNet and ScanNet, among others, are used for shape classification and contain columns like sample size, classes, training, testing data percentage, and other useful features. In addition to this, SHREC2018 and EndoSLAM are medical-related datasets. The latter is created through the recording of multiple endoscope cameras for six porcine organs, as well as synthetically generated records. However, the former, the SHREC2018 protein dataset, contains 2267 protein details. To record the details, the protein data bank (PDB) format has been used. The datasets, references, and available links are given in Table 4.

3. Overview of DTL

Arguably one of the top success stories of DL is DTL. Many applications in language and vision have benefited from the discovery that pretraining a network on a rich source set (e.g., ImageNet) can help boost performance once fine-tuned on a typically much smaller target set. Yet, very little is known about its usefulness in 3DPC understanding. We see this as an opportunity considering the effort required for annotating data in 3D.

3.1. Domain adaptation

Domain adaptation (DA) has shown significant improvements in various ML and CV tasks, such as classification, detection, and segmentation. However, there are limited methods that have achieved DA directly on 3DPC data, to the best of our knowledge. The challenge of point cloud data lies in its rich spatial geometric information, where the semantics of the entire object are contributed by regional geometric structures. Most general-purpose DA methods that focus on global feature alignment and disregard local geometric information may not be suitable for 3D domain alignment. Wu and their colleagues [153] discuss the challenges of generating and annotating large amounts of real-world data for DL-based approaches in robotics CV tasks. To overcome this, the authors propose using simulation-to-reality (sim2real) DTL for point cloud data in an industrial application case. They provide insights on generating and processing synthetic point cloud data to improve model performance when transferred to real-world data. The issue of imbalanced learning is also investigated, and the authors propose a novel patch-based attention network as a strategy to address this problem. Another work in [154], presents a new method called DTL-based sampling-attention network (TSANet) for semantic segmentation of 3D urban point clouds to facilitate the development of smart cities. The method includes a segmentation model with point downsampling–upsampling structure, embedding method, attention mechanism, and focal loss for feature processing and learning. The DTL technique aims to reduce data requirements and labeling efforts by leveraging prior knowledge. The method is evaluated on a realistic point cloud dataset of Cambridge and Birmingham cities, demonstrating promising performance, surpassing other state-of-the-art models in terms of accuracy and mean IoU. [116] introduces SSL for DA in 3D perception problems, specifically on point clouds. It describes a new family of pretext tasks called deformation reconstruction, inspired by sim-to-real transformations, and proposes a novel training procedure called point cloud mixup (PCM) motivated by the MixUp method for labeled point cloud data. Evaluations on DA datasets for classification and segmentation show significant improvement over existing and baseline methods, demonstrating the effectiveness of SSL-PCM-DA on point clouds. Similarly, [155] introduces a new model called SqueezeSegV2 for point cloud segmentation that is more robust to dropout noise in LiDAR point clouds. The improved model structure, training loss, batch normalization, and additional input channel result in significant accuracy improvement when trained on real data. To overcome the challenge of limited labeled point-cloud data, the proposed scheme employs DA training pipeline, consisting of learned intensity rendering, geodesic correlation alignment, and progressive domain calibration. When trained on real data,

Table 4

Dataset and evaluation metrics used by DTL methods for various 3DPC tasks.

Ref.	Dataset	Dataset availability	Evaluation metric	Best performance (%)
[117]	ShapeNet, ScanNet	http://www.scan-net.org/#code-and-data	-	-
[137]	PointNet [52], ShapeNet [147], and ModelNet-40	http://stanford.edu/rqi/pointnet/ https://shapenet.org/ https://modelnet.cs.princeton.edu/	-	-
[148]	UTD-MHAD	http://www.utdallas.edu/kehtar/Kinect2Dataset.zip	Recognition rate	92.50
[133]	ModelNet40	https://modelnet.cs.princeton.edu/	F1, precision, recall	F1 (91)
[149]	ModelNet	https://modelnet.cs.princeton.edu/	MAE-T, MAE-F	CA (97.6)
[128]	ShapeNet, ModelNet	https://shapenet.org/ https://modelnet.cs.princeton.edu/	OA	90.40
[138]	ISPRS, DFC	https://www.isprs.org/data/	F1, OA	F1 (83.62), OA (89.84)
[130]	KITTI 3D object detection, Ouster LiDAR-64	https://ouster.com/resources/lidar-sample-data/	FPS (frame per second)	FPS (30.6)
[150]	ImageNet, KITTI 2D, VLP-16	http://www.image-net.org/about-stats	IoU, F1, mAP	mAP(81.27), IoU(65.11), F1 (0.82)
[140]	Semantic3D dataset [22], Scaffolds dataset	http://www.semantic3d.net/view_dbase.php?chl=1	F1, precision, recall	F1 (90.84)
[139]	Campus3D	https://3d.nus.app/	OA, IoU, mIoU, CR, CP and WCov	OA(90.9), mIoU(61.5)
[129]	CMP façade dataset	https://cmp.felk.cvut.cz/tylcr1/facade/	Precision, recall, F1, Errors of commission, Errors of omission	Precision (85.97), recall (89.80), F1 (87.85)
[141]	Santa Monica point cloud data, KITTI 2D, VLP-16	http://www.cvlibs.net/datasets/kitti/	F1, precision, recall	-
[143]	PointDA-10	-	Accuracy	49.70
[145]	SHREC2018	-	precision, recall, NN, T1, T2, EM, DCG	-
[146]	EndoSLAM dataset	https://github.com/CapsuleEndoscope/EndoSLAM	RMSE	-
[131]	3DPC tunnel dataset	-	Average precision (mPrec), average recall (mRec)	mPrec (71.2)
[151]	2014 scans	-	MAPE, RMSE	MAPE (0.416), RMSE (0.112)
[152]	NYU	-	RMSE, Accuracy	(81.8),
[132]	ShapeNetPart	https://shapenet.org/	OA, mIoU, Cat. mIoU, Ins. mIoU	OA (94.5)

the new model exhibits significant segmentation accuracy improvements over the original SqueezeSeg. Moreover, when trained on synthetic data using the proposed DA pipeline, the test accuracy on real-world data nearly doubles. A similar scheme for segmentation is proposed in [156], introducing LiDARNet, a boundary-aware DA model tailored for semantic segmentation of LiDAR point cloud data. The model uses a two-branch structure to extract domain private and shared features, and incorporates Gated-SCNN to learn boundary information during segmentation. The domain gap is further reduced by learning a mapping between domains using shared and private features. They also introduce a new dataset, SemanticUSL, for DA in LiDAR semantic segmentation, which has the same format and ontology as Semantic KITTI. Experiments on real-world datasets show that LiDARNet achieves comparable performance on the SD and significant performance improvement (8-22% mIoU) on the TDs after adaptation.

Other researchers have advanced unsupervised DA approaches, demonstrated by the method outlined in [157], aimed at enhancing semantic labeling accuracy for 3DPC in autonomous driving scenarios. The proposed approach uses a complete and label approach, leveraging a sparse voxel completion network (SVCN) to recover underlying surfaces of sparse point clouds and transfer semantic labels across different LiDAR sensors. The approach does not require manual labeling for training pairs and introduces local adversarial learning to the model surface prior. Experimental results on a new benchmark dataset show significant performance improvements ranging from 8.2% to

36.6% compared to previous DA methods. Likewise, [158] introduces PointDAN, a 3D DA network tailored for point cloud data, aligning global and local features at multiple levels to achieve domain alignment. It introduces a Self-adaptive node module for local alignment, which models discriminative local structures, and a node-attention module for hierarchical feature representation. For global alignment, an adversarial-training strategy is employed. PointDAN outperforms state-of-the-art DA methods in terms of adapting 3DPC data across domains, as demonstrated on the benchmark dataset PointDA-10, created by the authors. Zhao et al. [159] proposes an end-to-end framework called ePointDA for simulation-to-real DA (SRDA) in LiDAR point cloud segmentation. ePointDA consists of three modules: self-supervised dropout noise rendering, statistics-invariant and spatially-adaptive feature alignment, and transferable segmentation learning. The framework bridges the domain shift at pixel-level and feature-level, without requiring real-world statistics. Experimental results on adapting from synthetic to real datasets demonstrate the superiority of ePointDA in LiDAR point cloud segmentation. Xu and their colleagues [160] propose semantic point generation to enhance the reliability of LiDAR-based object detectors against domain shifts in autonomous driving. The scheme generates semantic points to recover missing parts of foreground objects caused by occlusions, low reflectance, or weather interference. By merging the semantic points with the original points, an augmented point cloud is obtained, which significantly improves the performance of modern LiDAR-based detectors in unsupervised DA tasks. The method also benefits object detection in the original domain, surpassing KITTI when combined with PV-RCNN.

Lang et al. [161] utilize PointNets to represent point clouds organized in vertical columns. The scheme, called PointPillars, achieves superior speed and accuracy, surpassing KITTI benchmarks while running at a significantly higher frame rate of 62 Hz. A faster version achieves state-of-the-art performance at 105 Hz, making it a suitable encoding approach for object detection in point clouds in robotics applications like autonomous driving. For object detection from 3DPC, the authors [162] propose a Semi-Supervised DA method for 3D object detection that leverages a small amount of labeled target data to improve adaptation performance. The method consists of an inter-DA stage, which uses a Point-CutMix module to align point cloud distribution across domains, and an intra-domain generalization stage, which employs intra-domain Point-MixUp in semi-supervised learning to enhance model generalization on the unlabeled target set. Experimental results show that the proposed scheme, with only 10% labeled target data, outperforms a fully-supervised oracle model with 100% target labels on the Waymo to nuScenes domain shift. However, Du et al. [163] tackle the challenge of enhancing feature representation robustness in 3DPC by employing the DA approach. The severe spatial occlusion and point density variance in point cloud data make designing robust features crucial. The proposed approach bridges the gap between the perceptual domain (real scene) and the conceptual domain (augmented scene with non-occluded point clouds), mimicking the functionality of human perception. Experimental results show that this simple yet effective approach significantly improves the performance of 3DPC object detection, achieving state-of-the-art results.

3.2. Fine-tuning

Fine-tuning stands as a ubiquitous DTL approach, aiding pretrained models to adapt to new tasks through iterative training, often supplemented with additional layers known as the target model. [164]. The recent research studies, such as [165–167], have argued that even if the target task and source task are different, transferring features via DTL approaches outperforms random features selections. This characteristic has led to the great success of DTL in different spheres of real-life applications such as medical imaging [4, 168], recognition tasks like speech recognition [26], hand-gesture [169], face recognition [170], and recently, in the processing of 3DPC data [130, 171]. One of the major concerns raised in fine-tuning a pretrained model is to identify which layer to fine-tune. The authors in [172] have explicitly added regularization terms to the loss function for obtaining the parameters of the fine-tuned model close to the original pretrained model. AdaFilter [164], is an adaptive fine-tuning approach, which considers criterion for optimization by selecting only a part of the convolutional filters in the pretrained model. Furthermore, they have exploited a recurrent gated network and considered activation of the previous layer for carefully fine-tuning the desired convolutional filters only. The adaptive fine-tuning scheme considers the similarity between the source and target tasks and datasets to reuse more pretrained filters.

Many works that involve processing 3DPC data have exploited DTL for many tasks, include 3D reconstructions of scaffolds [140], 3DPC instance segmentation [131], classification of soft-story buildings using 3DPC data [141], 3DPC understanding [117], 3D orientation recognition [149], SSL on 3DPCs [148], and remaining useful life prediction [151], among others. Furthermore, some fine-tuning strategies involve all the pretrained parameters, whereas others fine-tuning the last few layers [164], as illustrated in Fig. 7 (a). G Diraco et al. [151] have performed an extensive experiment for a particular scenario in which the amount of data in the TD is small and explored how it behaves if only part of

the network is fine-tuned on the given target dataset. They have updated the decoder of their model, which has been trained on SDs and evaluated on the target dataset.

One factor contributing to the success of DTL is its ability to perform well with smaller datasets. In support of this, the authors [141] have employed DTL to address the challenge of training large parameters in deep convolutional networks. Their experimental results demonstrate the transferability of DTL from SDs to TD, as the dataset under consideration lacked sufficient data to train large parameters. Additionally, compared to traditional training methods, DTL consumes less time, making it a more efficient approach. To support this claim, the authors noted that models such as VGGNet, Inception and ResNet, which were trained using fine-tuning techniques, exhibited shorter training times by triggering the early stopping mechanism. This improvement in training time has enabled the workflow to quickly identify soft-story buildings on a city scale. Furthermore, the authors have shown that DTL can effectively reduce the risk of overfitting that can occur with DL techniques. By leveraging a pretrained network, DTL can transfer knowledge and prevent the model from memorizing the training data, leading to more robust and generalizable performance. Moving on, Xiu et al. [173] propose using airborne LiDAR to detect collapsed buildings during earthquake emergency response, as DTL-based damage detection with aerial images has limitations in detecting collapsed buildings with undamaged roofs. The authors develop a 3DPC-based dataset for building damage detection and propose a general extension framework and a visual explanation method to validate model decisions. The results conducted using PointNet [52], PointNet++ [53] and DGCNN [174] show that 3DPC-based methods can achieve high accuracy and are robust even with reduced training data. The model also achieves moderate accuracy on another dataset with different architectural styles without additional training.

3.3. Unsupervised DTL

Unsupervised DTL is mainly based on unsupervised domain adaptation (UDA) to remove the need or addressing the issue of lack for labeled data and allows any image to be used as a datapoint for any CV tasks [175, 176]. Numerous methods have been proposed for performing UDA on 2D images, which can be divided into two main categories: methods based on domain-invariant feature learning and methods for learning domain mapping. The former [177–181] aim to minimize the discrepancy between two distributions in the feature space, while the latter [182–184] use neural networks, such as CycleGAN [53], to directly learn the translation from the SD to the TDs. In [185], 2D translation is extended to depth images using a differential contrastive learning strategy for preserving underlying geometries. Despite their differences, these methods widely exploit domain adversarial training. Additionally, several useful techniques, such as pseudo-labeling [186] and batch normalization tailored for DA [187], have also been proposed.

Although there have been significant efforts made in UDA for 2D images and depth, UDA on 3DPC is still in its early stages. UDA on point clouds involves extending domain adversarial training from 2D images to 3DPC to align features on both local and global levels [188]. Nevertheless, adversarial methods on 3DPC struggle to balance local geometry alignment and global semantic alignment. CycleGAN [189] is utilized by both [159] and [190] to generate more realistic LiDAR point clouds from synthetic data. This Sim2Real approach is used to minimize feature distances between the SD and TD. The work in [157], on the other hand, leverages segmentation on completed surface reconstructed from sparse point cloud for better adaptation.

For object-level tasks, [158, 191] align global and local features, while [155] and [190] project point clouds to 2D and birds-eye view, respectively, to reduce sparsity. [163] creates a car model set and adapts their features for detection object features, but only targets general car 3D detection on a single point cloud domain. Recently, [192] published the first study targeting UDA for 3D LiDAR detection. They identify the vehicle size as the domain gap between KITTI [193] and other datasets and resize the vehicles in the data. In contrast, [160] identifies point cloud quality as the major domain gap between Waymo's two datasets [194] and proposes a learning-based approach to close the gap.

Recent works on UDA on point clouds mainly focus on designing suitable self-supervised tasks on point clouds to facilitate learning domain invariant features, which are discussed in detail in the following subsection. In addition to UDA on object point clouds, several methods have been proposed to address specific domain gaps on LiDAR point clouds. These methods commonly address depth missing and sampling difference between sensors. ST3D [195] presents a task-specific self-training pipeline with curriculum data augmentation to further improve the adaptation process

Alternatively, most existing UDA approaches focus on uni-modal data, despite the availability of multi-modal datasets. In [196], the authors propose a cross-modal UDA (xMUDA) approach for 3D semantic segmentation, where both 2D images and 3DPC are utilized. This is challenging as the two input modalities are heterogeneous

and can be affected differently by domain shift. In xMUDA, the modalities learn from each other through mutual mimicking, separate from the segmentation objective, to prevent the stronger modality from adopting false predictions from the weaker one. The proposed xMUDA approach is evaluated on various UDA scenarios, such as day-to-night, country-to-country, and dataset-to-dataset shifts, using recent autonomous driving datasets. Results show that xMUDA significantly improves over uni-modal UDA in all tested scenarios and complements state-of-the-art UDA techniques. Saltori et al. [197] introduces a novel source-free UDA (SF-UDA) framework for 3D object detection using LiDAR point clouds, which does not require any annotations from the SD or images/annotations from the TD. It addresses domain shift in LiDAR data, which is not only due to changes in environment and object appearances, but also to geometry (e.g., point density variations). SF-UDA^{3D} utilizes pseudo-annotations, reversible scale-transformations, and motion coherency for DA. Experimental results on large-scale datasets, KITTI and nuScenes, show that SF-UDA^{3D} outperforms previous methods based on feature alignment and state-of-the-art 3D object detection methods that use few-shot target annotations or target annotation statistics. Also, [198] introduces RefRec, an approach that investigate pseudo-labels and self-training for UDA in point cloud classification. Instead of relying on multi-task learning, RefRec proposes two innovations for effective self-training on 3D data. First, it refines noisy pseudo-labels by matching shape descriptors learned from the unsupervised task of shape reconstruction on both domains. Second, it proposes a novel self-training protocol that learns domain-specific decision boundaries and mitigates the negative impact of mislabelled target samples and in-domain intra-class variability. RefRec achieves state-of-the-art performance on standard benchmarks for UDA in point cloud classification, demonstrating the effectiveness of self-training for this emerging research problem. Additionally, [199] focuses on UDA in 3D CV tasks, specifically point cloud visual tasks. The proposed approach introduces a dual-branch feature alignment network (DFAN) architecture that leverages the characteristics of local and global features in point clouds. The approach utilizes different strategies for feature extraction and alignment in each branch, complementing each other. Hierarchical alignment for local features and distribution alignment for global features are also introduced. Experimental results on benchmark datasets demonstrate that the proposed approach achieves state-of-the-art performance in point cloud classification and segmentation tasks.

Previous studies on unsupervised 3D learning have principally concentrated on ShapeNet [147], which is a repository of single-object computer aided design (CAD) models. Typically, the idea is to use ShapeNet as the ImageNet counterpart in 3D so that the characteristics learned on single synthetic objects can be transferred to other real-world applications. In this regard, numerous works have then been proposed. For instance, [200] introduces a point-level DA by searched transformations. Typically, transformations of 3DPCs are learned via the search of the best combination of operations on 3DPCs, which transfers data from the SD to the TD while keeping the TD unlabeled. Besides, most 3DPC-based UDA techniques focus on extracting domain-invariant features in different domains for feature alignment. In this regard, UDA is advocated for the detection of 3D objects in the context of semantic point generation, as proposed in [160].

Moving on, in [157], a UDA problem approach for the semantic labeling of 3DPCs is proposed, focusing on domain gap reduction of LiDAR sensors. Based on the observation that sparse 3DPCs are sampled from 3D surfaces, a SVCN was designed to complete the 3D surfaces of a sparse 3DPC. Unlike semantic labels, obtaining training pairs for SVCN requires no manual labeling. A local adversarial learning to model the surface prior was also introduced. The recovered 3D surfaces serve as a canonical domain from which semantic labels can transfer across different LiDAR sensors. Experiments and ablation studies with benchmark for cross-domain semantic labeling of LiDAR data show that this approach provides 6.3-37.6% better performance than previous DA methods. Fig. 9 portrays the block diagram of the the UDA scheme introduced in [157] for semantic segmentation of LiDAR 3DPCs.

3.4. Semi-supervised DTL

The integration of semi-supervised DTL into 3DPC understanding for tasks like object detection and segmentation is rapidly transforming the field, particularly in contexts where labeled data are scarce. This approach leverages both labeled and unlabeled data, enhancing learning efficiency and model performance across various applications, from autonomous driving to tunnel monitoring. Typically, Tang et al. [201] develop a semi-supervised 3D object detection model that utilizes a novel network to transfer knowledge from well-labeled object classes to weakly labeled classes, improving detection in classes with only 2D labels. Moving on, Ji et al. [5] propose the Semi-supervised Learning-based Point Cloud Network (SPCNet) which integrates various learning modules to enhance tunnel scene segmentation from 3DPCs, significantly reducing the reliance on extensive labeled datasets. Imad et al. [130]: Focused on utilizing 3D LiDAR data for autonomous driving perception, enhancing object detection through a semi-supervised learning framework that minimizes the need for large-scale annotated datasets.

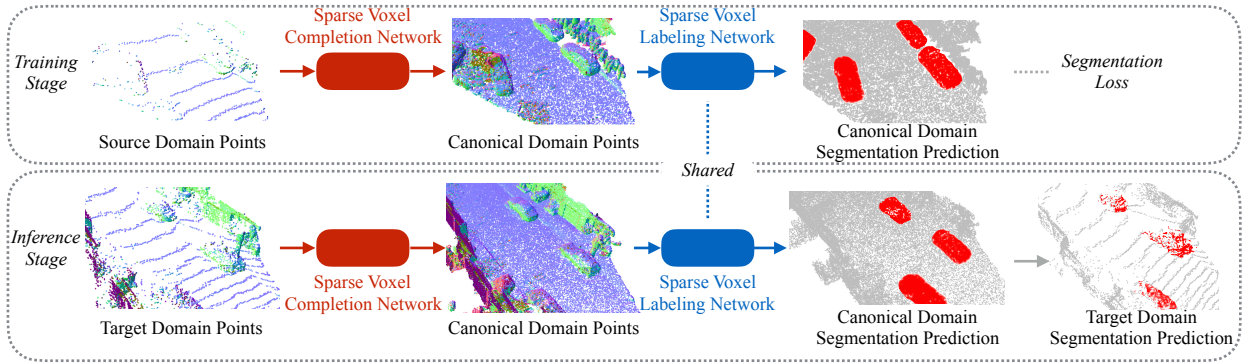


Figure 9: Flowchart of the UDA approach proposed in [157] for semantic segmentation of LiDAR 3DPCs

In this same direction, Huang et al. [202] present a point cloud registration framework that minimizes a feature-metric projection error without needing correspondences, using a semi-supervised approach. This method is particularly robust to noise and density differences in point clouds. Horache et al. [203] propose a method for generalizing deep learning for 3DPC registration on entirely different datasets using a combination of Multi-Scale Sparse Voxel Convolution and an unsupervised transfer algorithm, UDGE, enhancing adaptability across varied real-world datasets. Li et al. [204] introduce a semi-supervised point cloud segmentation method that utilizes both labeled and unlabeled data. By employing adversarial architecture for confidence discrimination of label predictions on unlabeled point clouds, their approach enhances segmentation performance.

Besides, Chen et al. [205] propose a multimodal semi-supervised learning framework that utilizes instance-level consistency and a novel multimodal contrastive prototype loss to enforce consistent representations across different 3D data modalities of the same object. Similarly, Xiao et al. [206] tackle the synthetic-to-real data gap in 3DPCs segmentation by developing a large-scale synthetic dataset and a novel translation method that decomposes and addresses the differences in appearance and sparsity between synthetic and real datasets. Moving on, Mei et al. [207] develop a system for the semantic segmentation of 3D LiDAR data in dynamic scenes, using a semi-supervised learning strategy that combines limited manual annotations with large amounts of constraint data to enhance scene adaptability. Additionally, Huang et al. [208] introduce a spatio-temporal representation learning framework for learning from unlabeled 3DPCs in a self-supervised manner, facilitating the generalization of pre-trained models to a variety of downstream tasks. Moreover, Qin et al. [209] propose a weakly supervised framework for 3D object detection that leverages unsupervised 3D proposal generation and cross-modal knowledge distillation, reducing the dependency on annotated 3D bounding boxes.

On the other hand, Yu et al. [210] tackle the data scarcity challenge in 3D tasks by transferring knowledge from robust 2D models to augment RGB-D images with pseudo-labels, significantly improving the pre-training of 3D models with limited labeled data. Xu et al. [211] develop a hierarchical point-based active learning strategy for 3DPC segmentation, which measures uncertainty at multiple levels and selects important points for manual labeling, effectively utilizing limited annotations. Zhang et al. [212] study weakly semi-supervised 3D object detection with point annotations to generate high-quality pseudo-bounding boxes, enabling 3D detectors to perform comparably to fully-supervised models with substantially fewer labeled data. Lastly, Wang et al. [213] introduce a Semi-Supervised Domain Adaptation method for 3D object detection (SSDA3D) that employs an Inter-domain Point-CutMix module to align point cloud distributions across domains and an Intra-domain Point-MixUp for enhancing model generalization on unlabeled target data. Table 5 summarizes and compares the above-discussed studies based on several aspects. This comparison underscores the dynamic evolution of semi-supervised DTL techniques in handling 3DPCs, which is pivotal for applications ranging from autonomous vehicles to environmental scanning and medical imaging. These advancements promise to drive significant improvements in how 3D data is processed and utilized across various fields.

3.5. Inductive transfer learning

In inductive transfer learning (ITL), usually SD and TD remain the same, however target task differs from the source task. In ITL setting, knowledge is transferred from source task to attain high performance in the target task. As

Table 5
Comparison of Studies on Semi-Supervised DTL in 3DPCs

Ref.	ML Model	Dataset	Application / Task	Advantage	Limitation
[201]	Semi-supervised 3D Object Detection	SUN-RGBD, KITTI	3D object detection from 2D and 3D labels	Efficiently transfers 3D info from strong to weak classes	Requires sufficient data in strong classes for effective transfer
[205]	Multimodal Semi-supervised Learning	ModelNet10, ModelNet40	3D classification and retrieval	Improves data efficiency using multimodal data consistency	Performance depends on the quality of multimodal data integration
[5]	SPCNet	Real tunnel point clouds	Multi-class object segmentation in tunnel scenes	Reduces reliance on labeled data, enhances segmentation performance	Specific to tunnel environments, may not generalize
[130]	DTL based Semantic Segmentation	KITTI, Ouster LiDAR-64	3D object detection in autonomous driving	Reduces need for large-scale datasets, fast processing	Limited by the initial data quality and transfer efficiency
[213]	Semi-Supervised Domain Adaptation (SSDA3D)	Waymo, nuScenes	3D object detection in diverse conditions	Adapts to new domains with minimal labeled data	Performance may degrade with severe domain shifts
[206]	DTL with PCT	SynLiDAR	3DPC segmentation	Bridges the gap between synthetic and real data, extensive dataset	Focuses on segmentation; may not directly apply to other 3D tasks
[202]	Semi-supervised or unsupervised feature-metric registration	N/A	Point cloud registration	Robust to noise and does not require correspondences; fast optimization	Limited details on specific dataset adaptability and real-world implementation
[203]	MS-SVConv and UDGE	3DMatch, ETH, TUM	3DPC registration	Generalizes across different datasets using unsupervised DTL	May require substantial computational resources; specific adaptation challenges not addressed
[207]	CNN-based classifier	Custom LiDAR dataset	Semantic segmentation of dynamic scenes	Combines few annotations with large constraint data for improved adaptability	Primarily tailored to dynamic scenes, may not generalize to static or varied environments
[208]	Spatio-Temporal Representation Learning (STRL)	Synthetic, indoor, outdoor datasets	3D scene understanding	Learns from unlabeled data; generalizes to multiple 3D tasks	Dependence on temporal correlation which may not be present in all datasets
[210]	DTL from 2D to 3D models	ScanNet	Semantic segmentation	Uses pseudo-labels for pre-training 3D models; enhances data efficiency	Relies on the quality and relevance of 2D model training to 3D tasks
[209]	Weakly supervised 3D object detection	KITTI	3D object detection	Reduces need for detailed annotations; uses unsupervised proposal generation	Performance may lag behind fully-supervised methods; adaptation to other datasets not detailed
[204]	Semi-supervised point cloud segmentation	N/A	Point cloud segmentation	Utilizes both labeled and unlabeled data; improves with self-training	Specifics on dataset and environmental adaptability are not detailed
[211]	Hierarchical point-based active learning	S3DIS, ScanNetV2	Point cloud semantic segmentation	Efficient use of very few labeled data; incorporates active learning	May require intricate setup for uncertainty measurement and point selection
[212]	Vision Transformer-based WSS3D	SUN RGBD, KITTI	3D object detection	Low reliance on fully labeled data; uses point annotations effectively	Challenges with varying detector compatibility and scene diversity

suggested in [214, 215], the target is labeled, whereas source may be labeled, unlabeled, or both. However, in the field of 3DPC, it is observed that only labeled source has been explored.

For instance, Chen et al. [141] focus on classifying soft-story buildings using CNNs and density features extracted from 3DPCs. More specifically, Once the 3DPC data of Santa Monica city is collected, density features are extracted and converted into 2D imagery data. The task of identifying a soft-story building is then approached as a binary classification problem, which has effectively been addressed using CNN models, including VGG, Inception, ResNet and Naive CNN. They have trained the SD with labeled settings exploiting more than 1.2 million images and 1,000 labeled categories, and surprisingly VGGNet has proved to be the best in 2014, with its different versions namely, VGG19 and VGG16. In addition to this, 138 million parameters are trained in the network. VGGNet uses 3 x 3 filters, contrary to this, Inception uses 1 x 1 filters, limiting the number of input channels. Hence, the trainable parameters for Inception is low, approximately 6.4 million trainable parameters. In another work, Murtiyoso et al. [129], have taken advantage of DeepLabv3+ network which they trained on labeled dataset of building façade images. The trained

network is deployed on TD, 2D orthoimages received from photogrammetry. Similarly, a DL-based encoder-decoder lightweight neural architecture, RandLA-Net, for the semantic segmentation of 3DPC data, has been utilized in [140] for performing per-point segmentation of large-scale 3DPCs, as detailed in [216], and demonstrated a good semantic segmentation performance in the Semantic 3D benchmark [140, 217].

In [218], authors have exploited ITL for 3DPC classification using an airborne laser scanning method. They have extracted deep features using deep residual network, and CNN was dedicated to classification task. To exploit CNN further, the unevenly distributed 3DPC is transformed into voxels [219]. However, this transformation can lead to information redundancy as well as some feature loss. PointNet and later PointNet++ were proposed in [52] and [53], respectively. They successfully directly classify the original 3DPC, leading to the proliferation of PointNet-like approaches for 3DPC classification. However, classification accuracy is affected when small range of multi-view projection influence the detailed description on each 3D point. In addition, there is a need of huge computing time for generating feature maps.

Lie and his team [138] have used DensNet201 for obtaining deep features, and make use of an improved fully CNN by incorporating it into the ITL. The result was very promising and superior to state-of-the-art on ISPRS dataset for OA. In many cases weight transfer has found to be instrumental in classification performance. For instance, Kamil and Marian [142] has suggested weights transfer while they use ITL to improve the classification accuracy of bidirectional LSTM (BiLSTM)-based approach for identifying human activities. Similarly, Sun et al. [220] has incorporated deep ITL to explore the options for solving the issues that are encountered with SAE networks in the prediction of remaining useful life by utilizing weight and feature transfer.

For semantic labeling of heritage, Arnold et al. [133] has utilized ITL by considering geometric shape characteristic for the purpose of segmentation of memorial objects from the scene. Further, they pretrained CNN on a model from ModelNet's labeled dataset. Similarly, for body measurement of cattle, Huang et al. [221] have pretrained the Kd-network by obtaining 3D deep model's initial parameters from ShapeNet. The authors extracted the 3DPC spatial feature information which are transferred for identifying cattle body silhouette. In addition, their ITL method is applicable even if the data distribution is different for source and target data.

3.6. Transductive transfer learning

The transductive transfer learning (TTL) was introduced by Arnold et al. [222] to solve a task in which domains are different however the source and target tasks remain same. The authors advocate that at the training time, all unlabeled data must be available in the TD, contrary to this, Pan and Yang [215] urges that for finding out marginal probability, it would be enough to seeing part of the unlabeled target data at the training time.

Applying DTL for different domain encounters many issues. One of these issues for SDs and TDs is distribution mismatching. There are few works based on UDA methods that have been reported in the literature for the adaptation of a model to an unlabeled TD from a labeled SD for various different applications [177, 223–226]. In addition to UDA, authors in [143] has suggested source-free unsupervised DA (SFUDA). They have used virtual domain modeling to address of one the most talked issue in SFUDA without requiring original source, reducing source and task data mismatching. To fill the gap between SD and TD distributions, they have introduced an intermediate virtual domain, reducing the distribution mismatch into two steps, minimizing the domain gap between SD and virtual domains and then between the virtual and TDs. To achieve this goal, the authors have generated the virtual domain samples in the feature space using an approximated Gaussian mixture model (GMM) and the pretrained source model, so that the virtual domain maintains a similar distribution to the SD without access to the original source data. On the other hand, they have proposed an effective distribution alignment method that gradually improves the compactness of the TD distribution through model learning to reduce the aforementioned distribution gap. However, the first SFUDA framework was proposed in [197], where the authors exploited the source model to fine-tune the TD data without access to the source data for 3D object detection. The paper [116] discussed the use of SSL to learn useful representations from unlabeled data in DA for 3D perception problems. The authors proposed a new family of pretext tasks employing SSL for DA on point clouds, called deformation reconstruction, along with a novel training procedure called point cloud mixup (PCM) for labeled point cloud data. The results demonstrated that employing SSL with this technique significantly improves classification and segmentation in DA datasets.

As the research on DA for 3DPC is evolving, researchers are working to improve the method to reduce the SD' differences from TD, and to maximize the domain adaptability so that it can be generalized. However, most of the research addresses DA through experimentation over different domain meant for different but related task. Table 6 summarizes some of the relevant studies, compares their characteristics and identifies their pros and cons.

The works [227, 228] require handling preprocessing tasks and additional data, which in turn increases complexity. Rist et al. [227] exploit cross-sensor DA via 3D voxels, while Wang et al. [228] utilize adversarial networks for global adaptation by exploiting cross-range adaptation. In this context, the authors in [229] present a potentially significant contribution. Their approach circumvents complex procedures and the need for additional data. Instead, they leverage the KITTI benchmark dataset to align strong-weak features and enhance feature representation, supplementing it with available data when necessary. Specifically, they focus on the 'car' example from the benchmark dataset, considering 'near-range' and 'far-range' objects as the SD and TD, respectively. In addition to the underlying issues in handling different domain for DA problems, distribution mismatch within a domain has also been raised by researchers. In this regard, to adapt the different scenario within a single domain, Zhang et al. [230] have taken the advantage of cross-dataset and considered several adaptation scenario like day-night adaptation and adaptation of different scenes (say, from different places) as in the case with nuScenes dataset consisting of driving scenes from different geographical locations, Boston and Singapore. Their extensive experiments enable understanding how researchers can leverage cross-datasets for UDA. Moreover, they have introduced range-aware and scale-aware detection mechanism for 3DPC tasks. In the similar direction, Jaritz et al. [196] has considered the same scenario, i.e., day-night adaptation and Boston-Singapore scenario, however they have primarily focused on cross-modality adaptation using their xMUDA model. By the virtue of their proposed method, they have shown a better performance can be achieved for cross-modality. Moreover, A2D2 and Semantic KITTI datasets were used as source and target respectively. Moving forward, Nunes et al. [231] present a new contrastive learning approach for representation learning of 3DPs point cloud data in the context of autonomous driving. The approach extracts class-agnostic segments and applies contrastive loss to discriminate between similar and dissimilar structures. The method is applied on data recorded with a 3D LiDAR and achieves competitive performance in comparison to other self-supervised contrastive point cloud methods. Fig. 10 presents an example of fine-tuning in 3DPC segmentation [196].

A UDA-based semantic labeling scheme of 3DPCs is proposed in [157], where domain discrepancies induced by different LiDAR sensors have been addressed. Typically, a complete and label technique that recovers 3D surfaces is developed before passing them to a segmentation network. More precisely, a SVCN to complete the 3D surfaces of a sparse 3DPC is designed. By contrast to semantic labeling, obtaining training pairs for SVCN does not require any manual labeling. Moreover, local adversarial learning has been introduced for modeling the surface priors. The recovered 3D surfaces serve as a canonical domain, from which semantic labels can transfer across different LiDAR sensors.

Table 6: A summary of unsupervised DA frameworks and their characteristics used in 3DPC understanding.

Work	SD	TD	ML model	SoDTs	SoDDs	Pros and cons
[116]	PointSegDA	PointSegDA	DefRec	S	D	The first study of SSL for DA on 3DPCs.
[142]	UTD-MHAD	UTD-MHAD	N/A	S	S	Computationally efficient and enable human activity detection using depth maps
[143]	ModelNet40	ShapeNet	VDM-DA	S	D	Enable virtual domain modeling for source data-free DA.
[155]	GTA-LiDAR	KITTI	SqueezesegV2	S	D	Enhance model structure and UDA for road-object segmentation.
[156]	Semantic (KITTI, POSS, USL)	Semantic (KITTI, POSS, USL)	LiDARNet	S	D	Preserve almost the same performance on the SD after adaptation and achieve 8%-22% mIoU performance increase in the TD.
[157]	Waymo	KITTI; nuScenes	SVCN	S	D	Provide 8.2-36.6% better performance than previous DA methods.
[158]	pointDA-10	pointDA-10	pointDAN	S	S	3DPC representation using a multi-scale 3D DA network.
[195]	Waymo	KITTI, nuSenses, Lyft	ST3D	S	D	Exceed fully supervised results on KITTI 3D object detection benchmark.
[197]	nuScenes	KITTI	SF-UDA	S	D	Enable SFUDA but requires to be tested beyond cars, to detect other types of objects.
[198]	PointDA-10; ScanObjectNN	ShapeNet, ModelNet40, ScanNet, ScanObjectNN	RefRec	S	D	Refine pseudolabels, offline and online, by leveraging shape descriptors learned to solve shape reconstruction on both domains
[228]	KITTI	nuScenes	CrAF	S	D	Conduct more challenging cross-device adaptation.
[230]	PreSIL; nuScenes	KITTI; nuScenes	SRDAN	S	D	Demonstrate the significance of geometric characteristics for cross-dataset 3D object detection.

Table 6 (Continue)

Work	SD	TD	ML model	SoDTs	SoDDs	Pros and cons
[232]	labeled data, VirtualKITTI	Semantic KITTI	CLDA	D	D	Improve segmentation performance for rare classes but still needs more enhancement.
[233]	PointDA-10	PointDA-10	BADM; PointDA-10	S	S	Achieve state-of-the-art performance and outperform other 3D DA techniques but not appropriate for different tasks or different domains.
[234]	bSSFP-MRI; MM-WHS	LGE-MRI; MRI and CT	UDA-GAN	D	D	Provide promising performance, compared to the state-of-the-art.
[235]	Video data	LiDAR	PALMAR	S	D	63% improvement of multi-person Tracking than state-of-the-art frameworks while maintaining efficient computation on the edge devices.
[236]	KITTI object; near-range	KITTI object; far-range	SCNET	S	S	Achieve a remarkable improvement in the adaptation capabilities but without enable knowledge transfer to different tasks.
[237]	GTA-V	Oxford Robot-Car	vLPD-Net R; vLPD-Net V	S	D	Achieve state-of-the-art performance on the real-world Oxford Robot-Car dataset but the investigation of the loop closure and re-localization in real-world is needed.
[238]	CadData	CamData	DANN; SSLPC; PoinDAN	S	D	Less time-consuming for implementation in production.
[239]	PointDA-10	PointDA-10	DSDAN	S	S	Exceed the state-of-the-art performance of cross-dataset 3DPC recognition tasks.
[240]	High resolution LiDar data	Low resolution LiDar data	LAMAR	S	D	94% Human activity recognition performance in multiple-inhabitant scenario.
[241]	A2D2	Semantic KITTI	xMUDA	S	D	Enable cross-modal learning DA (CLDA) in 3D semantic segmentation; however, knowledge cannot be transferred across different tasks.
[242]	KITTI	MDLS	CycleGAN; YOLOv3	S	D	Outperformed other compared baseline approaches with more than 39% improvement in F1-Measure score.

Abbreviations: Same or different tasks (SoDTs); Same or different domains (SoDDs); Different (D); Same(S).

4. Applications of TL-based 3DPCs

TL-based 3DPC can be applied in various applications, including robotics and autonomous systems, augmented reality and virtual reality, medical imaging, geo-spatial data analysis, industrial inspection, building information modeling, etc. In this section, we focus on some of the main applications that attract increasing research effort. Table 7 summarizes some of the pertinent DTL-based 3DPC frameworks proposed to perform different tasks.

4.1. Semantic labeling and segmentation

Semantic labeling of 3DPC is crucial for performing segmentation tasks to represent scans accurately, using manual as well as automatic labeling. For instance, recently, Xie et al. [117] have used the Stanford large-scale 3D indoor spaces (S3DIS) dataset for transferring knowledge to the target dataset. However, it contains a much smaller repository as compared to source dataset (ScanNet), and manual semantic labeling has been done with 13 categories. Arnold et al. [133] used simple MLP to learn the diversity of the feature space and acquire knowledge for semantic labeling.

One of the prime concerns is to identify similar labels and different data from the same labels separately. To address this, authors [243] have suggested a domain-independent approach for semantic labeling. Their proposed model considers similarity metrics as features to infer the correct semantic labels and learns a similarity function to identify if attributes have the same labels. Because the matching function is unrelated to specific labels, their model does not depend upon the label and thus are independent of domain ontologies. A similar approach for bridge 3DPC has been suggested in [244]. The authors have received an improved IoU with 94.29%.

The ability of DTL to reduce the need for large-scale dataset can be economical and hence can be exploited in 3DPC tasks for performing accurately without requiring more extensive data. For example, with the help of DTL, authors in [245] have explored the analogy between real and synthetic data for semantic segmentation and tried reducing their gap. Based on deep CNN (DCNN), authors in [246] have suggested a weakly-supervised semantic segmentation technique. Unlike others, they have considered auxiliary segmentation annotations for distinct categories to guide segmentation on pictures with only image-level class labels. They have used a decoupled encoder-decoder architecture with an attention model allowing segmentation knowledge to be transferable across categories.

Semantic segmentation is conducted in [206] by transferring knowledge from synthetic to real LiDAR 3DPCs. Typically, a large-scale synthetic LiDAR dataset, is first collected from multiple virtual environments with rich

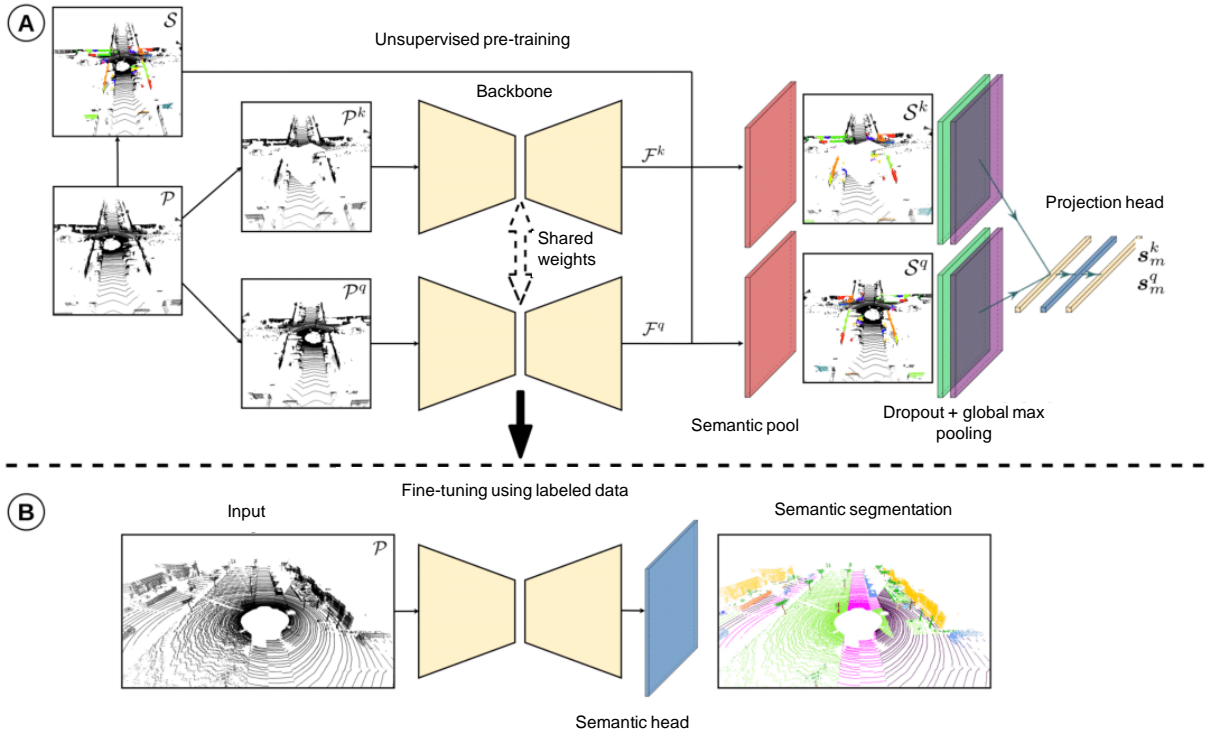


Figure 10: Example of using fine-tuning in 3DPC segmentation: (A) Data augmentation is used to generate the augmented views \mathcal{P}^q and \mathcal{P}^k from a point cloud \mathcal{P} , and class-agnostic segments \mathcal{S} are extracted from \mathcal{P} . The augmented segments \mathcal{S}^q and \mathcal{S}^k are determined with their point-wise features using the point indexes of \mathcal{S} extracted from \mathcal{P} . Point-wise features \mathcal{F}^q and \mathcal{F}^k are computed, followed by dropout and global max pooling over each segment. The segment feature vectors are projected using the projection head to obtain the final features \mathbf{s}_m^q and \mathbf{s}_m^k from the M segments, and the contrastive loss is computed, and (B) The pre-trained backbone is fine-tuned for the downstream task, i.e., semantic segmentation [231].

layouts and scenes. It includes point-wise labeled 3DPCs with accurate geometric shapes and comprehensive semantic classes. Moving on, a 3DPC translator (PCT) is designed to mitigate the discrepancy between real and synthetic 3DPCs. Typically, the synthetic-to-real discrepancy is decomposed into a sparsity and an appearance component before separately handling them. Fig. 11 explains the PCT approach adopted in [206], disentangling 3DPC translation into appearance and sparsity translation tasks. Accordingly, dense 3DPCs having similar appearances are first learned within the appearance translation. The sparsity translation then learns real sparsity distribution in 2D space and fuses it with the reconstructed 3DPC in 3D space. Then, real sparsity distributions in 2D space are learned within the sparsity translation before being fused with the reconstructed 3DPC in 3D space.

Moving forward, A. Murtiyoso et al. [129] has used DTL on a photogrammetric orthoimage by exploiting labeled and rectified images of building facades for training neural networks on them. Next, they allow the transition from 2D orthoimage to 3DPC by another program. With their promising results for photogrammetric data, their proposed work is a potential option to assist in automatic 3DPC semantic segmentation. Similarly, authors in [171] have claimed that semantic segmentation can perform equally competently to the latest ML approaches in modeling cultural heritage.

On the other hand, 3DPC instance segmentation is equally employed for many applications. For example, in [131], authors have taken a problem of height detection of a catenary conductor. For 3DPC instance segmentation, they have incorporated DTL and 3D-BoNet model with a multiscale grouping (MSG) structure on a smaller dataset, with loss curve converging better for their model. In addition to its applications in building, tunneling, and construction, DTL for 3DPC segmentation has found utility in robotics. Specifically, it is utilized for automatic toolpath generation to enable tasks such as masking, deburring, and polishing in various industrial applications. Z. Xie and his team [137] have utilized 3DPC segmentation and classification to extract the object features. Furthermore, they have exploited DTL to

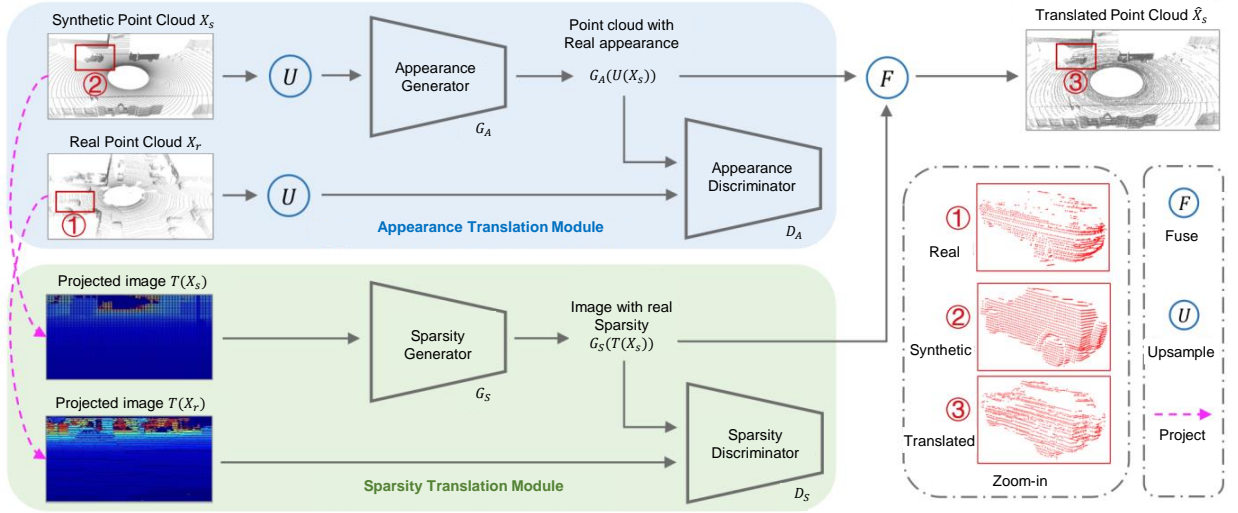


Figure 11: The PCT method separates the task of translating 3DPC into two parts: appearance translation and sparsity translation. Using synthetic 3DPC as input, the appearance translation learns to create dense 3DPC that look similar to real ones. The sparsity translation then learns the typical sparsity patterns found in real 2D point clouds, and combines these patterns with the dense 3DPC in 3D space. The end result is a 3DPC that looks and is sparse similarly to real 3DPC.

enhance performance and avoid investing much time in training data. Their toolpath recommendation automatically suggests patterns to choose from and does not require manual efforts. To identify human activities, authors [142] have carried out segmentation to separate the human figure from the background so that the descriptor can only be determined for a human figure.

4.2. Classification

3DPC classification is the process of classifying the features of 3D objects and categorizing the classes to which they belong. The 3DPC segmentation types and classification are illustrated in Fig. 12. In the diagram, it is shown how a building, with the help of CNN, can be classified based on different classifications e.g., concerning time (period), region, and structure. Recently, researchers have explored different ways of directly classifying 3DPC, mainly to avoid information loss during the conversion of 3DPC into non-3DPC. Automated classification of point cloud data has great potential for various applications, but a limited number of labelled points can lead to overfitting and poor generalization in ML models.

One of the pioneered works in the field is done by Qi et al. [52], reported being the first DL model to classify the original 3DPC directly. Their PointNet model is based on CNN, and its success has attracted many works to follow their proposed architecture. CNN has been widely used for classification tasks. For example, authors [129] have used CNN with DTL to classify improved fisher vectors used to represent 3DPC. The work [247] introduces a method called Atrous XCRF that induces controlled noise by invoking conditional random field similarity penalties using nearby features to improve generalization. The method achieves high OA and F1 score in a benchmark study using the ISPRS 3D labeling dataset and is on par with the current best model. Using DTL with Bergen 2018 dataset shows improvement in accuracy, but more work is needed to address generalization issues in DA and DTL. To overcome the requirement of large dataset, Lei et al. [138] have proposed a 3DPC classification method that integrates an improved CNN into DTL. They have used the DensNet201 model as a pretrained model for finding deep features able to accurately characterize the object. In addition, The authors [218] have proposed an ALS 3DPC classification method based on DTL using CNN. In [138], an ALS 3DPC classification approach for integrating an enhanced fully-CNN into DTL with multi-view and multiscale and deep features is proposed. Typically, the shallow features of the ALS 3DPC, such as height, intensity, and curvature change, are extracted to generate feature maps by multiscale voxel and multi-view projection. Second, these feature maps are fed into the pretrained DenseNet201 model to derive deep features. Experimental results show that OA and the average F1 scores obtained by the proposed method are 89.84% and 83.62%, respectively.

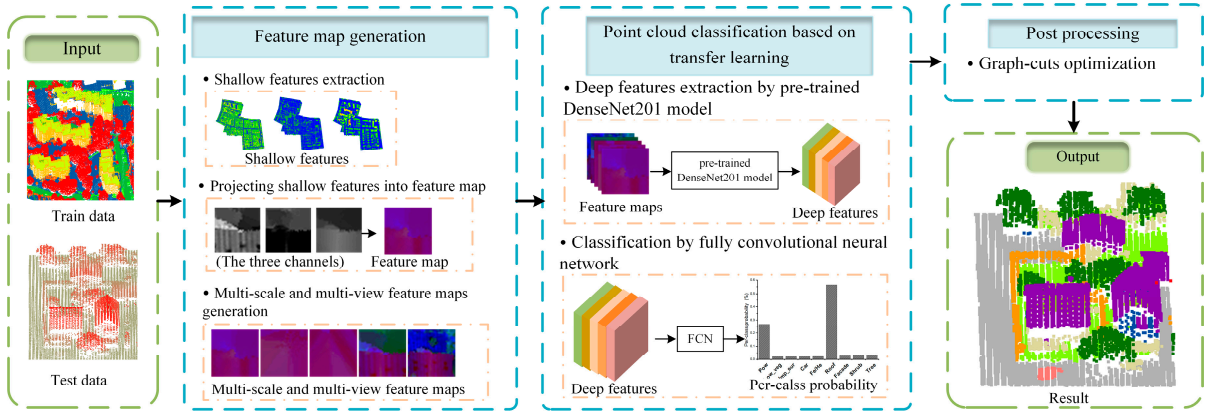


Figure 12: The flow chart of the proposed classification method.

4.3. Point-set registration

With the increasing number of 3D sensors and 3D data production, consolidating overlapping 3DPCs, which is called registration, has become a significant issue in many applications [248]. Registration can be used online (e.g., in a LiDAR SLAM pipeline for loop closure detection) or offline (e.g., in 3D reconstructions of RGB-D indoor scenes [249] or for outdoor LiDAR map building for autonomous vehicles). However, 3DPC registration can be challenging with real-world scans because of noise, incomplete 3D scans, outliers, etc. There are numerous existing approaches to this issue; however, recently, DL approaches have become very popular, especially for learning descriptors and computing transformations. These data-driven approaches, especially those that involve learning on large datasets with the ground truth pose as supervision, have effectively solved registration problems [237, 250]. Specifically, in [237], a registration-aided DA model for 3DPC-based place recognition is developed, called vLPD-Net. The method utilizes virtual large-scale point cloud descriptors and a structure-aware registration network, along with adversarial training, to minimize the gap between synthetic and real-world domains.

4.4. Scene understanding

The method proposed by Xu et al. [82] uses DTL technique by inflating weights to transform an image-pretrained model into a 3DPC model. Authors in [251] have proposed a model 'Shape Self-Correction' for 3DPC analysis where they have explored how unlabeled data can be utilized for a better 3DPC understanding. In addition, their approach can identify distorted points and automatically correct them by producing state-of-the-art results. Moreover, this model can be used as a pretrained model to be fine-tuned for related tasks. Going forward, Zhang et al. [252] also tried to exploit a pretrained large-scale 2D dataset to generalize it to 3DPC understanding using a contrastive vision-language pretraining (CLIP). Their model, PointCLIP, projects 3DPC into multi-view depth maps by encoding it, and successfully, view-wise zeroshot prediction is aggregated to transfer knowledge from 2D to 3D. Furthermore, many works exploit unsupervised approaches for 3DPC understanding. For example, Xie et al. [117] have suggested an unsupervised pretraining framework. To avoid the domain gap and utilize their approach across the different domains in the real world, they have directly made use of a complex network to pretrain the model. The major contribution they have is the examination of the transferability of learned representations generalization across the domain for 3DPC understanding. In addition, their architecture can also represent point-level information by capturing local features. To further exploit the geometric structure of the 3DPC and relationships of local features, Liu et al. [253] have suggested a convolution-based geometric-aware approach. Moreover, they proposed a filtering mechanism that identifies noise and outliers for a high-level understanding.

4.5. Object detection and denoising

The exploitation of DTL for various applications of 3DPC in 3D object detection and recognition has recently attracted researchers, ranging from medical science to biological research and robotics. For instance, authors in [145]

have used DTL for protein structure indexing using 3DPC. The suggested approach saves training time by fine-tuning the pretrained network, using Euclidean distance to extract shape-matching, with generic 3D objects. Furthermore, authors in [131] have proposed a detection method incorporating instance segmentation and DTL for overhead catenary height detection of a tunnel using a 3D 3DPC tunnel dataset. To recognize human activities, Sidor et al. [142] have suggested an approach by transforming depth maps into 3DPC. The authors have used DTL combined with multiple networks to improve the classification mechanism based on BiLSTM. In [143], 3DPC semantic segmentation based on DTL is used for 3D object detection. The advantage of this method is that it reduces large-scale training datasets requirement, and consequently, the training duration is reduced as DTL exploits knowledge from prior classification tasks, aiding object detection after preprocessing, thereby promoting cross-task generalization.

Denoising is an important 3DPC task to remove noise usually found in acquiring images from scanning devices. These noises can influence many downstream tasks such as segmentation, detection, reconstruction and classification, etc. To remove these noises at different scales of 3DPC data, several algorithms have been suggested. The first DTL-based 3DPC denoising scheme was proposed in [254]. It involved denoising patches of points by projecting them onto a learned local frame and repositioning the points onto the surface using a CNN. Some interesting 3DPC denoising approaches include score-based 3DPC denoising [255], graph Laplacian regularization [256], bipartite graph approximation and total variation [257], weighted multi-projection [258], and feature graph learning [259], etc.

4.6. Upsampling and downsampling

Point clouds obtained through 3D scanning are often incomplete, unevenly distributed, and corrupted by noise. Upsampling, on the other hand, involves generating a dense set of points that not only restores uniformity and proximity to the surface but can also address small gaps in the data, all through a single network. For instance, authors have proposed Segnet [260], and they designed decoder to upsamples their input feature map(s) having lower resolution enabling non-linear upsampling to produce dense feature maps. In a similar way, Eltner et al. [261] have used an encoder that extracts a low-resolution activation map while the decoder upsamples it to obtain a pixel-wise classification. More recently, an upsampling method for 3DPC to reduce human annotation cost is presented in [262]. They relied solely on the upsampling operation to perform effective feature learning of 3DPCs. Similarly, Imad et al. [130] have added more convolutional layers to the decoder stage, which has been coupled with upsampling layers to increase the size of the spatial tensor and generate high-resolution segmentation outputs.

Down-sampling point clouds refers to the process of reducing the number of points contained within them. This is commonly done to decrease the processing time required, or to select a specific number of points for use in training, among other purposes. Moreover, downsampling is also used to transform 3DPC into 2D representations. Typically, in [263], a 2D scene modelling method is described that effectively and meaningfully transforms the 3D data to a 2.5D representation and then to a 2D grid map. In addition to this, downsampling has been used in 3D data processing to remove the noise. For example, [264] have used growing neural gas (GNG) based downsampling technique for noise removal. However, downsampling necessitates careful consideration of whether the points are significant for the output, so that all important points are passed to the next layer and not removed. To this end, critical points layer (CPL) has been proposed in [265], an adaptive downsampling layer that learns to downsize an unordered 3DPC while keeping the crucial (critical) points. Downsampling has also been used in building and automation, for instance, a downsampling technique to optimize Terrestrial laser scanning (TLS) dataset is suggested in [266].

Table 7: Summary of DTL-based 3DPC frameworks describing different tasks.

Ref.	MoN	Task/application	DTL	Limitations	Contribution/advantage/key point
[117]	ResNet-34, Pointcontrast	3DPC understanding	FT	Testing for generalizability across multiple datasets and verifying computational costs after applying DTL were not conducted.	transferability of learned representation in 3DPCs to high-level scene understanding.
[128]	UFF	Segmentation and classification	UDTL	they optimize the classifiers in a single stage, a multi-stage classifier that can reduce the redefined cost function could enhance the result.	Propose a learning system with an unsupervised feedforward feature (UFF) by incorporating encoder-decoder architecture.
[129]	DeepLabv3+	Semantic segmentation	ITL	Due to the terrestrial nature of the data acquisition, several parts of the orthophoto, notably blind spots were distorted by the orthorectification algorithm	An improved automated procedure for 3DPC semantic segmentation, especially for photogrammetric data.

Table 7 (Continue)

Ref.	MoN	Task/application	DTL	Limitations	Contribution/advantage/key point
[130]	AE	3DPC semantic segmentation for 3D object detection	ITL	The method does not work for raw 3DPCs.	A 3DPC is projected into a birds-eye-view by which the amount of annotated data and time required for training has been minimized
[131]	3D BoNet + MSG structure	3DPC instance segmentation	ITL	The proposed RKT method is costly	New tunnel dataset is generated for 3DPC segmentation.
[133]	ConvPoint network, MLP	3DPC segmentation for classification	ITL	Semantic interpretation of objects with fewer visual features is missing	automation of extraction and labeling of memorial objects from cultural heritage sites using 3DPC data.
[138]	DenseNet201	3DPC classification	TTL	Algorithms are not integrated efficiently, which makes the feature maps generation complex	This algorithm can quickly and accurately extract the features and reduce the effect of ground object size on classification results.
[140]	RandLA-Net	3DPC semantic segmentation	ITL	The SLAM algorithm is not efficient for indoor spaces, LiDAR can be located to a limited height only, which provides a minimal view for acquired data	Robot dog has been exploited for data acquisition instead of human which saves time and minimize the monetary efforts.
[141]	CNN	Classification	ITL	The 3DPC data is used instead of street-view images, which needs open space. Buildings with irregularities and reinforcing shapes can misclassify as soft-story buildings.	To accurately classify the soft-story building using CNN model pretrained with DTL
[142]	BiLSTM	Segmentation and classification	TTL	eigenvalue-based descriptors for human activity recognition and other state-of-the-art methods are not discussed	With the help of 3DPCs and VFH descriptor, human activities are recognized.
[143]	SFUDMA	Object recognition	UDA	The proposed Virtual Domain Modeling needs to be deployed for a variety of tasks.	They successfully achieve the goal of distribution alignment between the SD and TD by training deep networks without accessing the SD data
[144]	DenesNet-121	Depth estimation	ITL	Testing for generalizability across multiple datasets was not performed.	Depth and surface estimation with a higher resolution
[145]	GLT4IP, point-Net	Protein structure indexing	FT	The validation of real-time performance improvements through transfer learning was not conducted.	DTL based indexing of protein structures using 3DPCs
[146]	Endo-SfMLearner	Depth estimation	UTL	Unresolved aspects: enhancing data adaptability, resolving issues, integrating with segmentation, abnormality detection, and classification tasks for improved performance.	Presented a new dataset for endoscopy, "EndoSLAM"
[148]	GMM	Segmentation and classification	ITL	Further research into novel pretext tasks tailored specifically to the idiosyncrasies of 3D data has not been conducted.	For representation learning, the method does not require any procedure like transformation/data augmentation.
[149]	POCO	3D orientation, and classification	ITL	Orientation accuracy can be improved further	Experimentally shown how DTL can be used for a model to serve as a platform for 3D object's orientation representation.
[150]	YOLO	Object detection	ITL	Method heavily relies on LiDAR data only and may not be that beneficial for another domain of image dataset	Suggest a method efficient enough and compatible for any LiDARs, even containing a different number of channels. Moreover, they do not require a re-training step.
[151]	GoogleNet, AlexNet, VGG	Classification	ITL	verification of the degree of dependence of the DNN architecture on the characteristics of the mechanical system subject to degradation	representation of punch deformation with depth and normal vector maps (DNVMs) obtained from 3D scan 3DPCs
[221]	Kd-network	Shape classification, feature recognition	ITL	This method not applicable for any cattle and may produce heavy mistakes and significant errors for adult Qinghai yaks	Livestock can be observed without any physical involvement of human
[260]	Segnet	Upsampling	UDTL	This method needs to separate the roles between the optimizer and the model to achieve the desired outcome.	It is much smaller and can be trained end-to-end using stochastic gradient descent. It has been engineered to be effective for memory and processing time during inference.
[262]	UAE	upsampling	SSTL	The complexity increased with the double-head architecture. Additionally, mechanical systems with different geometry and material from the punch tool were not investigated.	It allows classification and segmentation tasks to benefit from pretrained models. And it reduces the human annotation cost.
[265]	CPL	downsampling	DA	The complexity of CP-Net is high, potentially leading to increased computation costs.	an adaptive downsampling layer that learns to downsize an unordered 3DPC while keeping the crucial (critical) points
[254]	PointProNets	denoising	S	The 3DPC data utilized in the method was created by adding random noise; hence it is ineffective for 3DPCs that were legitimately created using LiDAR.	The first TL based 3DPC denoising scheme.

Abbreviations: Unsupervised TL (UTL); supervised DTL (STL); self-supervised DTL (SSTL); supervised (S); upsampling auto-encoder (UAE); model or network (MoN); fine-tuning (FT).

4.7. Scene generation

3D point cloud scene generation or reconstruction is of paramount importance in various fields, including robotics, autonomous driving, virtual reality, and architecture. By capturing the precise three-dimensional coordinates of a scene, 3D point clouds provide a detailed and accurate representation of the environment. This capability is crucial for tasks such as object recognition, navigation, and interaction within a space, enabling robots and autonomous vehicles to perceive and understand their surroundings effectively. In architecture and construction, 3D reconstruction facilitates accurate modeling and analysis of structures, aiding in design, inspection, and renovation processes. Furthermore, in virtual reality and gaming, 3D point cloud generation enhances the realism and immersion of digital environments, providing users with a more engaging and interactive experience. The ability to create detailed and accurate 3D models from point clouds revolutionizes various industries by improving precision, efficiency, and safety in numerous applications.

The SGFormer study [267] introduces a Semantic Graph Transformer for point cloud-based 3D scene graph generation, addressing the limitations of graph convolutional networks (GCNs) by using Transformer layers for global information passing. The model includes graph embedding and semantic injection layers to enhance object visual features with linguistic knowledge from large-scale language models. Benchmarked on the 3DSSG dataset, SGFormer demonstrates significant improvements in relationship prediction over state-of-the-art methods. The Sat2Scene study [268] proposes a novel architecture for direct 3D scene generation from satellite imagery using diffusion models and neural rendering techniques. This method generates texture colors at the point level and transforms them into a scene representation for rendering arbitrary views, showing proficiency in generating photo-realistic street-view image sequences and cross-view urban scenes, validated through experiments on city-scale datasets.

The ART3D study [269] introduces a framework combining diffusion models and 3D Gaussian splatting for 3D artistic scene generation, utilizing depth information and initial artistic images to generate point cloud maps and enhance 3D scene consistency. ART3D shows superior performance in content and structural consistency metrics compared to existing methods. Liu et al. [16] propose a high-precision 3D building model generation method using multi-source 3D data fusion, achieving state-of-the-art performance in multi-source 3D data quality evaluation and large-scale, high-precision building model generation. Chung et al. [270] present LucidDreamer, a domain-free 3D scene generation pipeline leveraging large-scale diffusion-based generative models, producing highly detailed Gaussian splats and outperforming previous methods in reconstruction quality. The S2HGrasp study [271] explores generating human grasps from single-view scene point clouds, addressing challenges of incomplete object point clouds and scene points, showcasing strong generalization capabilities and effective grasp generation. Lastly, the SGRec3D study [272] presents a self-supervised pre-training method for 3D scene graph prediction, achieving significant improvements in 3D scene graph prediction with reduced labeled data requirements during fine-tuning, demonstrating state-of-the-art performance. In [273], Liu et al. introduce the Pyramid Discrete Diffusion model (PDD), a framework employing scale-varied diffusion models to generate high-quality large-scale 3D scenes. Using a coarse-to-fine paradigm, PDD addresses the complexity and size challenges of 3D scenery data, particularly for outdoor scenes. The model demonstrates effective generation capabilities and data compatibility, allowing easy fine-tuning across different datasets.

Table 8 compares various studies on 3D scene generation and reconstruction, highlighting key aspects such as models used, datasets, contributions, performance values, and limitations. The models range from SGFormer, utilizing a Semantic Graph Transformer, to MS3DQE-Net for multi-source 3D data fusion, and Pyramid Discrete Diffusion (PDD) for large-scale scene generation. Datasets include 3DSSG, city-scale datasets from satellite imagery, artistic images with depth information, and MLS 3D point clouds.

Each study offers unique contributions: SGFormer excels in relationship prediction, Sat2Scene integrates diffusion models for urban scenes, and ART3D bridges artistic and realistic images. MS3DQE-Net focuses on high-precision building models, LucidDreamer achieves domain-free scene generation, S2HGrasp generates human grasps from incomplete point clouds, and SGRec3D enhances 3D scene graph prediction. Performance metrics show significant improvements, such as 40.94% R@50 for SGFormer, FID of 71.98 for Sat2Scene, and PSNR of 34.24 for LucidDreamer. Limitations include over-smoothing in GCNs, handling significant view changes, and managing the complexity of 3D data. These challenges highlight areas for future research in 3D scene generation and reconstruction.

Table 8
Comparison of 3D Scene Generation/Reconstruction Studies

Ref.	Model(s) Used	Dataset/Data Type	Main Contribution	Best Performance Value	Limitation
[267]	SGFormer	3DSSG	Semantic Graph Transformer for 3D scene graph generation	40.94% R@50, 88.36% boost in complex scenes	Over-smoothing in GCNs
[268]	Diffusion Models, Neural Rendering	City-scale datasets, satellite imagery	Direct 3D scene generation from satellite imagery	FID: 71.98, KID: 5.91	Handling significant view changes and scene scale
[269]	Diffusion Models, 3D Gaussian Splatting	Artistic images, depth information	3D artistic scene generation	PSNR: 24.041, SSIM: 0.863, LPIPS: 0.214	Bridging artistic and realistic images
[16]	MS3DQE-Net, Deep Learning	MLS 3D point clouds, 3D mesh data	High-precision 3D building model generation	State-of-the-art performance in data quality evaluation	Balancing local accuracy and overall integrity
[270]	Diffusion-based Generative Model	Various datasets, VR content	Domain-free 3D scene generation	PSNR: 34.24, SSIM: 0.9781, LPIPS: 0.0164	Limited by training on 3D scan datasets
[271]	S2HGrasp (Global Perception, Diffu-Grasp)	S2HGD dataset, single-view scene point clouds	Generating human grasps from single-view point clouds	Contact Ratio: 99.41%, Volume: 6.58cm ³	Handling incomplete object point clouds
[272]	SGRec3D	Various 3D scene understanding datasets	Self-supervised pre-training for 3D scene graph prediction	+10% on object prediction, +4% on relationship prediction	Requires object-level and relationship labels
[273]	Pyramid Discrete Diffusion (PDD)	Large-scale 3D scenes, outdoor scenes	Coarse-to-fine 3D scene generation	mIoU: 68.0, MA: 85.7, F3D: 0.20	Complexity and size of 3D scenery data

5. Open Challenges

DTL and DA can be effective techniques for 3DPC understanding, but they also come with their own set of challenges. Typically, DL models require large amounts of labeled data to achieve high accuracy. However, in the case of 3DPC understanding, it can be challenging to obtain large amounts of labeled data due to the time-consuming and expensive process of manually annotating point clouds [274]. Additionally, 3DPC data can be highly variable in terms of size, shape, and orientation. This variability can make it challenging to develop DTL and DA models that can generalize well to new datasets [275, 276]. Moreover, DA is needed when the distribution of the source and TDs is different. In the context of 3DPC understanding, domain shift can occur due to changes in sensor modalities, lighting conditions, and other environmental factors. To that end, DA techniques must be used to adapt the model to the TD and prevent performance degradation. Moving on, 3DPC data can contain complex geometric structures, such as non-uniformly distributed points, non-planar surfaces, and varying levels of detail. These complexities can make it challenging to develop effective DL models that can accurately capture the structure and features of the data [274]. DTL and DA models can be computationally expensive, especially when dealing with large 3DPC datasets. This can limit their practical applicability and require specialized hardware to achieve acceptable performance [277, 278].

DA methods have shown significant improvements in various ML and CV tasks, such as classification, detection, and segmentation. However, to date, there are only a few methods that have been successful in applying DA directly to 3DPC data. The unique challenge in working with 3DPC data is its large amount of spatial geometric information, and the object's semantics which depend on the regional geometric structures. This means that general-purpose DA methods, which focus on global feature alignment and neglect local geometric information, are not effective for aligning 3D domains, as stated in [158].

5.1. The problem of negative transfer

Negative transfer refers to a situation when knowledge transfer can negatively influence the model's accuracy, possibly because the SD and TD are significantly different or they are supposed to perform different tasks [215]. Moreover, not taking adequate advantage of the relationship between the SD and TD can also lead to negative transfer [151]. In such situations, random and forced knowledge transfer without identifying the specific knowledge that can be useful and without considering "what", "when" and "how" to transfer can further propel negative transfer [37]. Hence, it can be inferred that high affinity among source and target tasks is of great importance for a successful DTL and to avoid the negative transfer. To this end, researchers have suggested clustering methods for tasks and identifying similar tasks by keeping them in the same cluster. In addition to this, an approach to group learning tasks together is suggested

in [279]. This approach enables what and when to transfer by identifying tasks within a group. Similarly, imbalanced training samples can increase negative transfer chances in a UDA scenario. For Example, for 3DPC representation, Qin et al. [158] have suggested a 3D DA network and have argued that for domain alignment, unique parts can induce negative transfer and hence covering standard features in 3D space can help to avoid the negative transfer. Furthermore, to address negative transfer while dealing with different domains/modalities for 3DPC, Gong et al. [280] have suggested a multi-SD adaptation and label unification approach. They have used attention-guided adversarial alignment for a strong distribution alignment between the SD and TD. Additionally, their proposed uncertainty maximization module limits the self-assured predictions for unlabeled samples in the SDs. To make their approach more promising, they have introduced a fusion module based on pseudo-labeling. Especially for unlabeled samples, they perform pseudo-labeling for the SDs and all samples in the TD.

5.2. The problem of overfitting

The established successful model, such as PointCNN and other DNN models, despite their widespread use and success for 3DPC tasks, still face some potential challenges, especially when the dataset available is relatively small. One possible reason for this is significant parameters, even in several million. It requires a large amount of data to fit this many parameters adequately. Since 3DPC data suffer from the scarcity of labeled data, this limitation makes 3DPC tasks prone to overfitting, and poor generalization [247].

Several mechanisms help in tackling the overfitting issue. For instance, [221] have used DTL on a Kd-network, they have frozen the weights of all network layers except the last fully connected layer, and only the fully connected layer is modified so that the gradients during backpropagation are not calculated, which can avoid the occurrence of overfitting and improve training efficiency [281]. Entropy minimization (EM), a regularization method, has also been suggested by [234] in addressing overfitting. EM helps improve generalization and, hence, robustness for preventing overfitting. Arief et al. proposed a solution to address the overfitting problem of PointCNN, a DNN-based model, by using the Atrous XCRF model, which is a combination of conditional random field (CRF) and recurrent neural network (RNN) [247]. DNN-based models such as PointCNN are highly susceptible to overfitting when the available dataset is relatively small, this is because of the large number of parameters in such models which requires a large number of training data. To tackle this problem, they introduced controlled noise during the training of a DNN-classifier, the method works by retraining a validated model using unlabeled test data. The training process is guided using the hierarchical structure of the CRF penalty procedure. With the proposed algorithm XCRF and addition of A-XCRF layer, they were able to improve the model's accuracy by utilizing the unlabelled data.

5.3. Domain discrepancies

Recently, UDA has gained a good deal of attraction by the research community, especially for various complex 3DPC tasks like semantic segmentation [140] and object recognition [143]. However, domain discrepancy exists due to the *domain shift* [282]; hence, it becomes difficult for a model to perform across domains accurately. Different solutions have been proposed to minimize the domain discrepancy for 3DPC tasks. To this end, DL methods based on the adversarial network, such as domain adversarial neural networks [18], have improved performance for UDA tasks. The primary job of bridging the domain gap is performed by introducing a generator that keeps fooling the discriminator until it identifies the discrepancies [238]. Moving forward, for classification purposes, a model is presented in [158] that focuses on aligning the local and global features. Similarly, for 3D segmentation on LiDAR sensors, authors in [155] have considered aligning activation correlation [282]. The out space alignment and entropy minimization has been integrated by the authors in [234] for addressing the above UDA issues. Domain discrepancies that can arise due to LiDAR sensors are handled by Yi et al. [157]. Accordingly, a SSL framework to improve UDA performance has been suggested in [116].

The proliferation in related research has paved the way for an increased interest in domain-invariant representations (DiR). The primary aim of the DiR is to facilitate a way that there should be insignificant discrepancies for features coming from different domains. To this end, Jaritz et al. [241] have leveraged the cross-modal discrepancies while preserving the best performance of each sensor from self-driving data from cameras and LiDAR 3DPC sensors because domain gaps are different for different sensors. For example, comparing a LiDAR and a camera, the former is more robust to lighting changes with respect to the latter. Whereas there are always dense images that come as output from a camera while LiDAR sensing density is proportional to the sensor setup. Notably, 'cross-modality' differ from multi-modal fusion [241] as multi-modal implies training a single model in a supervised way for combining inputs like LiDAR and camera [283], RGB-D [284], etc. This cross-modality DiR can help avoid the limitations of UDA across

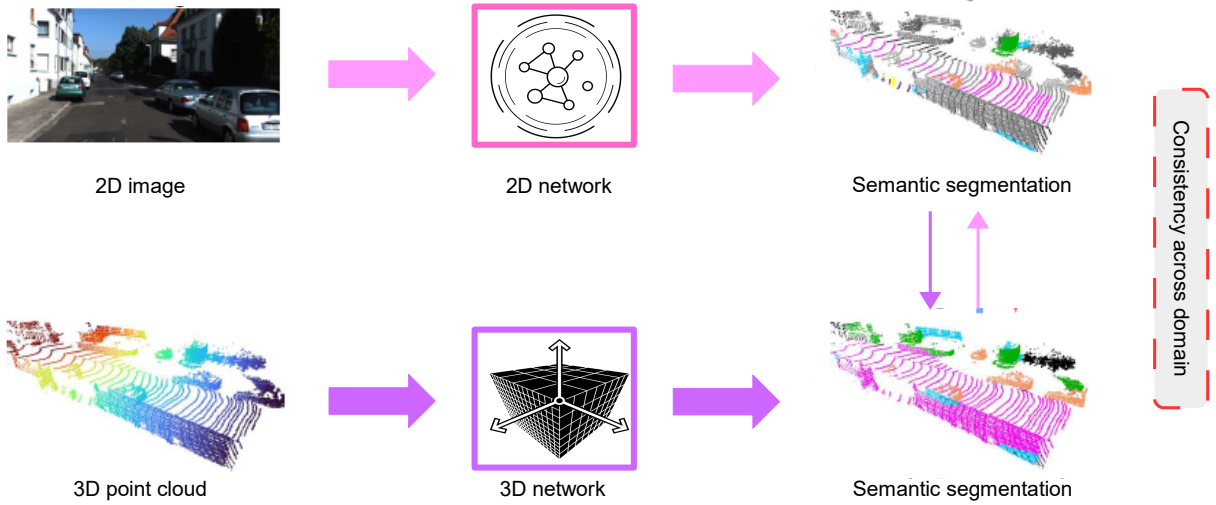


Figure 13: The CLDA proposed in [241], where consistency has been ensured through mutual mimicking.

modalities in which one modality influences the performance of the other modality in a negative way. In Fig. 13, an overview of CLDA is presented. Here, a prediction of 3D segmentation labels is performed through 2D and a 3D network by providing an image and a 3DPC as input to this network. 3D predictions are converted to 3D while consistency is ensured through mutual mimicking. This approach is proved to be advantageous for UDA.

5.4. Reproducibility of scientific results

Despite the growing interest in using DTL for various energy applications, there are still several factors that hinder the widespread adoption of DTL-based models and impact reproducibility, and the ability to compare DTL-based solutions. Firstly, it is difficult to evaluate the generality of DTL models as most of the frameworks are evaluated on datasets collected under similar conditions, such as the same climate [285]. Secondly, there is a lack of consistency in using the same datasets and benchmarks to validate new DTL models, due to the limited availability of open-source, benchmarked datasets [286]. Finally, different metrics and parameter settings have been used to measure the distance between the source and TDs and evaluate the performance of DTL-based solutions on different datasets. This makes it challenging, and even impossible, to compare DTL techniques uniformly [287]. Despite that, there are some studies already uploaded on GitHub and other online platforms to facilitate the reproducibility and comparison tasks; the effort put in this direction still needs to consider the challenges introduced by DTL for 3DPCs.

5.5. Measuring knowledge gains

Assessing the knowledge gained when using DTL models for specific tasks is crucial, yet this challenge has not been fully addressed in the literature. Bengio et al. in [288] proposed four measures, transfer error, transfer loss, transfer ratio, and in-domain ratio, to quantify the gain of knowledge in DTL. However, it is unclear how these measures would perform with other DTL-based methods, particularly in the energy sector, where the class sets are different between problems. Moreover, these measures can lead to non-definite performance evaluations if a perfect baseline model is achieved. To address these issues, simpler measures such as accuracy, F1 score, MSE, RMSE, MAE, performance improvement ratio (PIR) or other statistically-inspired coefficients have been widely used to evaluate DTL-based solutions in the energy sector. These measures provide additional information, such as class agreement, and are better suited to the specific requirements of the energy sector.

5.6. Unification of DTL

The evolution of DTL in energy applications has been rapid and innovative but also rather fragmented. This is due to the range of unique mathematical formulations utilized to delineate DTL algorithms. Numerous researchers have developed and proposed various versions of DTL, each bearing its unique label and implementation approach.

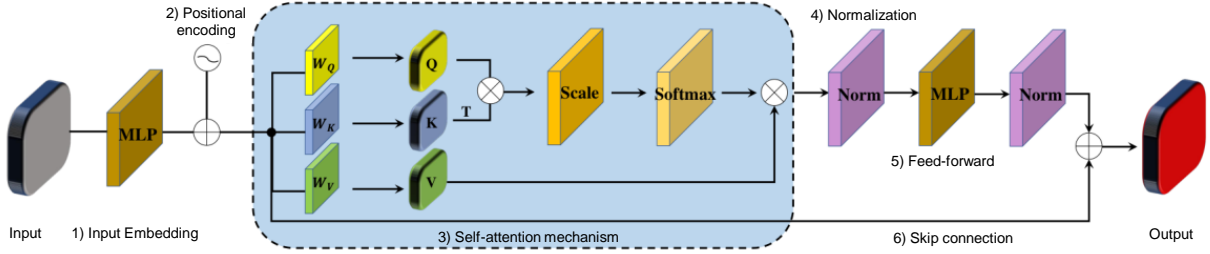


Figure 14: Example of a Transformer's encoder architecture.

Examples of these include "Heterogeneous DTL" as proposed in [289], "Statistical investigations" in [290], and "DA-DTL" in [291]. This multiplicity of terms and methods can often lead to confusion among scholars in the field. It is clear that there is a pressing need to homogenize the terminologies and conceptual underpinnings of DTL to foster better comprehension and collaboration within the research community. A seminal step towards this unification was taken in [292], laying a foundation upon which future studies can build. However, the exploration remains incomplete with respect to 3DPC applications in particular.

The unification of DTL concepts entails collating, comparing, and reconciling the differing methodologies, with an ultimate aim to develop a more cohesive and comprehensive framework. A unified approach would facilitate the application of DTL in 3DPC applications by standardizing algorithm descriptions, mitigating confusion, and making it easier for researchers to implement, adapt, and build upon existing algorithms. This, in turn, would expedite the progression of DTL-based solutions, thereby accelerating advancements in the realm of energy applications. Therefore, it is paramount to expand the unification efforts initiated in [292] to include 3DPC applications. Future research endeavors should prioritize developing a harmonized approach that accommodates the diverse range of DTL methodologies while also meeting the specific needs of 3DPC applications. This would not only streamline the use of DTL in the field but also pave the way for more innovative developments in energy applications.

6. Future Research directions

6.1. 3DPC Transformers

Transformer models have greatly improved NLP [293] and CV, but their application in 3DPC processing remains uncertain. Questions remain about their ability to handle irregular and unordered data in 3D, their suitability for different 3D representations and their competence in various 3D processing tasks. Fig. 14 illustrates an example of a Transformer encoder architecture.

One important challenge when using transformers is that they require large amounts of training data. In the field of 3DPC, obtaining large datasets is a challenge and this makes training Transformers for 3D tasks difficult. The authors in [294] have investigated the use of knowledge from multiple images for 3DPC understanding. They proposed a pipeline called *Pix4Point* that allows for utilizing pretrained Transformers in the image domain to improve downstream 3DPC tasks. This is achieved by using a modality-agnostic pure Transformer backbone with tokenizer and decoder layers specialized in the 3D domain. Another model named "Point-BERT" which is based on BERT's architecture [295] to learn Transformers for generalizing the idea of BERT to 3DPC is proposed in [119]. Point-BERT is trained using a masked point modeling task. The pipeline of Point-BERT is illustrated in Fig. 15, where the input 3DPC is first partitioned into several point patches.

6.2. Further generalization

Enhancing the generalization capabilities of DTL algorithms for 3DPC understanding involves some unique challenges and strategies due to the distinctive nature of 3D data. For instance, data augmentation techniques for 3D data can be more complex than for images or text. Techniques could include rotations, translations, adding Gaussian noise, or mirroring the point cloud along a plane. This would create a more diverse training dataset and can help the model generalize better. In order to reduce the domain shift between the source and target task, techniques such

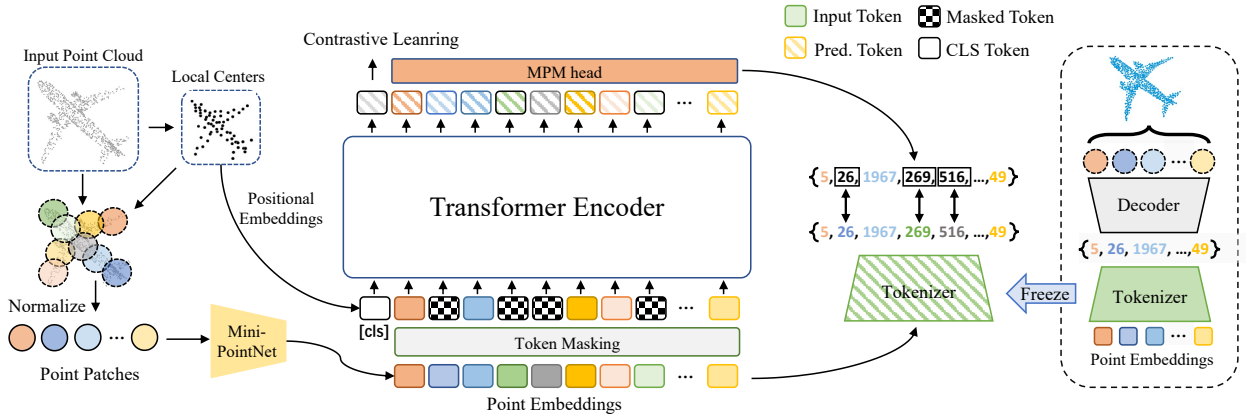


Figure 15: An illustration of CNN based DTL for 3DPC segmentation and its types

as feature alignment can be used. This involves minimizing the difference between the distributions of the source and target features. Moreover, utilizing architectures that maintain geometric invariance can be helpful as 3DPC data can be rotated or scaled. Networks, such as PointNet or PointNet++ which are invariant to permutations and transformations of the input points can be utilized. Additionally, methods such as PointNet++ use hierarchical neural networks to capture local structures induced by the metric space points live in, and also model global structures. This can help with generalization as it learns at different scales. Moving on, regularization methods such as dropout or weight decay can be implemented to prevent overfitting and ensure the model generalizes better. Lastly, designing loss functions that better capture the properties of 3D data can also help with generalization.

6.3. Multi-task learning

6.3.1. Segmentation and Detection

This section focuses on frameworks that handle multiple tasks like segmentation, detection, and sometimes additional tasks like classification or instance identification within point clouds. Typically, Pham et al. 2019 [296] and Zou et al. 2022 [297] both explore multi-task learning frameworks that handle segmentation and classification simultaneously. Pham et al. focus on combining semantic and instance segmentation, while Zou et al. integrate classification and segmentation tasks to enhance each other, utilizing a Y-shaped graph neural network. Moving on, Chen et al. 2022 [298] propose a method for joint semantic and instance segmentation using a shared encoder and dual decoders, focusing on enhancing feature representation through cross-task interactions. Similarly, Ye et al. 2023 [299] extend the multi-task approach to LiDAR-based perception tasks, unifying object detection, semantic segmentation, and panoptic segmentation in a single network to optimize performance across tasks. These studies collectively push the boundaries in efficient multi-task handling, demonstrating that integrating tasks can improve overall performance and reduce computational costs by sharing learned features across tasks.

6.3.2. Advanced Architectures for Enhanced Feature Extraction

MTL can be used for developing sophisticated neural network architectures to better handle the complexities of point cloud data. In this regard, Dubey et al. 2022 [300] introduce an attention-based architecture for radar point cloud data, focusing on enhancing target localization and classification through an anchor-free network design. Similarly, Hassani et al. 2019 [301] leverage an unsupervised multi-task model to learn point and shape features effectively, employing a graph-based encoder that tackles tasks like clustering and reconstruction simultaneously. Moving forward, Lin et al. 2022 [302] use a multi-task learning framework to improve semantic segmentation efficiency in Mobile Laser Scanning point clouds by integrating color prediction as an auxiliary task.

6.3.3. Specific Enhancements

Many studies have focused on applying multi-task learning to achieve specific enhancements in processing or understanding point cloud data. In this direction, Zhao et al. 2024 [303] develop a robust network for preprocessing

LiDAR data, tackling denoising, segmentation, and completion tasks within a shared framework to improve data quality. Similarly, Rios et al. 2021 [304] employ a multi-task approach in an evolutionary optimization context, using a 3DPC autoencoder to unify different design representations in a common latent space. Feng et al. 2021 [305] propose a multi-task network to handle various perception tasks for autonomous driving, demonstrating how a unified approach can enhance both detection and road understanding tasks.

Besides, the study in [306] introduces FFT-RadNet, a novel HD radar sensing model that optimizes the computation of angular positions from radar data, facilitating vehicle detection and free driving space segmentation. Moving on, Shan et al. 2023 [307] propose a no-reference point cloud quality assessment metric, GPA-Net, which utilizes a multi-task framework to enhance the accuracy of quality regression by also predicting distortion type and degree. Besides, the authors in [308] present Point-TTA, a test-time adaptation framework for point cloud registration that improves model generalization and performance on unknown testing environments through self-supervised auxiliary tasks. On the other hand, Zhang et al. 2022 [309] - The study proposes an improved multi-task network for roof plane segmentation from airborne laser scanning point clouds, which effectively segments and identifies roof planes. Wei et al. 2021 [310] - This paper proposes a multi-task network for 3D keypoint detection, which efficiently captures local and global features for accurate keypoint localization and semantic labeling. Lastly, the work in [311] introduces a multi-task network for machining feature recognition from point cloud data, aiming to accurately segment and identify complex machining features.

6.4. Cross-Modal Transfer Learning

6.4.1. Enhancing 3DPC Understanding Through 2D-3D Correspondences

Many studies employ contrastive learning and knowledge distillation strategies to align and enhance features between 2D images and 3DPCs. These methods focus on leveraging the rich textual and visual information available in 2D data to augment the spatial understanding provided by 3DPCs, significantly boosting performance in tasks such as classification, segmentation, and dense captioning. For instance, Afham et al. [312] introduce CrossPoint, utilizing self-supervised contrastive learning to map 2D image features to 3DPCs for better object classification and segmentation. The PointCMT, proposed in Yan et al. [313], adopts a teacher-student framework for cross-modal training, using 2D images to enhance 3DPC classification through knowledge distillation. Wu et al. [314] propose CrossNet, a method that aligns 3DPC features with both colored and grayscale images to enhance classification and segmentation tasks across different domains. Group 2: Cross-Modal and Cross-Domain Adaptation for Comprehensive 3D Understanding

6.4.2. Comprehensive 3D Understanding

CMTL can be employed in various works to tackle the challenge of transferring knowledge across not just modalities but also different domains, aiming to improve the performance of 3D perception tasks under varying conditions and datasets, without relying heavily on labeled data. Typically, Zhang et al. [315] develop a novel adaptation strategy that aligns features between images and point clouds to enhance semantic segmentation without requiring 3D labels. The X4D-SceneFormer, introduced by Jing et al. [316], uses a dual-branch Transformer architecture to transfer dynamic textual and visual cues from 2D video sequences to 4D point cloud sequences, focusing on temporal and semantic coherence. Zhou et al. [317] introduce PointCMC, which utilizes a Local-to-Local (L2L) module and a Cross-Modal Local-Global Contrastive (CLGC) loss to enhance cross-modal knowledge transfer between image and point cloud data.

6.4.3. Innovative Cross-Modal Applications in Robotics and Dynamic Environments

This section discusses the group of studies that applies cross-modal transfer learning to specific, challenging scenarios such as robotic tactile recognition and dynamic 4D scene understanding, demonstrating the flexibility and potential of cross-modal learning in practical and dynamic applications. Specifically, Falco et al. [318] explore visuo-tactile object recognition, where a robot uses visual data to enhance its tactile recognition capabilities, effectively bridging the gap between seeing and touching. Additionally, the authors in [316] focus on enhancing 4D point cloud understanding by transferring knowledge from RGB video sequences, improving the dynamic scene comprehension significantly. Murali et al. [319] propose xAVTNet, a visuo-tactile cross-modal framework for object recognition by autonomous robotic systems, utilizing active learning and perception strategies.

6.4.4. *Enhanced Sensory Perception and Retrieval*

CMTL can be used to improve sensory perception and retrieval tasks, enabling more effective and efficient recognition and classification across different sensory inputs. For example, Shen et al. [320] implement a simple cross-modal transfer from 2D to 3D sensors, using Vision Transformers to handle occlusions and improve performance in low-light scenarios. Jing et al. [321] enhances cross-modal retrieval capabilities by training a network to minimize feature discrepancies across 2D images, 3DPCs, and mesh data, ensuring robust retrieval performance across modalities.

6.4.5. *Point Cloud Completion and Enhancement*

Zhu et al. [322] introduce a cross-modal shape-transfer dual-refinement network (CSDN) designed for point cloud completion, utilizing images to guide the geometry generation of missing regions and refine the output through dual refinement processes. Li et al. [323] propose a model integrating Cross-Domain and Cross-Modal Knowledge Distillation to mitigate domain shifts and enhance the interaction between LiDAR and camera data, improving adaptation in unsupervised settings. Zhang et al. [317] explore PointMCD, a multi-view cross-modal distillation architecture, which aligns features between 2D visual and 3D geometric domains to boost the learning capacity of point cloud encoders.

6.4.6. *Domain Adaptation and Generalization in Cross-Modal Settings*

Peng et al. [324] discuss leveraging 2D images for 3D domain adaptation through cross-modal learning, addressing the loss of useful 2D features and promoting high-level modal complementarity. Nitsch et al. [325] propose a transductive transfer learning approach that uses a multi-modal adversarial autoencoder to transfer knowledge from images to point clouds, focusing on object detection. Li et al. [326] introduce a bird's-eye view approach for cross-modal learning under Domain Generalization (DG) for 3D semantic segmentation, optimizing domain-irrelevant representation modeling.

6.4.7. *Semantic Segmentation*

The ProtoTransfer, proposed in [327], explores knowledge transfer from multi-modal sources, such as LiDAR points and images, to enhance point cloud semantic segmentation, using a class-wise prototype bank to fully exploit image representations and transfer multi-modal knowledge to point cloud features. This approach effectively handles the challenge of unmatched point and pixel features by employing a pseudo-labeling scheme to integrate these features into the prototype bank, demonstrating superior performance on large-scale benchmarks. Similarly, Jaritz et al. [196] explore xMUDA, a cross-modal UDA technique for 3D semantic segmentation, leveraging mutual mimicking between 2D images and 3DPCs. Xing et al. [328] discuss enhancing domain adaptation for 3D semantic segmentation using cross-modal contrastive learning to improve interactions between 2D-pixel features and 3D point features.

Table 9 presents a comprehensive comparison of various studies focused on cross-modal learning and point cloud analysis, highlighting significant contributions and challenges in the field. For example, CrossPoint utilizes a self-supervised approach to establish 3D-2D correspondence, improving 3D object classification and segmentation, although it faces complexities in cross-modal alignment. Similarly, PointCMT enhances the representation of point clouds by incorporating view images derived from 2D image quality, thereby boosting 3DPC classification capabilities. Other notable methodologies include CrossNet, which excels in both intra- and cross-modal learning across multiple benchmark datasets, and X-Trans2Cap, which demonstrates effective cross-modal knowledge transfer in 3D dense captioning, albeit at a high computational cost.

The studies also outline several limitations inherent in current cross-modal and point cloud analysis techniques. For instance, many models, like the Cross-modal adaptation and simCrossTrans, struggle with domain shifts or performance variations across different 3D tasks, respectively. Additionally, while technologies such as the Visuotactile object recognition and xAVTNet offer high accuracy in specific applications such as object recognition in robotics, they are limited by their dependency on particular datasets and high system complexities. Other common challenges include the sensitivity to hyperparameters, as seen in Dual-Cross for cross-modal UDA, and the difficulty in feature alignment and generalization across different domains, which affects models like PointMCD and BEV-DG.

Table 9: Comparison of Studies on Cross-Modal Learning and Point Cloud Analysis

Ref.	ML Model	Dataset	Application / Task	Advantage	Limitation
[312]	CrossPoint	Varied	3D object classification, segmentation	Uses 3D-2D correspondence; self-supervised	May require complex cross-modal alignment
[313]	PointCMT	ModelNet40, ScanObjectNN	3DPC classification	Enhances point-only representation; uses view-images	Depends on 2D image quality
[314]	CrossNet	Multiple benchmarks	3DPC classification, segmentation	Intra- and cross-modal learning; versatile	Complex model structure for fine-tuning
[329]	X-Trans2Cap	ScanRefer, Nr3D	3D dense captioning	Effective cross-modal knowledge transfer; high accuracy	High computational cost in training
[315]	Cross-modal adaptation	SemanticKITTI, KITTI360, GTA5	3DPC semantic segmentation	Leverages 2D datasets; unsupervised	May struggle with substantial domain shifts
[318]	Visuo-tactile object recognition	15 objects dataset	Object recognition	High accuracy; cross-modal transfer	Limited to specific tactile and visual datasets
[316]	X4D-SceneFormer	HOI4D	4D point cloud tasks	Incorporates temporal dynamics; high performance	Complex model, heavy on resources
[320]	simCrossTrans	SUN RGB-D	3D sensor performance	Utilizes ViTs; robust to occlusions	Performance may vary across different 3D tasks
[321]	Cross-modal retrieval	ModelNet10, ModelNet40	Cross-modal retrieval	Efficient feature learning; high retrieval accuracy	Depends on network's feature extraction ability
[327]	ProtoTransfer	nuScenes, SemanticKITTI	Point cloud semantic segmentation	Exploits multi-modal fusion; high accuracy	May miss benefits for unmatched features
[322]	CSDN	Varied	Point cloud completion	Coarse-to-fine approach with dual-refinement; cross-modal data use	Complex model structure
[319]	xAVTNet	Robotics system	Visuo-tactile object recognition	Integrates visuo-tactile data; uses active learning	Specific to robotics; high system complexity

Continued on next page

Table 9 continued from previous page

Ref.	ML Model	Dataset	Application Task	Advantage	Limitation
[323]	Dual-Cross	Multi-modal	Cross-modal UDA	Integrates CDKD and CMKD for domain adaptation	Highly sensitive to hyperparameters
[324]	DsCML, CMAL	Multi-modal	3D semantic segmentation	Enhances cross-modal learning; diverse domain adaptation	Potential feature mismatch
[325]	Adversarial Auto Encoder	KITTI	Object detection	Transductive transfer from images to point clouds	Requires multi-modal data
[330]	PointCMC	Varied	3D object classification, segmentation	Enhances fine-grained cross-modal knowledge transfer	Alignment challenges
[196]	xMUDA	Autonomous driving datasets	3D semantic segmentation	Utilizes mutual mimicking in multi-modality	Complexity in heterogeneous input spaces
[328]	Cross-modal contrastive learning	Varied	3D semantic segmentation	Improves adaptation effects; uses neighborhood feature aggregation	Depends on precise feature correspondence
[317]	PointMCD	3D datasets	3D shape classification, segmentation	Uses cross-modal distillation; aligns features across modalities	Complicated feature alignment process
[326]	BEV-DG	3D datasets	3D semantic segmentation	Implements BEV-based cross-modal learning; robust to misalignment	Domain generalization complexity

6.5. Diffusion models for 3DPC understanding

Diffusion models are increasingly used for 3DPC applications due to their ability to generate high-quality, detailed structures, which is crucial for tasks such as 3D modeling and virtual reality. These models excel in handling complex distributions characteristic of 3DPCs, which are typically unordered and involve intricate spatial relationships. Their gradual denoising process allows them to implicitly learn the nuances of geometric structures, making them suitable for a range of tasks including reconstruction, up-sampling, and completion. Additionally, diffusion models are robust to noisy data, a common challenge with real-world 3D sensor data, and can be integrated with specialized 3D neural network architectures like PointNet, enhancing their effectiveness in processing 3DPCs. This flexibility and robustness make diffusion models a promising approach for advanced 3D applications across various industries.

The studies on diffusion model-based 3DPCs offer innovative solutions across various domains. Zheng et al. [331] introduce PointDif, a pre-training method for 3D models that employs a conditional point generator to enhance feature aggregation and guide point-to-point recovery, showing notable improvements in classification and segmentation tasks. Kasten et al. [332] describe SDS-Complete, a text-to-image diffusion model for completing 3D objects from partial point clouds, demonstrating its effectiveness in handling Out-Of-Distribution objects. Liu's study [333] focuses on a Diffusion Probabilistic Network for point cloud segmentation, utilizing a reverse diffusion process to refine topological structures. Jiang et al. [334] develop an SE(3) diffusion model-based framework for 3D registration, achieving precise

object pose alignment by manipulating noise in the SE(3) manifold. Jin introduces [335] a multiway point cloud mosaicking approach, employing a diffusion-based denoising process for enhanced registration accuracy. Feng's [336] DiffPoint combines Vision Transformers with diffusion models for 2D-to-3D reconstruction, achieving superior results in both single and multi-view tasks. Sharma [337] proposes a class-conditioned diffusion model to generate synthetic point cloud embeddings, significantly enhancing classification performance. Mo's [338] DiT-3D uses a Diffusion Transformer to generate high-quality 3D shapes from voxelized point clouds, integrating 3D window attention for computational efficiency. Yi's [339] GaussianDreamer leverages both 2D and 3D diffusion models for rapid, high-quality 3D generation from text prompts. Lastly, Ho [340] introduces Diffusion-SS3D, integrating diffusion models into a semi-supervised learning framework for 3D object detection, improving the quality of pseudo-labels and enhancing detection accuracy in diverse 3D spaces. These advancements collectively highlight the versatility and effectiveness of diffusion models in enhancing 3DPC processing and analysis.

Ohno et al. (2024) present a privacy-centric pedestrian tracking system using 3D LiDARs, capturing pedestrians as anonymous point clouds and leveraging a generative diffusion model to predict trajectories in unmonitored areas, achieving a high F-measure of 0.98 [341]. In a different approach, Bi et al. (2024) introduce DiffusionEMIS, a novel paradigm that models 3-D electromagnetic inverse scattering as a denoising diffusion process, significantly improving performance and noise resistance over conventional methods [342]. Dutt (2024) develops Diff3F, which distills diffusion features onto untextured shapes, demonstrating robustness and reliability across several benchmarks [343]. Simultaneously, Li (2024) proposes a framework for generating stable crystal structures using a point cloud-based diffusion model, enhancing material design [344]. Expanding the applications, Ze (2024) integrates 3D visual representations into diffusion models for robotic imitation learning with the 3D Diffusion Policy (DP3), which shows remarkable success rates and generalizability [345]. Addressing point cloud registration, She (2024) utilizes graph neural PDEs and heat kernel signatures to enhance keypoint matching accuracy and robustness [346]. Meanwhile, Li (2024) details a method for reconstructing 3D colored objects from images using a conditional diffusion model, achieving high fidelity in shape and color reconstruction [347]. Chen (2024) introduces V3D, adapting video diffusion models for 3D generation that produce high-quality outputs rapidly with impressive multi-view consistency [348]. Further, Hu (2024) presents a novel generative model combining latent diffusion with topological features, enabling diverse and adaptable 3D shape generation [349]. Finally, Dong (2024) proposes a novel generative model for man-made shapes, incorporating diffusion processes with a quality checker to ensure geometric feasibility and physical stability, significantly outperforming traditional methods on ShapeNet-v2 [350].

Several future directions can be suggested to further improve the use of diffusion models in 3DPC. These include enhancing privacy while utilizing detailed data, improving computational efficiency in model adaptation with minimal trainable parameters, and increasing robustness against data quality variations. Additionally, there's a trend toward cross-domain applications and interdisciplinary approaches, such as integrating 2D image processing techniques. The generation of complex and detailed 3D structures, especially in dynamic environments, is also a focal point, along with the development of semi-supervised and fully automated learning systems. Innovations in incorporating topological and geometric features into diffusion processes highlight the potential for more precise and versatile models. Finally, there's a growing need for standardization in benchmarking methods to evaluate and compare the performance of diffusion models in handling 3DPCs. These insights indicate a move towards more efficient, robust, and application-diverse uses of diffusion models in the realm of 3D data analysis.

7. Conclusion

With the rapid advancement of 3D scanning technologies, such as LiDAR and RGB-D cameras, capturing and processing 3DPC data has become increasingly popular in various fields, including robotics, CV, virtual reality, and autonomous vehicles. On the other hand, deep DTL, a cutting-edge technique in ML and DL, has emerged as a powerful approach to leverage pre-trained DNNs and transfer their knowledge to new 3DPC tasks overcome several challenges to using DL. To shed light on the latest innovations related to using DTL in 3DPCs, this article presented a comprehensive review of the state-of-the-art techniques for 3DPC understanding using DTL and DA, including 3DPC object detection, 3DPC semantic labeling, segmentation and classification, 3DPC registration, downsampling/upsampling and 3DPC denoising. In doing so, a well-defined taxonomy has been introduced, and detailed comparisons have been conducted, presented with reference to different aspects, such as the types of adopted DL models, obtained performance, and knowledge transfer strategies (fine-tuning, DA, UDA, etc.). Moving forward, the pros and cons of presented frameworks have been covered before identifying open challenges. Lastly, potential research directions have been listed.

Point cloud understanding has made significant progress through years of research, but as it becomes more widely used in real-world applications, it faces new challenges. One major challenge is partial overlap in sensor-acquired point clouds, which makes direct registration difficult. While some solutions have been developed for alignment under partial overlap, the rate of overlap is often limited. Finding a comprehensive solution to this problem, therefore, is a valuable and promising area of research. Moreover, only simple objects can currently be solved for alignment, despite the fact that the 3DPC registration techniques that combine DTL and conventional methods have made significant advancements. For instance, when dealing with complex scenarios and large-scale 3DPCs, these approaches fall short of the desired outcomes and continue to use the conventional algorithms. However, these algorithms are stochastic, and the number of iterations rise exponentially with outliers. By combining DTL and conventional ML methods, better results are obtained. Specifically, traditional ML approaches are transparent, whereas DTL schemes excel at fitting data. Hence, one of the trends for the future research is how to combine the benefits of both.

Besides, the need for generalizing 3DPC scene understanding algorithms arises from the fact that different application scenarios present the algorithms with different challenges. Nevertheless, given the state of the research, it is difficult to suggest a general algorithm. For instance, an aircraft's skin is very large, its surface is smooth, and it has few features with a curvature. When feature-based methods are used in the registration process, significant misalignment will consequently happen. The development of targeted, lightweight, and efficient algorithms for particular application scenarios is thus an attractive research hotspot in the near future.

References

- [1] Y. Himeur, S. Al-Maadeed, H. Kheddar, N. Al-Maadeed, K. Abualsaud, A. Mohamed, T. Khattab, Video surveillance using deep transfer learning and deep domain adaptation: Towards better generalization, *Engineering Applications of Artificial Intelligence* 119 (2023) 105698.
- [2] A. Copiaco, Y. Himeur, A. Amira, W. Mansoor, F. Fadli, S. Atalla, S. S. Sohail, An innovative deep anomaly detection of building energy consumption using energy time-series images, *Engineering Applications of Artificial Intelligence* 119 (2023) 105775.
- [3] Y. Zhou, A. Ji, L. Zhang, X. Xue, Attention-enhanced sampling point cloud network (aspcnet) for efficient 3d tunnel semantic segmentation, *Automation in Construction* 146 (2023) 104667.
- [4] Y. Habchi, Y. Himeur, H. Kheddar, A. Boukabou, S. Atalla, A. Chouchane, A. Ouamane, W. Mansoor, Ai in thyroid cancer diagnosis: Techniques, trends, and future directions, *Systems* 11 (10) (2023) 519.
- [5] A. Ji, Y. Zhou, L. Zhang, R. L. Tiong, X. Xue, Semi-supervised learning-based point cloud network for segmentation of 3d tunnel scenes, *Automation in Construction* 146 (2023) 104668.
- [6] O. Kerdjadj, Y. Himeur, S. Atalla, A. Copiaco, A. Amira, F. Fadli, S. S. Sohail, W. Mansoor, A. Gawanmeh, S. Miniaoui, Exploiting 2d representations for enhanced indoor localization: A transfer learning approach, *IEEE Sensors Journal* (2024).
- [7] C. Fotsing, P. Hahn, D. Cunningham, C. Bobda, Volumetric wall detection in unorganized indoor point clouds using continuous segments in 2d grids, *Automation in Construction* 141 (2022) 104462.
- [8] X. Lai, J. Liu, L. Jiang, L. Wang, H. Zhao, S. Liu, X. Qi, J. Jia, Stratified transformer for 3d point cloud segmentation, in: *Proceedings of the IEEE/CVF Conference on Computer Vision and Pattern Recognition*, IEEE, New Orleans, LA, USA, 2022, pp. 8500–8509.
- [9] A. Bechar, Y. Elmir, Y. Himeur, R. Medjoudj, A. Amira, Federated and transfer learning for cancer detection based on image analysis, *arXiv preprint arXiv:2405.20126* (2024).
- [10] R. Abbasi, A. K. Bashir, H. J. Alyamani, F. Amin, J. Doh, J. Chen, Lidar point cloud compression, processing and learning for autonomous driving, *IEEE Transactions on Intelligent Transportation Systems* (2022).
- [11] D. Liu, W. Hu, Imperceptible transfer attack and defense on 3d point cloud classification, *IEEE Transactions on Pattern Analysis and Machine Intelligence* (2022).
- [12] Q. Yu, C. Yang, H. Wei, Part-wise atlasnet for 3d point cloud reconstruction from a single image, *Knowledge-Based Systems* 242 (2022) 108395.
- [13] Z. Li, Z. Chen, A. Li, L. Fang, Q. Jiang, X. Liu, J. Jiang, B. Zhou, H. Zhao, Simipu: Simple 2d image and 3d point cloud unsupervised pre-training for spatial-aware visual representations, in: *Proceedings of the AAAI Conference on Artificial Intelligence*, Vol. 36, AAAI, online/virtual, 2022, pp. 1500–1508.
- [14] O. Elharrouss, S. Al-Maadeed, N. Subramanian, N. Ottakath, N. Almaadeed, Y. Himeur, Panoptic segmentation: a review, *arXiv preprint arXiv:2111.10250* (2021).
- [15] S. Cao, H. Zhao, P. Liu, Semantic segmentation for point clouds via semantic-based local aggregation and multi-scale global pyramid, *Machines* 11 (1) (2023) 11.
- [16] W. Liu, Y. Zang, Z. Xiong, X. Bian, C. Wen, X. Lu, C. Wang, J. M. Junior, W. N. Gonçalves, J. Li, 3d building model generation from mls point cloud and 3d mesh using multi-source data fusion, *International Journal of Applied Earth Observation and Geoinformation* 116 (2023) 103171.
- [17] X. Yang, E. del Rey Castillo, Y. Zou, L. Wotherspoon, Y. Tan, Automated semantic segmentation of bridge components from large-scale point clouds using a weighted superpoint graph, *Automation in Construction* 142 (2022) 104519.
- [18] W. Liu, Y. Shao, K. Chen, C. Li, H. Luo, Whale optimization algorithm-based point cloud data processing method for sewer pipeline inspection, *Automation in Construction* 141 (2022) 104423.
- [19] I. Ahmed, G. Jeon, F. Piccialli, A deep-learning-based smart healthcare system for patient's discomfort detection at the edge of internet of things, *IEEE Internet of Things Journal* 8 (13) (2021) 10318–10326.

- [20] N. Mehdiyev, J. Evermann, P. Fettke, A novel business process prediction model using a deep learning method, *Business & information systems engineering* 62 (2) (2020) 143–157.
- [21] R. Kiran, P. Kumar, B. Bhasker, Dnnrec: A novel deep learning based hybrid recommender system, *Expert Systems with Applications* 144 (2020) 113054.
- [22] Y. Himeur, K. Ghanem, A. Alsalemi, F. Bensaali, A. Amira, Artificial intelligence based anomaly detection of energy consumption in buildings: A review, current trends and new perspectives, *Applied Energy* 287 (2021) 116601.
- [23] P. K. Kashyap, S. Kumar, A. Jaiswal, M. Prasad, A. H. Gandomi, Towards precision agriculture: Iot-enabled intelligent irrigation systems using deep learning neural network, *IEEE Sensors Journal* 21 (16) (2021) 17479–17491.
- [24] D. De Gregorio, A. Tonioni, G. Palli, L. Di Stefano, Semiautomatic labeling for deep learning in robotics, *IEEE Transactions on Automation Science and Engineering* 17 (2) (2019) 611–620.
- [25] A. N. Sayed, Y. Himeur, F. Bensaali, Deep and transfer learning for building occupancy detection: A review and comparative analysis, *Engineering Applications of Artificial Intelligence* 115 (2022) 105254.
- [26] H. Kheddar, Y. Himeur, S. Al-Maadeed, A. Amira, F. Bensaali, Deep transfer learning for automatic speech recognition: Towards better generalization, *Knowledge-Based Systems* 277 (2023) 110851. doi:10.1016/j.knsys.2023.110851.
- [27] H. Kheddar, Y. Himeur, A. I. Awad, Deep transfer learning for intrusion detection in industrial control networks: A comprehensive review, *J. Netw. Comput. Appl.* 220 (2023) 103760.
- [28] B. Kitchenham, Procedures for performing systematic reviews, Keele, UK, Keele University 33 (2004) (2004) 1–26.
- [29] Y. Himeur, A. Alsalemi, A. Al-Kababji, F. Bensaali, A. Amira, C. Sardianos, G. Dimitrakopoulos, I. Varlamis, A survey of recommender systems for energy efficiency in buildings: Principles, challenges and prospects, *Information Fusion* 72 (2021) 1–21.
- [30] S. A. Bello, S. Yu, C. Wang, J. M. Adam, J. Li, Deep learning on 3d point clouds, *Remote Sensing* 12 (11) (2020) 1729.
- [31] Y. Guo, H. Wang, Q. Hu, H. Liu, L. Liu, M. Bennamoun, Deep learning for 3d point clouds: A survey, *IEEE transactions on pattern analysis and machine intelligence* 43 (12) (2020) 4338–4364.
- [32] Y. Li, Deep reinforcement learning: An overview, arXiv preprint arXiv:1701.07274 (2017).
- [33] P. Z. Ramirez, A. Tonioni, S. Salti, L. D. Stefano, Learning across tasks and domains, in: *Proceedings of the IEEE/CVF International Conference on Computer Vision, IEEE, Seoul, Korea (South), 2019*, pp. 8110–8119.
- [34] M. A. Morid, A. Borjali, G. Del Fiol, A scoping review of transfer learning research on medical image analysis using imagenet, *Computers in biology and medicine* 128 (2021) 104115.
- [35] W. Li, W. Huan, B. Hou, Y. Tian, Z. Zhang, A. Song, Can emotion be transferred?—a review on transfer learning for eeg-based emotion recognition, *IEEE Transactions on Cognitive and Developmental Systems* (2021).
- [36] Z. Alyafeai, M. S. AlShaibani, I. Ahmad, A survey on transfer learning in natural language processing, arXiv preprint arXiv:2007.04239 (2020).
- [37] R. Ribani, M. Marengoni, A survey of transfer learning for convolutional neural networks, in: *2019 32nd SIBGRAPI conference on graphics, patterns and images tutorials (SIBGRAPI-T)*, IEEE, Rio de Janeiro, Brazil, 2019, pp. 47–57.
- [38] Z. Wan, R. Yang, M. Huang, N. Zeng, X. Liu, A review on transfer learning in eeg signal analysis, *Neurocomputing* 421 (2021) 1–14.
- [39] Z.-H. Liu, L.-B. Jiang, H.-L. Wei, L. Chen, X.-H. Li, Optimal transport-based deep domain adaptation approach for fault diagnosis of rotating machine, *IEEE Transactions on Instrumentation and Measurement* 70 (2021) 1–12.
- [40] C. Tan, F. Sun, T. Kong, W. Zhang, C. Yang, C. Liu, A survey on deep transfer learning, in: *International conference on artificial neural networks*, Springer, Rhodes, Greece, 2018, pp. 270–279.
- [41] S. Niu, Y. Jiang, B. Chen, J. Wang, Y. Liu, H. Song, Cross-modality transfer learning for image-text information management, *ACM Transactions on Management Information System (TMIS)* 13 (1) (2021) 1–14.
- [42] J. Si, H. Shi, J. Chen, C. Zheng, Unsupervised deep transfer learning with moment matching: A new intelligent fault diagnosis approach for bearings, *Measurement* 172 (2021) 108827.
- [43] Y. Zhou, J. Yang, H. Li, T. Cao, S.-Y. Kung, Adversarial learning for multiscale crowd counting under complex scenes, *IEEE transactions on cybernetics* 51 (11) (2020) 5423–5432.
- [44] Y. Ganin, E. Ustinova, H. Ajakan, P. Germain, H. Larochelle, F. Laviolette, M. Marchand, V. Lempitsky, Domain-adversarial training of neural networks, *The journal of machine learning research* 17 (1) (2016) 2096–2030.
- [45] Z. Shen, Y. Xu, B. Ni, M. Wang, J. Hu, X. Yang, Crowd counting via adversarial cross-scale consistency pursuit, in: *Proceedings of the IEEE conference on computer vision and pattern recognition*, 2018, pp. 5245–5254.
- [46] M.-I. Georgescu, R. T. Ionescu, F. S. Khan, M. Popescu, M. Shah, A background-agnostic framework with adversarial training for abnormal event detection in video, arXiv preprint arXiv:2008.12328 (2020).
- [47] W. Choi, W. Yang, J. Na, J. Park, G. Lee, W. Nam, Unsupervised gait phase estimation with domain-adversarial neural network and adaptive window, *IEEE Journal of Biomedical and Health Informatics* (2021).
- [48] E. Soleimani, E. Nazerfard, Cross-subject transfer learning in human activity recognition systems using generative adversarial networks, *Neurocomputing* 426 (2021) 26–34.
- [49] J. Wang, Y. Chen, W. Feng, H. Yu, M. Huang, Q. Yang, Transfer learning with dynamic distribution adaptation, *ACM Transactions on Intelligent Systems and Technology (TIST)* 11 (1) (2020) 1–25.
- [50] Z. Zou, X. Qu, P. Zhou, S. Xu, X. Ye, W. Wu, J. Ye, Coarse to fine: Domain adaptive crowd counting via adversarial scoring network, in: *Proceedings of the 29th ACM International Conference on Multimedia*, ACM, online, 2021, pp. 2185–2194.
- [51] J. Sun, Y. Cao, C. B. Choy, Z. Yu, A. Anandkumar, Z. M. Mao, C. Xiao, Adversarially robust 3d point cloud recognition using self-supervisions, *Advances in Neural Information Processing Systems* 34 (2021) 15498–15512.
- [52] C. R. Qi, H. Su, K. Mo, L. J. Guibas, Pointnet: Deep learning on point sets for 3d classification and segmentation, in: *Proceedings of the IEEE conference on computer vision and pattern recognition*, IEEE, Honolulu, HI, USA, 2017, pp. 652–660.

- [53] C. R. Qi, L. Yi, H. Su, L. J. Guibas, Pointnet++: Deep hierarchical feature learning on point sets in a metric space, *Advances in neural information processing systems* 30 (2017).
- [54] R. Li, Y. Zhang, D. Niu, G. Yang, N. Zafar, C. Zhang, X. Zhao, Pointvgg: Graph convolutional network with progressive aggregating features on point clouds, *Neurocomputing* 429 (2021) 187–198.
- [55] Y. Shi, C. Zhang, X. Zhang, K. Wang, Y. Zhang, X. Zhao, Pointpavgg: An incremental algorithm for extraction of points' positional feature using vgg on point clouds, in: *Intelligent Computing Theories and Application: 17th International Conference, ICIC 2021, Shenzhen, China, August 12–15, 2021, Proceedings, Part II*, Springer, 2021, pp. 718–731.
- [56] Y. Xu, T. Fan, M. Xu, L. Zeng, Y. Qiao, Spidercnn: Deep learning on point sets with parameterized convolutional filters, in: *Proceedings of the European conference on computer vision (ECCV)*, Springer, Munich, Germany, 2018, pp. 87–102.
- [57] Y. Li, R. Bu, M. Sun, W. Wu, X. Di, B. Chen, Pointcnn: Convolution on x-transformed points, *Advances in neural information processing systems* 31 (2018).
- [58] H. Su, V. Jampani, D. Sun, S. Maji, E. Kalogerakis, M.-H. Yang, J. Kautz, Splatnet: Sparse lattice networks for point cloud processing, in: *Proceedings of the IEEE conference on computer vision and pattern recognition*, 2018, pp. 2530–2539.
- [59] W. Wang, R. Yu, Q. Huang, U. Neumann, Sgpn: Similarity group proposal network for 3d point cloud instance segmentation, in: *Proceedings of the IEEE conference on computer vision and pattern recognition*, 2018, pp. 2569–2578.
- [60] Y. Yang, C. Feng, Y. Shen, D. Tian, Foldingnet: Point cloud auto-encoder via deep grid deformation, in: *Proceedings of the IEEE conference on computer vision and pattern recognition*, 2018, pp. 206–215.
- [61] L. Yu, X. Li, C.-W. Fu, D. Cohen-Or, P.-A. Heng, Pu-net: Point cloud upsampling network, in: *Proceedings of the IEEE conference on computer vision and pattern recognition*, 2018, pp. 2790–2799.
- [62] T. Le, Y. Duan, Pointgrid: A deep network for 3d shape understanding, in: *Proceedings of the IEEE conference on computer vision and pattern recognition*, 2018, pp. 9204–9214.
- [63] L. Ge, Y. Cai, J. Weng, J. Yuan, Hand pointnet: 3d hand pose estimation using point sets, in: *Proceedings of the IEEE conference on computer vision and pattern recognition*, 2018, pp. 8417–8426.
- [64] M. A. Uy, G. H. Lee, Pointnetvlad: Deep point cloud based retrieval for large-scale place recognition, in: *Proceedings of the IEEE conference on computer vision and pattern recognition*, 2018, pp. 4470–4479.
- [65] S. Huang, Z. Gojcic, M. Usvyatsov, A. Wieser, K. Schindler, Predator: Registration of 3d point clouds with low overlap, in: *Proceedings of the IEEE/CVF Conference on computer vision and pattern recognition*, 2021, pp. 4267–4276.
- [66] H. Wang, Y. Cong, O. Litany, Y. Gao, L. J. Guibas, 3dioumatch: Leveraging iou prediction for semi-supervised 3d object detection, in: *Proceedings of the IEEE/CVF Conference on Computer Vision and Pattern Recognition*, 2021, pp. 14615–14624.
- [67] A. Dai, A. X. Chang, M. Savva, M. Halber, T. Funkhouser, M. Nießner, Scannet: Richly-annotated 3d reconstructions of indoor scenes, in: *Proceedings of the IEEE conference on computer vision and pattern recognition*, 2017, pp. 5828–5839.
- [68] G. Riegler, A. Osman Ulusoy, A. Geiger, Octnet: Learning deep 3d representations at high resolutions, in: *Proceedings of the IEEE conference on computer vision and pattern recognition*, 2017, pp. 3577–3586.
- [69] J. Li, B. M. Chen, G. H. Lee, So-net: Self-organizing network for point cloud analysis, in: *Proceedings of the IEEE conference on computer vision and pattern recognition*, 2018, pp. 9397–9406.
- [70] B. Yang, W. Luo, R. Urtasun, Pixor: Real-time 3d object detection from point clouds, in: *Proceedings of the IEEE conference on Computer Vision and Pattern Recognition*, 2018, pp. 7652–7660.
- [71] Y. Zhou, O. Tuzel, Voxelnet: End-to-end learning for point cloud based 3d object detection, in: *Proceedings of the IEEE conference on computer vision and pattern recognition*, 2018, pp. 4490–4499.
- [72] H. Deng, T. Birdal, S. Ilic, Ppfnnet: Global context aware local features for robust 3d point matching, in: *Proceedings of the IEEE conference on computer vision and pattern recognition*, 2018, pp. 195–205.
- [73] D. Xu, D. Anguelov, A. Jain, Pointfusion: Deep sensor fusion for 3d bounding box estimation, in: *Proceedings of the IEEE conference on computer vision and pattern recognition*, 2018, pp. 244–253.
- [74] C. R. Qi, W. Liu, C. Wu, H. Su, L. J. Guibas, Frustum pointnets for 3d object detection from rgb-d data, in: *Proceedings of the IEEE conference on computer vision and pattern recognition*, 2018, pp. 918–927.
- [75] Z. J. Yew, G. H. Lee, 3dfeat-net: Weakly supervised local 3d features for point cloud registration, in: *Proceedings of the European conference on computer vision (ECCV)*, 2018, pp. 607–623.
- [76] B. Wu, A. Wan, X. Yue, K. Keutzer, Squeezeseg: Convolutional neural nets with recurrent crf for real-time road-object segmentation from 3d lidar point cloud, in: *2018 IEEE international conference on robotics and automation (ICRA)*, IEEE, 2018, pp. 1887–1893.
- [77] X. Yan, J. Gao, C. Zheng, C. Zheng, R. Zhang, S. Cui, Z. Li, 2dpass: 2d priors assisted semantic segmentation on lidar point clouds, in: *European Conference on Computer Vision*, Springer, 2022, pp. 677–695.
- [78] W. Chen, J. Duan, H. Basevi, H. J. Chang, A. Leonardis, Pointposenet: Point pose network for robust 6d object pose estimation, in: *Proceedings of the IEEE/CVF Winter Conference on Applications of Computer Vision*, 2020, pp. 2824–2833.
- [79] H. Cao, Y. Lu, C. Lu, B. Pang, G. Liu, A. Yuille, Asap-net: Attention and structure aware point cloud sequence segmentation, *arXiv preprint arXiv:2008.05149* (2020).
- [80] S. Biswas, J. Liu, K. Wong, S. Wang, R. Urtasun, Muscle: Multi sweep compression of lidar using deep entropy models, *Advances in Neural Information Processing Systems* 33 (2020) 22170–22181.
- [81] Y. Zhang, D. Huang, Y. Wang, Pc-rgnn: Point cloud completion and graph neural network for 3d object detection, in: *Proceedings of the AAAI conference on artificial intelligence*, Vol. 35, 2021, pp. 3430–3437.
- [82] C. Xu, S. Yang, B. Zhai, B. Wu, X. Yue, W. Zhan, P. Vajda, K. Keutzer, M. Tomizuka, Image2point: 3d point-cloud understanding with 2d image pretrained models (2021).
- [83] L. Mattheuwsen, M. Vergauwen, Manhole cover detection on rasterized mobile mapping point cloud data using transfer learned fully convolutional neural networks, *Remote Sensing* 12 (22) (2020) 3820.

- [84] Y. Liao, M. E. Mohammadi, R. L. Wood, Deep learning classification of 2d orthomosaic images and 3d point clouds for post-event structural damage assessment, *Drones* 4 (2) (2020) 24.
- [85] S. Bourbia, A. Karine, A. Chetouani, M. El Hassouni, Blind projection-based 3d point cloud quality assessment method using a convolutional neural network., in: VISIGRAPP (4: VISAPP), SCITEPRES, online, 2022, pp. 518–525.
- [86] R. Leroy, P. Trouvé-Pelouas, F. Champagnat, B. Le Saux, M. Carvalho, Pix2point: Learning outdoor 3d using sparse point clouds and optimal transport, in: 2021 17th International Conference on Machine Vision and Applications (MVA), IEEE, online, 2021, pp. 1–5.
- [87] J. Balado, R. Sousa, L. Diaz-Vilarino, P. Arias, Transfer learning in urban object classification: Online images to recognize point clouds, *Automation in Construction* 111 (2020) 103058.
- [88] V. Stojanovic, M. Trapp, R. Richter, J. Döllner, Service-oriented semantic enrichment of indoor point clouds using octree-based multiview classification, *Graphical Models* 105 (2019) 101039.
- [89] W. Dongyu, H. Fuwen, T. Mikolajczyk, H. Yunhua, Object detection for soft robotic manipulation based on rgb-d sensors, in: 2018 WRC Symposium on Advanced Robotics and Automation (WRC SARA), IEEE, Beijing, China, 2018, pp. 52–58.
- [90] C. Zhao, H. Guo, J. Lu, D. Yu, D. Li, X. Chen, Als point cloud classification with small training data set based on transfer learning, *IEEE Geoscience and Remote Sensing Letters* 17 (8) (2020) 1406–1410. doi:10.1109/LGRS.2019.2947608.
- [91] K. He, X. Zhang, S. Ren, J. Sun, Deep residual learning for image recognition, in: Proceedings of the IEEE conference on computer vision and pattern recognition, IEEE, Las Vegas, NV, USA, 2016, pp. 770–778.
- [92] M. Liu, L. Sheng, S. Yang, J. Shao, S.-M. Hu, Morphing and sampling network for dense point cloud completion, in: Proceedings of the AAAI conference on artificial intelligence, Vol. 34, 2020, pp. 11596–11603.
- [93] D. Zong, S. Sun, J. Zhao, Ashf-net: Adaptive sampling and hierarchical folding network for robust point cloud completion, in: Proceedings of the AAAI Conference on Artificial Intelligence, Vol. 35, 2021, pp. 3625–3632.
- [94] W. Yuan, T. Khot, D. Held, C. Mertz, M. Hebert, Pcn: Point completion network, in: 2018 international conference on 3D vision (3DV), IEEE, 2018, pp. 728–737.
- [95] X. Wen, T. Li, Z. Han, Y.-S. Liu, Point cloud completion by skip-attention network with hierarchical folding, in: Proceedings of the IEEE/CVF conference on computer vision and pattern recognition, 2020, pp. 1939–1948.
- [96] Y. Nie, Y. Lin, X. Han, S. Guo, J. Chang, S. Cui, J. Zhang, et al., Skeleton-bridged point completion: From global inference to local adjustment, *Advances in Neural Information Processing Systems* 33 (2020) 16119–16130.
- [97] Y. Li, L. Ma, W. Tan, C. Sun, D. Cao, J. Li, Grnet: Geometric relation network for 3d object detection from point clouds, *ISPRS Journal of Photogrammetry and Remote Sensing* 165 (2020) 43–53.
- [98] X. Wang, M. H. Ang, G. H. Lee, Voxel-based network for shape completion by leveraging edge generation, in: Proceedings of the IEEE/CVF international conference on computer vision, 2021, pp. 13189–13198.
- [99] Y. Tang, R. Zhang, Z. Guo, X. Ma, B. Zhao, Z. Wang, D. Wang, X. Li, Point-peft: Parameter-efficient fine-tuning for 3d pre-trained models, in: Proceedings of the AAAI Conference on Artificial Intelligence, Vol. 38, 2024, pp. 5171–5179.
- [100] X. Zhou, D. Liang, W. Xu, X. Zhu, Y. Xu, Z. Zou, X. Bai, Dynamic adapter meets prompt tuning: Parameter-efficient transfer learning for point cloud analysis, in: Proceedings of the IEEE/CVF Conference on Computer Vision and Pattern Recognition, 2024, pp. 14707–14717.
- [101] G. Song, H. Xu, J. Liu, T. Zhi, Y. Shi, J. Zhang, Z. Jiang, J. Feng, S. Sang, L. Luo, Agile3d: Few-shot 3d portrait stylization by augmented transfer learning, in: Proceedings of the IEEE/CVF Conference on Computer Vision and Pattern Recognition, 2024, pp. 765–774.
- [102] M. A. Shoukat, A. B. Sargano, L. You, Z. Habib, 3d estimation of single-view 2d images using shape priors and transfer learning, *Multimedia Tools and Applications* (2024) 1–13.
- [103] M. Zaheer, S. Kottur, S. Ravanbakhsh, B. Póczos, R. R. Salakhutdinov, A. J. Smola, Deep sets, *Advances in neural information processing systems* 30 (2017).
- [104] R. Klokov, V. Lempitsky, Escape from cells: Deep kd-networks for the recognition of 3d point cloud models, in: Proceedings of the IEEE international conference on computer vision, Venice, Italy, 2017, pp. 863–872.
- [105] W. Zeng, T. Gevers, 3dcontextnet: Kd tree guided hierarchical learning of point clouds using local and global contextual cues, in: Proceedings of the European Conference on Computer Vision (ECCV) Workshops, Springer, Munich, Germany, 2018, pp. 0–0.
- [106] B.-S. Hua, M.-K. Tran, S.-K. Yeung, Pointwise convolutional neural networks, in: Proceedings of the IEEE conference on computer vision and pattern recognition, IEEE, Salt Lake City, UT, USA, 2018, pp. 984–993.
- [107] Z. Zhang, B.-S. Hua, S.-K. Yeung, Shellnet: Efficient point cloud convolutional neural networks using concentric shells statistics, in: Proceedings of the IEEE/CVF international conference on computer vision, IEEE, Seoul, Korea (South), 2019, pp. 1607–1616.
- [108] G. Te, W. Hu, A. Zheng, Z. Guo, Rgcn: Regularized graph cnn for point cloud segmentation, in: Proceedings of the 26th ACM international conference on Multimedia, ACM, Seoul Republic of Korea, 2018, pp. 746–754.
- [109] C. Wang, B. Samari, K. Siddiqi, Local spectral graph convolution for point set feature learning, in: Proceedings of the European conference on computer vision (ECCV), Springer, Munich, Germany, 2018, pp. 52–66.
- [110] S. Xie, S. Liu, Z. Chen, Z. Tu, Attentional shapecontextnet for point cloud recognition, in: Proceedings of the IEEE conference on computer vision and pattern recognition, IEEE, Salt Lake City, UT, USA, 2018, pp. 4606–4615.
- [111] N. Verma, E. Boyer, J. Verbeek, Feastnet: Feature-steered graph convolutions for 3d shape analysis, in: Proceedings of the IEEE conference on computer vision and pattern recognition, IEEE, Salt Lake City, UT, USA, 2018, pp. 2598–2606.
- [112] A. Boulch, Convpoint: Continuous convolutions for point cloud processing, *Computers & Graphics* 88 (2020) 24–34.
- [113] Z. Yang, O. Litany, T. Birdal, S. Sridhar, L. Guibas, Continuous geodesic convolutions for learning on 3d shapes, in: Proceedings of the IEEE/CVF winter conference on applications of computer vision, IEEE, online, 2021, pp. 134–144.
- [114] J. Sauder, B. Sievers, Self-supervised deep learning on point clouds by reconstructing space, *Advances in Neural Information Processing Systems* 32 (2019).
- [115] O. Poursaeed, T. Jiang, H. Qiao, N. Xu, V. G. Kim, Self-supervised learning of point clouds via orientation estimation, in: 2020 International Conference on 3D Vision (3DV), IEEE, 2020, pp. 1018–1028.

- [116] I. Achituve, H. Maron, G. Chechik, Self-supervised learning for domain adaptation on point clouds, in: Proceedings of the IEEE/CVF winter conference on applications of computer vision, IEEE, online, 2021, pp. 123–133.
- [117] S. Xie, J. Gu, D. Guo, C. R. Qi, L. Guibas, O. Litany, Pointcontrast: Unsupervised pre-training for 3d point cloud understanding, in: Computer Vision—ECCV 2020: 16th European Conference, Glasgow, UK, August 23–28, 2020, Proceedings, Part III 16, Springer, online, 2020, pp. 574–591.
- [118] H. Wang, Q. Liu, X. Yue, J. Lasenby, M. J. Kusner, Unsupervised point cloud pre-training via occlusion completion, in: Proceedings of the IEEE/CVF international conference on computer vision, Montreal, BC, Canada, 2021, pp. 9782–9792.
- [119] X. Yu, L. Tang, Y. Rao, T. Huang, J. Zhou, J. Lu, Point-bert: Pre-training 3d point cloud transformers with masked point modeling, in: Proceedings of the IEEE/CVF Conference on Computer Vision and Pattern Recognition, IEEE, New Orleans, LA, USA, 2022, pp. 19313–19322.
- [120] R. Zhang, Z. Guo, P. Gao, R. Fang, B. Zhao, D. Wang, Y. Qiao, H. Li, Point-m2ae: multi-scale masked autoencoders for hierarchical point cloud pre-training, arXiv preprint arXiv:2205.14401 (2022).
- [121] C. Choy, J. Gwak, S. Savarese, 4d spatio-temporal convnets: Minkowski convolutional neural networks, in: Proceedings of the IEEE/CVF conference on computer vision and pattern recognition, IEEE, Long Beach, CA, USA, 2019, pp. 3075–3084.
- [122] B. Graham, M. Engelcke, L. Van Der Maaten, 3d semantic segmentation with submanifold sparse convolutional networks, in: Proceedings of the IEEE conference on computer vision and pattern recognition, IEEE, Salt Lake City, UT, USA, 2018, pp. 9224–9232.
- [123] O. Ronneberger, P. Fischer, T. Brox, U-net: Convolutional networks for biomedical image segmentation, in: Medical Image Computing and Computer-Assisted Intervention—MICCAI 2015: 18th International Conference, Munich, Germany, October 5–9, 2015, Proceedings, Part III 18, Springer, 2015, pp. 234–241.
- [124] H. Kheddar, M. Hemis, Y. Himeur, Automatic speech recognition using advanced deep learning approaches: A survey, Information Fusion (2024) 102422.
- [125] R. Zhang, Z. Guo, W. Zhang, K. Li, X. Miao, B. Cui, Y. Qiao, P. Gao, H. Li, Pointclip: Point cloud understanding by clip, in: Proceedings of the IEEE/CVF Conference on Computer Vision and Pattern Recognition, IEEE, New Orleans, Louisiana, USA, 2022, pp. 8552–8562.
- [126] X. Huang, T. Xie, Z. Wang, L. Chen, Q. Zhou, Z. Hu, A transfer learning-based multi-fidelity point-cloud neural network approach for melt pool modeling in additive manufacturing, ASCE-ASME J Risk and Uncert in Engrg Sys Part B Mech Engrg 8 (1) (2022).
- [127] W. Zhao, H. Zhang, Y. Yan, Y. Fu, H. Wang, A semantic segmentation algorithm using fcn with combination of bslic, Applied Sciences 8 (4) (2018) 500.
- [128] M. Zhang, P. Kadam, S. Liu, C.-C. J. Kuo, Unsupervised feedforward feature (uff) learning for point cloud classification and segmentation, in: 2020 IEEE International Conference on Visual Communications and Image Processing (VCIP), IEEE, online, 2020, pp. 144–147.
- [129] A. Murtiyoso, C. Lhenry, T. Landes, P. Grussenmeyer, E. Alby, Semantic segmentation for building façade 3d point cloud from 2d orthophoto images using transfer learning, ISPRS-International Archives of the Photogrammetry, Remote Sensing and Spatial Information Sciences 43 (2021) 201–206.
- [130] M. Imad, O. Doukhi, D.-J. Lee, Transfer learning based semantic segmentation for 3d object detection from point cloud, Sensors 21 (12) (2021) 3964.
- [131] C. Zong, H. Wang, et al., An improved 3d point cloud instance segmentation method for overhead catenary height detection, Computers & Electrical Engineering 98 (2022) 107685.
- [132] D. Bazazian, D. Nahata, Dcg-net: Dynamic capsule graph convolutional network for point clouds, IEEE Access 8 (2020) 188056–188067.
- [133] N. Arnold, P. Angelov, T. Viney, P. Atkinson, Automatic extraction and labelling of memorial objects from 3d point clouds, Journal of Computer Applications in Archaeology 4 (1) (2021).
- [134] D. Urbach, Y. Ben-Shabat, M. Lindenbaum, Dpdist: Comparing point clouds using deep point cloud distance, in: Computer Vision—ECCV 2020: 16th European Conference, Glasgow, UK, August 23–28, 2020, Proceedings, Part XI 16, Springer, 2020, pp. 545–560.
- [135] D. P. Huttenlocher, G. A. Klanderman, W. J. Rucklidge, Comparing images using the hausdorff distance, IEEE Transactions on pattern analysis and machine intelligence 15 (9) (1993) 850–863.
- [136] T. Nguyen, Q.-H. Pham, T. Le, T. Pham, N. Ho, B.-S. Hua, Point-set distances for learning representations of 3d point clouds, in: Proceedings of the IEEE/CVF International Conference on Computer Vision, Montreal, BC, Canada, 2021, pp. 10478–10487.
- [137] Z. Xie, N. Somani, Y. J. S. Tan, J. C. Y. Seng, Automatic toolpath pattern recommendation for various industrial applications based on deep learning, in: 2021 IEEE/SICE International Symposium on System Integration (SII), IEEE, 2021, pp. 60–65.
- [138] X. Lei, H. Wang, C. Wang, Z. Zhao, J. Miao, P. Tian, Als point cloud classification by integrating an improved fully convolutional network into transfer learning with multi-scale and multi-view deep features, Sensors 20 (23) (2020) 6969.
- [139] X. Li, C. Li, Z. Tong, A. Lim, J. Yuan, Y. Wu, J. Tang, R. Huang, Campus3d: A photogrammetry point cloud benchmark for hierarchical understanding of outdoor scene, in: Proceedings of the 28th ACM International Conference on Multimedia, 2020, pp. 238–246.
- [140] J. Kim, D. Chung, Y. Kim, H. Kim, Deep learning-based 3d reconstruction of scaffolds using a robot dog, Automation in Construction 134 (2022) 104092.
- [141] P.-Y. Chen, Z. Y. Wu, E. Taciroglu, Classification of soft-story buildings using deep learning with density features extracted from 3d point clouds, Journal of Computing in Civil Engineering 35 (3) (2021) 04021005.
- [142] K. Sidor, M. Wysocki, Recognition of human activities using depth maps and the viewpoint feature histogram descriptor, Sensors 20 (10) (2020) 2940.
- [143] J. Tian, J. Zhang, W. Li, D. Xu, Vdm-da: Virtual domain modeling for source data-free domain adaptation, IEEE Transactions on Circuits and Systems for Video Technology (2021).
- [144] K. Huang, X. Qu, S. Chen, Z. Chen, W. Zhang, H. Qi, F. Zhao, Superb monocular depth estimation based on transfer learning and surface normal guidance, Sensors 20 (17) (2020) 4856.
- [145] H. Benhabiles, K. Hammoudi, F. Windal, M. Melkemi, A. Cabani, A transfer learning exploited for indexing protein structures from 3d point clouds, in: Sipaim—Miccai Biomedical Workshop, Springer, 2018, pp. 82–89.

- [146] K. B. Ozyoruk, G. I. Gokceler, T. L. Bobrow, G. Coskun, K. Incetan, Y. Almalioglu, F. Mahmood, E. Curto, L. Perdigoto, M. Oliveira, et al., Endoslam dataset and an unsupervised monocular visual odometry and depth estimation approach for endoscopic videos, *Medical image analysis* 71 (2021) 102058.
- [147] A. X. Chang, T. Funkhouser, L. Guibas, P. Hanrahan, Q. Huang, Z. Li, S. Savarese, M. Savva, S. Song, H. Su, et al., Shapenet: An information-rich 3d model repository, *arXiv preprint arXiv:1512.03012* (2015).
- [148] B. Eckart, W. Yuan, C. Liu, J. Kautz, Self-supervised learning on 3d point clouds by learning discrete generative models, in: *Proceedings of the IEEE/CVF Conference on Computer Vision and Pattern Recognition*, IEEE, Nashville, TN, USA, 2021, pp. 8248–8257.
- [149] S. Lee, Y. Yang, Progressive deep learning framework for recognizing 3d orientations and object class based on point cloud representation, *Sensors* 21 (18) (2021) 6108.
- [150] B. Dai, C. Le Gentil, T. Vidal-Calleja, Connecting the dots for real-time lidar-based object detection with yolo, in: *Australasian Conference on Robotics and Automation*, ACRA, ARAA, Lincoln, Canterbury, New Zealand, 2018.
- [151] G. Diraco, P. Siciliano, A. Leone, Remaining useful life prediction from 3d scan data with genetically optimized convolutional neural networks, *Sensors* 21 (20) (2021) 6772.
- [152] J. Kang, M. Körner, Y. Wang, H. Taubenböck, X. X. Zhu, Building instance classification using street view images, *ISPRS journal of photogrammetry and remote sensing* 145 (2018) 44–59.
- [153] C. Wu, X. Bi, J. Pfrommer, A. Cebulla, S. Mangold, J. Beyerer, Sim2real transfer learning for point cloud segmentation: An industrial application case on autonomous disassembly, in: *Proceedings of the IEEE/CVF Winter Conference on Applications of Computer Vision*, IEEE, Waikoloa, HI, USA, 2023, pp. 4531–4540.
- [154] Y. Zhou, A. Ji, L. Zhang, X. Xue, Sampling-attention deep learning network with transfer learning for large-scale urban point cloud semantic segmentation, *Engineering Applications of Artificial Intelligence* 117 (2023) 105554.
- [155] B. Wu, X. Zhou, S. Zhao, X. Yue, K. Keutzer, Squeezesegv2: Improved model structure and unsupervised domain adaptation for road-object segmentation from a lidar point cloud, in: *2019 International Conference on Robotics and Automation (ICRA)*, IEEE, Montreal, Canada, 2019, pp. 4376–4382.
- [156] P. Jiang, S. Saripalli, Lidarnet: A boundary-aware domain adaptation model for point cloud semantic segmentation, in: *2021 IEEE International Conference on Robotics and Automation (ICRA)*, IEEE, Xi'an, China, 2021, pp. 2457–2464.
- [157] L. Yi, B. Gong, T. Funkhouser, Complete & label: A domain adaptation approach to semantic segmentation of lidar point clouds, in: *Proceedings of the IEEE/CVF Conference on Computer Vision and Pattern Recognition*, IEEE, Nashville, TN, USA, 2021, pp. 15363–15373.
- [158] C. Qin, H. You, L. Wang, C.-C. J. Kuo, Y. Fu, Pointdan: A multi-scale 3d domain adaption network for point cloud representation, *Advances in Neural Information Processing Systems* 32 (2019).
- [159] S. Zhao, Y. Wang, B. Li, B. Wu, Y. Gao, P. Xu, T. Darrell, K. Keutzer, epointda: An end-to-end simulation-to-real domain adaptation framework for lidar point cloud segmentation, in: *Proceedings of the AAAI Conference on Artificial Intelligence*, Vol. 35, online, 2021, pp. 3500–3509.
- [160] Q. Xu, Y. Zhou, W. Wang, C. R. Qi, D. Anguelov, Spg: Unsupervised domain adaptation for 3d object detection via semantic point generation, in: *Proceedings of the IEEE/CVF International Conference on Computer Vision*, Montreal, BC, Canada, 2021, pp. 15446–15456.
- [161] A. H. Lang, S. Vora, H. Caesar, L. Zhou, J. Yang, O. Beijbom, Pointpillars: Fast encoders for object detection from point clouds, in: *Proceedings of the IEEE/CVF conference on computer vision and pattern recognition*, IEEE, Long Beach, CA, USA, 2019, pp. 12697–12705.
- [162] Y. Wang, J. Yin, W. Li, P. Frossard, R. Yang, J. Shen, Ssda3d: Semi-supervised domain adaptation for 3d object detection from point cloud, *arXiv preprint arXiv:2212.02845* (2022).
- [163] L. Du, X. Ye, X. Tan, J. Feng, Z. Xu, E. Ding, S. Wen, Associate-3ddet: Perceptual-to-conceptual association for 3d point cloud object detection, in: *Proceedings of the IEEE/CVF conference on computer vision and pattern recognition*, Seattle, WA, USA, 2020, pp. 13329–13338.
- [164] Y. Guo, Y. Li, L. Wang, T. Rosing, Adafilter: Adaptive filter fine-tuning for deep transfer learning, in: *Proceedings of the AAAI Conference on Artificial Intelligence*, Vol. 34, AAAI, New York Midtown, New York, USA, 2020, pp. 4060–4066.
- [165] A. Kumar, P. Sattigeri, K. Wadhawan, L. Karlinsky, R. Feris, B. Freeman, G. Wornell, Co-regularized alignment for unsupervised domain adaptation, *Advances in Neural Information Processing Systems* 31 (2018).
- [166] Z. Li, X. Li, Y. Wei, L. Bing, Y. Zhang, Q. Yang, Transferable end-to-end aspect-based sentiment analysis with selective adversarial learning, *arXiv preprint arXiv:1910.14192* (2019).
- [167] W. Ge, Y. Yu, Borrowing treasures from the wealthy: Deep transfer learning through selective joint fine-tuning, in: *Proceedings of the IEEE conference on computer vision and pattern recognition*, IEEE, Honolulu, HI, USA, 2017, pp. 1086–1095.
- [168] M. Maqsood, F. Nazir, U. Khan, F. Aadil, H. Jamal, I. Mehmood, O.-y. Song, Transfer learning assisted classification and detection of alzheimer's disease stages using 3d mri scans, *Sensors* 19 (11) (2019) 2645.
- [169] U. Côté-Allard, C. L. Fall, A. Drouin, A. Campeau-Lecours, C. Gosselin, K. Glette, F. Laviolette, B. Gosselin, Deep learning for electromyographic hand gesture signal classification using transfer learning, *IEEE transactions on neural systems and rehabilitation engineering* 27 (4) (2019) 760–771.
- [170] C.-X. Ren, D.-Q. Dai, K.-K. Huang, Z.-R. Lai, Transfer learning of structured representation for face recognition, *IEEE Transactions on image processing* 23 (12) (2014) 5440–5454.
- [171] F. Matrone, M. Martini, Transfer learning and performance enhancement techniques for deep semantic segmentation of built heritage point clouds, *Virtual Archaeology Review* 12 (25) (2021) 73–84.
- [172] L. Xuhong, Y. Grandvalet, F. Davoine, Explicit inductive bias for transfer learning with convolutional networks, in: *International Conference on Machine Learning*, PMLR, PMLR, tockholm, Sweden, 2018, pp. 2825–2834.
- [173] H. Xiu, T. Shinohara, M. Matsuoka, M. Inoguchi, K. Kawabe, K. Horie, Collapsed building detection using 3d point clouds and deep learning, *Remote Sensing* 12 (24) (2020) 4057.

- [174] Y. Wang, Y. Sun, Z. Liu, S. E. Sarma, M. M. Bronstein, J. M. Solomon, Dynamic graph cnn for learning on point clouds, *Acm Transactions On Graphics (tog)* 38 (5) (2019) 1–12.
- [175] K. Jeon, G. Lee, S. Yang, H. D. Jeong, Named entity recognition of building construction defect information from text with linguistic noise, *Automation in Construction* 143 (2022) 104543.
- [176] M.-Y. Cheng, R. R. Khasani, K. Setiono, Image quality enhancement using hybridgan for automated railway track defect recognition, *Automation in Construction* 146 (2023) 104669.
- [177] G. Kang, L. Jiang, Y. Yang, A. G. Hauptmann, Contrastive adaptation network for unsupervised domain adaptation, in: *Proceedings of the IEEE/CVF Conference on Computer Vision and Pattern Recognition*, Long Beach, CA, USA, 2019, pp. 4893–4902.
- [178] J. Geyer, Y. Kassahun, M. Mahmudi, X. Ricou, R. Durgesh, A. S. Chung, L. Hauswald, V. H. Pham, M. Mühlegg, S. Dorn, T. Fernandez, M. Jänicke, S. Mirashi, C. Savani, M. Sturm, O. Vorobiov, M. Oelker, S. Garreis, P. Schuberth, A2d2: Audi autonomous driving dataset (2020). [arXiv:2004.06320](https://arxiv.org/abs/2004.06320).
- [179] R. Wang, Z. Wu, Z. Weng, J. Chen, G.-J. Qi, Y.-G. Jiang, Cross-domain contrastive learning for unsupervised domain adaptation, *IEEE Transactions on Multimedia* (2022) 1–1 [doi:10.1109/TMM.2022.3146744](https://doi.org/10.1109/TMM.2022.3146744).
- [180] B. Xie, S. Li, F. Lv, C. H. Liu, G. Wang, D. Wu, A collaborative alignment framework of transferable knowledge extraction for unsupervised domain adaptation, *IEEE Transactions on Knowledge and Data Engineering* (2022). [doi:10.1109/TKDE.2022.3185233](https://doi.org/10.1109/TKDE.2022.3185233).
- [181] C.-X. Ren, Y.-H. Liu, X.-W. Zhang, K.-K. Huang, Multi-source unsupervised domain adaptation via pseudo target domain, *IEEE Transactions on Image Processing* 31 (2022) 2122–2135. [doi:10.1109/TIP.2022.3152052](https://doi.org/10.1109/TIP.2022.3152052).
- [182] B. Fernando, A. Habrard, M. Sebban, T. Tuytelaars, Unsupervised visual domain adaptation using subspace alignment, in: *2013 IEEE International Conference on Computer Vision, IEEE*, Sydney, Australia, 2013, pp. 2960–2967. [doi:10.1109/ICCV.2013.368](https://doi.org/10.1109/ICCV.2013.368).
- [183] M. M. Bronstein, J. Bruna, Y. LeCun, A. Szlam, P. Vandergheynst, Geometric deep learning: Going beyond euclidean data, *IEEE Signal Processing Magazine* 34 (4) (2017) 18–42. [doi:10.1109/MSP.2017.2693418](https://doi.org/10.1109/MSP.2017.2693418).
- [184] C.-Y. Lee, T. Batra, M. H. Baig, D. Ulbricht, Sliced wasserstein discrepancy for unsupervised domain adaptation, in: *2019 IEEE/CVF Conference on Computer Vision and Pattern Recognition (CVPR)*, IEEE, Long Beach, CA, USA, 2019, pp. 10277–10287. [doi:10.1109/CVPR.2019.01053](https://doi.org/10.1109/CVPR.2019.01053).
- [185] C. Ledig, L. Theis, F. Huszar, J. Caballero, A. Cunningham, A. Acosta, A. Aitken, A. Tejani, J. Totz, Z. Wang, W. Shi, Photo-realistic single image super-resolution using a generative adversarial network (2017). [arXiv:1609.04802](https://arxiv.org/abs/1609.04802).
- [186] J. Huang, H. Zhang, L. Yi, T. Funkhouser, M. NieBner, L. Guibas, Texturenet: Consistent local parametrizations for learning from high-resolution signals on meshes, in: *2019 IEEE/CVF Conference on Computer Vision and Pattern Recognition (CVPR)*, IEEE, Long Beach, CA, USA, 2019, pp. 4435–4444.
- [187] B. Gong, K. Grauman, F. Sha, Reshaping visual datasets for domain adaptation, *Advances in Neural Information Processing Systems* 26 (2013).
- [188] Y. Shen, Y. Yang, M. Yan, H. Wang, Y. Zheng, L. J. Guibas, Domain adaptation on point clouds via geometry-aware implicits, in: *Proceedings of the IEEE/CVF Conference on Computer Vision and Pattern Recognition*, New Orleans, LA, USA, 2022, pp. 7223–7232.
- [189] J.-Y. Zhu, T. Park, P. Isola, A. A. Efros, Unpaired image-to-image translation using cycle-consistent adversarial networks, in: *Proceedings of the IEEE international conference on computer vision*, IEEE, Venice, Italy, 2017, pp. 2223–2232.
- [190] K. Saleh, A. Abobakr, M. Attia, J. Iskander, D. Nahavandi, M. Hossny, S. Nahvandi, Domain adaptation for vehicle detection from bird’s eye view lidar point cloud data, in: *Proceedings of the IEEE/CVF International Conference on Computer Vision Workshops*, IEEE, Seoul, Korea, 2019, pp. 0–0.
- [191] X. Zhou, A. Karpur, C. Gan, L. Luo, Q. Huang, Unsupervised domain adaptation for 3d keypoint estimation via view consistency, in: *Proceedings of the European conference on computer vision (ECCV)*, IEEE, Munich, Germany, 2018, pp. 137–153.
- [192] Y. Wang, X. Chen, Y. You, L. E. Li, B. Hariharan, M. Campbell, K. Q. Weinberger, W.-L. Chao, Train in germany, test in the usa: Making 3d object detectors generalize, in: *Proceedings of the IEEE/CVF Conference on Computer Vision and Pattern Recognition*, IEEE, Seattle, WA, USA, 2020, pp. 11713–11723.
- [193] A. Geiger, P. Lenz, C. Stiller, R. Urtasun, Vision meets robotics: The kitti dataset, *The International Journal of Robotics Research* 32 (11) (2013) 1231–1237.
- [194] P. Sun, H. Kretschmar, X. Dotiwalla, A. Chouard, V. Patnaik, P. Tsui, J. Guo, Y. Zhou, Y. Chai, B. Caine, et al., Scalability in perception for autonomous driving: Waymo open dataset, in: *Proceedings of the IEEE/CVF conference on computer vision and pattern recognition*, IEEE, Seattle, WA, USA, 2020, pp. 2446–2454.
- [195] J. Yang, S. Shi, Z. Wang, H. Li, X. Qi, St3d: Self-training for unsupervised domain adaptation on 3d object detection, in: *Proceedings of the IEEE/CVF conference on computer vision and pattern recognition*, IEEE, Nashville, TN, USA, 2021, pp. 10368–10378.
- [196] M. Jaritz, T.-H. Vu, R. d. Charette, E. Wirbel, P. Pérez, xmuda: Cross-modal unsupervised domain adaptation for 3d semantic segmentation, in: *Proceedings of the IEEE/CVF conference on computer vision and pattern recognition*, Seattle, WA, USA, 2020, pp. 12605–12614.
- [197] C. Saltori, S. Lathuilière, N. Sebe, E. Ricci, F. Galasso, Sf-uda 3d: Source-free unsupervised domain adaptation for lidar-based 3d object detection, in: *2020 International Conference on 3D Vision (3DV)*, IEEE, Fukuoka, Japan, 2020, pp. 771–780.
- [198] A. Cardace, R. Spezialetti, P. Z. Ramirez, S. Salti, L. Di Stefano, Refrec: Pseudo-labels refinement via shape reconstruction for unsupervised 3d domain adaptation, in: *2021 International Conference on 3D Vision (3DV)*, IEEE, 2021, pp. 331–341.
- [199] L. Shi, Z. Yuan, M. Cheng, Y. Chen, C. Wang, Dfan: Dual-branch feature alignment network for domain adaptation on point clouds, *IEEE Transactions on Geoscience and Remote Sensing* 60 (2022) 1–12.
- [200] D. Kang, Y. Nam, D. Kyung, J. Choi, Unsupervised domain adaptation for 3d point clouds by searched transformations, *IEEE Access* 10 (2022) 56901–56913.
- [201] Y. S. Tang, G. H. Lee, Transferable semi-supervised 3d object detection from rgb-d data, in: *Proceedings of the IEEE/CVF international conference on computer vision*, 2019, pp. 1931–1940.

- [202] X. Huang, G. Mei, J. Zhang, Feature-metric registration: A fast semi-supervised approach for robust point cloud registration without correspondences, in: Proceedings of the IEEE/CVF conference on computer vision and pattern recognition, 2020, pp. 11366–11374.
- [203] S. Horache, J.-E. Deschaud, F. Goulette, 3d point cloud registration with multi-scale architecture and unsupervised transfer learning, in: 2021 international conference on 3D vision (3DV), IEEE, 2021, pp. 1351–1361.
- [204] H. Li, Z. Sun, Y. Wu, Y. Song, Semi-supervised point cloud segmentation using self-training with label confidence prediction, *Neurocomputing* 437 (2021) 227–237.
- [205] Z. Chen, L. Jing, Y. Liang, Y. Tian, B. Li, Multimodal semi-supervised learning for 3d objects, arXiv preprint arXiv:2110.11601 (2021).
- [206] A. Xiao, J. Huang, D. Guan, F. Zhan, S. Lu, Transfer learning from synthetic to real lidar point cloud for semantic segmentation, in: Proceedings of the AAAI conference on artificial intelligence, Vol. 36, 2022, pp. 2795–2803.
- [207] J. Mei, B. Gao, D. Xu, W. Yao, X. Zhao, H. Zhao, Semantic segmentation of 3d lidar data in dynamic scene using semi-supervised learning, *IEEE Transactions on Intelligent Transportation Systems* 21 (6) (2019) 2496–2509.
- [208] S. Huang, Y. Xie, S.-C. Zhu, Y. Zhu, Spatio-temporal self-supervised representation learning for 3d point clouds, in: Proceedings of the IEEE/CVF International Conference on Computer Vision, 2021, pp. 6535–6545.
- [209] Z. Qin, J. Wang, Y. Lu, Weakly supervised 3d object detection from point clouds, in: Proceedings of the 28th ACM International Conference on Multimedia, 2020, pp. 4144–4152.
- [210] P.-C. Yu, C. Sun, M. Sun, Data efficient 3d learner via knowledge transferred from 2d model, in: European Conference on Computer Vision, Springer, 2022, pp. 182–198.
- [211] Z. Xu, B. Yuan, S. Zhao, Q. Zhang, X. Gao, Hierarchical point-based active learning for semi-supervised point cloud semantic segmentation, in: Proceedings of the IEEE/CVF International Conference on Computer Vision, 2023, pp. 18098–18108.
- [212] D. Zhang, D. Liang, Z. Zou, J. Li, X. Ye, Z. Liu, X. Tan, X. Bai, A simple vision transformer for weakly semi-supervised 3d object detection, in: Proceedings of the IEEE/CVF International Conference on Computer Vision, 2023, pp. 8373–8383.
- [213] Y. Wang, J. Yin, W. Li, P. Frossard, R. Yang, J. Shen, Ssd3d: Semi-supervised domain adaptation for 3d object detection from point cloud, in: Proceedings of the AAAI Conference on Artificial Intelligence, Vol. 37, 2023, pp. 2707–2715.
- [214] F. Zhuang, Z. Qi, K. Duan, D. Xi, Y. Zhu, H. Zhu, H. Xiong, Q. He, A comprehensive survey on transfer learning, *Proceedings of the IEEE* 109 (1) (2020) 43–76.
- [215] S. J. Pan, Q. Yang, A survey on transfer learning, *IEEE Transactions on knowledge and data engineering* 22 (10) (2009) 1345–1359.
- [216] Q. Hu, B. Yang, L. Xie, S. Rosa, Y. Guo, Z. Wang, N. Trigoni, A. Markham, Randa-net: Efficient semantic segmentation of large-scale point clouds, in: Proceedings of the IEEE/CVF Conference on Computer Vision and Pattern Recognition, Seattle, WA, USA, 2020, pp. 11108–11117.
- [217] T. Hackel, N. Savinov, L. Ladicky, J. D. Wegner, K. Schindler, M. Pollefeys, Semantic3d. net: A new large-scale point cloud classification benchmark, arXiv preprint arXiv:1704.03847 (2017).
- [218] C. Zhao, H. Guo, J. Lu, D. Yu, D. Li, X. Chen, Als point cloud classification with small training data set based on transfer learning, *IEEE Geoscience and Remote Sensing Letters* 17 (8) (2019) 1406–1410.
- [219] Z. Liu, H. Tang, Y. Lin, S. Han, Point-voxel cnn for efficient 3d deep learning, *Advances in Neural Information Processing Systems* 32 (2019).
- [220] C. Sun, M. Ma, Z. Zhao, S. Tian, R. Yan, X. Chen, Deep transfer learning based on sparse autoencoder for remaining useful life prediction of tool in manufacturing, *IEEE Transactions on Industrial Informatics* 15 (4) (2018) 2416–2425.
- [221] L. Huang, H. Guo, Q. Rao, Z. Hou, S. Li, S. Qiu, X. Fan, H. Wang, Body dimension measurements of qinchuan cattle with transfer learning from lidar sensing, *Sensors* 19 (22) (2019) 5046.
- [222] A. Arnold, R. Nallapati, W. W. Cohen, A comparative study of methods for transductive transfer learning, in: Seventh IEEE international conference on data mining workshops (ICDMW 2007), IEEE, IEEE, Omaha, NE, 2007, pp. 77–82.
- [223] K. Bousmalis, N. Silberman, D. Dohan, D. Erhan, D. Krishnan, Unsupervised pixel-level domain adaptation with generative adversarial networks, in: Proceedings of the IEEE conference on computer vision and pattern recognition, IEEE, Honolulu, HI, USA, 2017, pp. 3722–3731.
- [224] L. Duan, I. W. Tsang, D. Xu, Domain transfer multiple kernel learning, *IEEE Transactions on Pattern Analysis and Machine Intelligence* 34 (3) (2012) 465–479.
- [225] M. Long, H. Zhu, J. Wang, M. I. Jordan, Deep transfer learning with joint adaptation networks, in: International conference on machine learning, PMLR, PMLR, Sydney, Australia, 2017, pp. 2208–2217.
- [226] W. Zhang, W. Ouyang, W. Li, D. Xu, Collaborative and adversarial network for unsupervised domain adaptation, in: Proceedings of the IEEE conference on computer vision and pattern recognition, IEEE, Salt Lake City, UT, USA, 2018, pp. 3801–3809.
- [227] C. B. Rist, M. Enzweiler, D. M. Gavrila, Cross-sensor deep domain adaptation for lidar detection and segmentation, in: 2019 IEEE Intelligent Vehicles Symposium (IV), IEEE, 2019, pp. 1535–1542.
- [228] Z. Wang, S. Ding, Y. Li, M. Zhao, S. Roychowdhury, A. Wallin, G. Sapiro, Q. Qiu, Range adaptation for 3d object detection in lidar, in: Proceedings of the IEEE/CVF International Conference on Computer Vision Workshops, Seoul, Korea, 2019, pp. 0–0.
- [229] Z. Wang, L. Wang, B. Dai, Strong-weak feature alignment for 3d object detection, *Electronics* 10 (10) (2021) 1205.
- [230] W. Zhang, W. Li, D. Xu, Srdan: Scale-aware and range-aware domain adaptation network for cross-dataset 3d object detection, in: Proceedings of the IEEE/CVF Conference on Computer Vision and Pattern Recognition, Nashville, TN, USA, 2021, pp. 6769–6779.
- [231] L. Nunes, R. Marcuzzi, X. Chen, J. Behley, C. Stachniss, Segcontrast: 3d point cloud feature representation learning through self-supervised segment discrimination, *IEEE Robotics and Automation Letters* 7 (2) (2022) 2116–2123.
- [232] W. Liu, Z. Luo, Y. Cai, Y. Yu, Y. Ke, J. M. Junior, W. N. Gonçalves, J. Li, Adversarial unsupervised domain adaptation for 3d semantic segmentation with multi-modal learning, *ISPRS Journal of Photogrammetry and Remote Sensing* 176 (2021) 211–221.
- [233] H. Tang, C. Xu, J. Yang, Bi-adversarial discrepancy minimization for unsupervised domain adaptation on 3d point cloud, in: 2021 International Joint Conference on Neural Networks (IJCNN), IEEE, IEEE, online, 2021, pp. 1–8.

- [234] S. Vesal, M. Gu, R. Kosti, A. Maier, N. Ravikumar, Adapt everywhere: unsupervised adaptation of point-clouds and entropy minimization for multi-modal cardiac image segmentation, *IEEE Transactions on Medical Imaging* 40 (7) (2021) 1838–1851.
- [235] M. A. U. Alam, M. M. Rahman, J. Q. Widberg, Palmar: Towards adaptive multi-inhabitant activity recognition in point-cloud technology, in: *IEEE INFOCOM 2021-IEEE Conference on Computer Communications*, IEEE, IEEE, online, 2021, pp. 1–10.
- [236] Z. Wang, L. Wang, L. Xiao, B. Dai, Unsupervised subcategory domain adaptive network for 3d object detection in lidar, *Electronics* 10 (8) (2021) 927.
- [237] Z. Qiao, H. Hu, W. Shi, S. Chen, Z. Liu, H. Wang, A registration-aided domain adaptation network for 3d point cloud based place recognition, in: *2021 IEEE/RSJ International Conference on Intelligent Robots and Systems (IROS)*, IEEE, IEEE, Prague, Czech Republic, 2021, pp. 1317–1322.
- [238] X. Zhu, H. Manamasa, J. L. J. Sánchez, A. Maki, L. Hanson, Automatic assembly quality inspection based on an unsupervised point cloud domain adaptation model, *Procedia CIRP* 104 (2021) 1801–1806.
- [239] F. Wang, W. Li, D. Xu, Cross-dataset point cloud recognition using deep-shallow domain adaptation network, *IEEE Transactions on Image Processing* 30 (2021) 7364–7377.
- [240] M. A. U. Alam, F. Mazzoni, M. M. Rahman, J. Widberg, Lamar: Lidar based multi-inhabitant activity recognition, in: *MobiQuitous 2020-17th EAI International Conference on Mobile and Ubiquitous Systems: Computing, Networking and Services*, EAI, online, 2020, pp. 1–9.
- [241] M. Jaritz, T.-H. Vu, R. De Charette, É. Wirbel, P. Pérez, Cross-modal learning for domain adaptation in 3d semantic segmentation, *IEEE Transactions on Pattern Analysis and Machine Intelligence* 45 (2) (2022) 1533–1544.
- [242] K. Saleh, A. Abobakr, D. Nahavandi, J. Iskander, M. Attia, M. Hossny, S. Nahavandi, Cyclist intent prediction using 3d lidar sensors for fully automated vehicles, in: *2019 IEEE Intelligent Transportation Systems Conference (ITSC)*, IEEE, IEEE, Auckland, New Zealand, 2019, pp. 2020–2026.
- [243] M. Pham, S. Aise, C. A. Knoblock, P. Szekely, Semantic labeling: a domain-independent approach, in: *International Semantic Web Conference*, Springer, Springer, Kobe, Japan, 2016, pp. 446–462.
- [244] T. Xia, J. Yang, L. Chen, Automated semantic segmentation of bridge point cloud based on local descriptor and machine learning, *Automation in Construction* 133 (2022) 103992.
- [245] R. Sun, X. Zhu, C. Wu, C. Huang, J. Shi, L. Ma, Not all areas are equal: Transfer learning for semantic segmentation via hierarchical region selection, in: *Proceedings of the IEEE/CVF Conference on Computer Vision and Pattern Recognition*, Long Beach, CA, USA, 2019, pp. 4360–4369.
- [246] S. Hong, J. Oh, H. Lee, B. Han, Learning transferrable knowledge for semantic segmentation with deep convolutional neural network, in: *Proceedings of the IEEE Conference on Computer Vision and Pattern Recognition*, IEEE, Las Vegas, NV, USA, 2016, pp. 3204–3212.
- [247] H. A. Arief, U. G. Indahl, G.-H. Strand, H. Tveite, Addressing overfitting on point cloud classification using atrous xcrf, *ISPRS Journal of Photogrammetry and Remote Sensing* 155 (2019) 90–101.
- [248] H. Yang, J. Shi, L. Carlone, Teaser: Fast and certifiable point cloud registration, *IEEE Transactions on Robotics* 37 (2) (2020) 314–333.
- [249] S. Choi, Q.-Y. Zhou, V. Koltun, Robust reconstruction of indoor scenes, in: *Proceedings of the IEEE Conference on Computer Vision and Pattern Recognition*, IEEE, Boston, MA, USA, 2015, pp. 5556–5565.
- [250] Y. Wang, J. M. Solomon, Deep closest point: Learning representations for point cloud registration, in: *Proceedings of the IEEE/CVF international conference on computer vision*, Seoul, Korea (South), 2019, pp. 3523–3532.
- [251] Y. Chen, J. Liu, B. Ni, H. Wang, J. Yang, N. Liu, T. Li, Q. Tian, Shape self-correction for unsupervised point cloud understanding, in: *Proceedings of the IEEE/CVF International Conference on Computer Vision*, Montreal, BC, Canada, 2021, pp. 8382–8391.
- [252] R. Zhang, Z. Guo, W. Zhang, K. Li, X. Miao, B. Cui, Y. Qiao, P. Gao, H. Li, Pointclip: Point cloud understanding by clip, *arXiv preprint arXiv:2112.02413* (2021).
- [253] K. Liu, Z. Gao, F. Lin, B. M. Chen, Fg-net: A fast and accurate framework for large-scale lidar point cloud understanding, *IEEE Transactions on Cybernetics* (2022).
- [254] R. Roveri, A. C. Öztireli, I. Pandele, M. Gross, Pointpronet: Consolidation of point clouds with convolutional neural networks, in: *Computer Graphics Forum*, Vol. 37, Wiley Online Library, 2018, pp. 87–99.
- [255] S. Luo, W. Hu, Score-based point cloud denoising, in: *Proceedings of the IEEE/CVF International Conference on Computer Vision*, Montreal, BC, Canada, 2021, pp. 4583–4592.
- [256] J. Zeng, G. Cheung, M. Ng, J. Pang, C. Yang, 3d point cloud denoising using graph laplacian regularization of a low dimensional manifold model, *IEEE Transactions on Image Processing* 29 (2019) 3474–3489.
- [257] C. Dinesh, G. Cheung, I. V. Bajic, C. Yang, Fast 3d point cloud denoising via bipartite graph approximation & total variation, *arXiv preprint arXiv:1804.10831* (2018).
- [258] C. Duan, S. Chen, J. Kovačević, Weighted multi-projection: 3d point cloud denoising with estimated tangent planes, *arXiv preprint arXiv:1807.00253* (2018).
- [259] W. Hu, X. Gao, G. Cheung, Z. Guo, Feature graph learning for 3d point cloud denoising, *IEEE Transactions on Signal Processing* 68 (2020) 2841–2856.
- [260] V. Badrinarayanan, A. Kendall, R. Cipolla, Segnet: A deep convolutional encoder-decoder architecture for image segmentation, *IEEE transactions on pattern analysis and machine intelligence* 39 (12) (2017) 2481–2495.
- [261] A. Eltner, P. O. Bressan, T. Akiyama, W. N. Gonçalves, J. Marcato Junior, Using deep learning for automatic water stage measurements, *Water Resources Research* 57 (3) (2021) e2020WR027608.
- [262] C. Zhang, J. Shi, X. Deng, Z. Wu, Upsampling autoencoder for self-supervised point cloud learning, *arXiv preprint arXiv:2203.10768* (2022).
- [263] L. Garrote, J. Rosa, J. Paulo, C. Premebida, P. Peixoto, U. J. Nunes, 3d point cloud downsampling for 2d indoor scene modelling in mobile robotics, in: *2017 IEEE international conference on autonomous robot systems and competitions (ICARSC)*, IEEE, IEEE, Coimbra, Portugal, 2017, pp. 228–233.

- [264] S. Orts-Escolano, V. Morell, J. García-Rodríguez, M. Cazorla, Point cloud data filtering and downsampling using growing neural gas, in: The 2013 International Joint Conference on Neural Networks (IJCNN), IEEE, IEEE, Dallas, Texas, USA, 2013, pp. 1–8.
- [265] E. Nezhadarya, E. Taghavi, R. Razani, B. Liu, J. Luo, Adaptive hierarchical down-sampling for point cloud classification, in: Proceedings of the IEEE/CVF Conference on Computer Vision and Pattern Recognition, Seattle, WA, USA, 2020, pp. 12956–12964.
- [266] C. Suchocki, W. Błaszczak-Bąk, Down-sampling of point clouds for the technical diagnostics of buildings and structures, *Geosciences* 9 (2) (2019) 70.
- [267] C. Lv, M. Qi, X. Li, Z. Yang, H. Ma, Sgformer: Semantic graph transformer for point cloud-based 3d scene graph generation, in: Proceedings of the AAAI Conference on Artificial Intelligence, Vol. 38, 2024, pp. 4035–4043.
- [268] Z. Li, Z. Li, Z. Cui, M. Pollefeys, M. R. Oswald, Sat2scene: 3d urban scene generation from satellite images with diffusion, in: Proceedings of the IEEE/CVF Conference on Computer Vision and Pattern Recognition, 2024, pp. 7141–7150.
- [269] P. Li, C. Tang, Q. Huang, Z. Li, Art3d: 3d gaussian splatting for text-guided artistic scenes generation, arXiv preprint arXiv:2405.10508 (2024).
- [270] J. Chung, S. Lee, H. Nam, J. Lee, K. M. Lee, Luciddreamer: Domain-free generation of 3d gaussian splatting scenes, arXiv preprint arXiv:2311.13384 (2023).
- [271] Y.-K. Wang, C. Xing, Y.-L. Wei, X.-M. Wu, W.-S. Zheng, Single-view scene point cloud human grasp generation, in: Proceedings of the IEEE/CVF Conference on Computer Vision and Pattern Recognition, 2024, pp. 831–841.
- [272] S. Koch, P. Hermosilla, N. Vaskevicius, M. Colosi, T. Ropinski, Sgrec3d: Self-supervised 3d scene graph learning via object-level scene reconstruction, in: Proceedings of the IEEE/CVF Winter Conference on Applications of Computer Vision, 2024, pp. 3404–3414.
- [273] Y. Liu, X. Li, X. Li, L. Qi, C. Li, M.-H. Yang, Pyramid diffusion for fine 3d large scene generation, arXiv preprint arXiv:2311.12085 (2023).
- [274] T. Mathes, D. Seidel, K.-H. Häberle, H. Pretzsch, P. Annighöfer, What are we missing? occlusion in laser scanning point clouds and its impact on the detection of single-tree morphologies and stand structural variables, *Remote Sensing* 15 (2) (2023) 450.
- [275] Y. Zhang, L. Wang, Y. Dai, Plot: a 3d point cloud object detection network for autonomous driving, *Robotica* (2023) 1–17.
- [276] Y. Himeur, M. Elnour, F. Fadli, N. Meskin, I. Petri, Y. Rezgui, F. Bensaali, A. Amira, Next-generation energy systems for sustainable smart cities: Roles of transfer learning, *Sustainable Cities and Society* (2022) 104059.
- [277] C. Romanengo, A. Raffo, S. Biasotti, B. Falcidieno, Recognising geometric primitives in 3d point clouds of mechanical cad objects, *Computer-Aided Design* (2023) 103479.
- [278] Y. Himeur, S. Al-Maadeed, I. Varlamis, N. Al-Maadeed, K. Abualsaud, A. Mohamed, Face mask detection in smart cities using deep and transfer learning: Lessons learned from the covid-19 pandemic, *Systems* 11 (2) (2023) 107.
- [279] A. Argyriou, A. Maurer, M. Pontil, An algorithm for transfer learning in a heterogeneous environment, in: Joint European Conference on Machine Learning and Knowledge Discovery in Databases, Springer, Springer, Antwerp, Belgium, 2008, pp. 71–85.
- [280] R. Gong, D. Dai, Y. Chen, W. Li, L. Van Gool, mdalu: Multi-source domain adaptation and label unification with partial datasets, in: Proceedings of the IEEE/CVF International Conference on Computer Vision, Montreal, BC, Canada, 2021, pp. 8876–8885.
- [281] L. Wang, X. Geng, X. Ma, D. Zhang, Q. Yang, Ridesharing car detection by transfer learning, *Artificial Intelligence* 273 (2019) 1–18.
- [282] P. Morerio, J. Cavazza, V. Murino, Minimal-entropy correlation alignment for unsupervised deep domain adaptation, arXiv preprint arXiv:1711.10288 (2017).
- [283] M. Liang, B. Yang, Y. Chen, R. Hu, R. Urtasun, Multi-task multi-sensor fusion for 3d object detection, in: Proceedings of the IEEE/CVF Conference on Computer Vision and Pattern Recognition, Long Beach, CA, USA, 2019, pp. 7345–7353.
- [284] A. Valada, R. Mohan, W. Burgard, Self-supervised model adaptation for multimodal semantic segmentation, *International Journal of Computer Vision* 128 (5) (2020) 1239–1285.
- [285] Y. Himeur, S. Al-Maadeed, N. Almadeed, K. Abualsaud, A. Mohamed, T. Khatib, O. Elharrouss, Deep visual social distancing monitoring to combat covid-19: A comprehensive survey, *Sustainable Cities and Society* (2022) 104064.
- [286] G. Mateo-García, V. Laparra, D. López-Puigdollers, L. Gómez-Chova, Transferring deep learning models for cloud detection between landsat-8 and proba-v, *ISPRS Journal of Photogrammetry and Remote Sensing* 160 (2020) 1–17.
- [287] X. Ling, R. Qin, A graph-matching approach for cross-view registration of over-view and street-view based point clouds, *ISPRS Journal of Photogrammetry and Remote Sensing* 185 (2022) 2–15.
- [288] X. Glorot, A. Bordes, Y. Bengio, Domain adaptation for large-scale sentiment classification: A deep learning approach, in: ICML, 2011.
- [289] W. Hu, Y. Luo, Z. Lu, Y. Wen, Heterogeneous transfer learning for thermal comfort modeling, in: Proceedings of the 6th ACM International Conference on Systems for Energy-Efficient Buildings, Cities, and Transportation, ACM, New York, NY, USA, 2019, pp. 61–70.
- [290] C. Fan, Y. Sun, F. Xiao, J. Ma, D. Lee, J. Wang, Y. C. Tseng, Statistical investigations of transfer learning-based methodology for short-term building energy predictions, *Applied Energy* 262 (2020) 114499.
- [291] J. Lin, J. Ma, J. Zhu, H. Liang, Deep domain adaptation for non-intrusive load monitoring based on a knowledge transfer learning network, *IEEE Transactions on Smart Grid* (2021).
- [292] N. Patricia, B. Caputo, Learning to learn, from transfer learning to domain adaptation: A unifying perspective, in: Proceedings of the IEEE Conference on Computer Vision and Pattern Recognition, IEEE, Columbus, OH, USA, 2014, pp. 1442–1449.
- [293] N. Djeflal, H. Kheddar, D. Addou, A. C. Mazari, Y. Himeur, Automatic speech recognition with bert and ctc transformers: A review, in: 2023 2nd International Conference on Electronics, Energy and Measurement (IC2EM), Vol. 1, IEEE, 2023, pp. 1–8.
- [294] G. Qian, X. Zhang, A. Hamdi, B. Ghanem, Pix4point: Image pretrained transformers for 3d point cloud understanding, arXiv preprint arXiv:2208.12259 (2022).
- [295] J. Devlin, M.-W. Chang, K. Lee, K. Toutanova, Bert: Pre-training of deep bidirectional transformers for language understanding, arXiv preprint arXiv:1810.04805 (2018).
- [296] Q.-H. Pham, T. Nguyen, B.-S. Hua, G. Roig, S.-K. Yeung, Jsis3d: Joint semantic-instance segmentation of 3d point clouds with multi-task pointwise networks and multi-value conditional random fields, in: Proceedings of the IEEE/CVF conference on computer vision and pattern recognition, 2019, pp. 8827–8836.

- [297] X. Zou, K. Li, Y. Li, W. Wei, C. Chen, Multi-task y-shaped graph neural network for point cloud learning in autonomous driving, *IEEE Transactions on Intelligent Transportation Systems* 23 (7) (2022) 9568–9579.
- [298] F. Chen, F. Wu, G. Gao, Y. Ji, J. Xu, G.-P. Jiang, X.-Y. Jing, Jspnet: Learning joint semantic & instance segmentation of point clouds via feature self-similarity and cross-task probability, *Pattern Recognition* 122 (2022) 108250.
- [299] D. Ye, Z. Zhou, W. Chen, Y. Xie, Y. Wang, P. Wang, H. Foroosh, Lidarmultinet: Towards a unified multi-task network for lidar perception, in: *Proceedings of the AAAI Conference on Artificial Intelligence*, Vol. 37, 2023, pp. 3231–3240.
- [300] A. Dubey, A. Santra, J. Fuchs, M. Lübke, R. Weigel, F. Lurz, Haradnet: Anchor-free target detection for radar point clouds using hierarchical attention and multi-task learning, *Machine Learning with Applications* 8 (2022) 100275.
- [301] K. Hassani, M. Haley, Unsupervised multi-task feature learning on point clouds, in: *Proceedings of the IEEE/CVF International Conference on Computer Vision*, 2019, pp. 8160–8171.
- [302] X. Lin, H. Luo, W. Guo, C. Wang, J. Li, A multi-task learning framework for semantic segmentation in mls point clouds, in: *International Conference on Adaptive and Intelligent Systems*, Springer, 2022, pp. 382–392.
- [303] L. Zhao, Y. Hu, X. Yang, Z. Dou, L. Kang, Robust multi-task learning network for complex lidar point cloud data preprocessing, *Expert Systems with Applications* 237 (2024) 121552.
- [304] T. Rios, B. van Stein, T. Bäck, B. Sendhoff, S. Menzel, Multitask shape optimization using a 3-d point cloud autoencoder as unified representation, *IEEE Transactions on Evolutionary Computation* 26 (2) (2021) 206–217.
- [305] D. Feng, Y. Zhou, C. Xu, M. Tomizuka, W. Zhan, A simple and efficient multi-task network for 3d object detection and road understanding, in: *2021 IEEE/RSJ International Conference on Intelligent Robots and Systems (IROS)*, IEEE, 2021, pp. 7067–7074.
- [306] J. Rebut, A. Ouaknine, W. Malik, P. Pérez, Raw high-definition radar for multi-task learning, in: *Proceedings of the IEEE/CVF Conference on Computer Vision and Pattern Recognition*, 2022, pp. 17021–17030.
- [307] Z. Shan, Q. Yang, R. Ye, Y. Zhang, Y. Xu, X. Xu, S. Liu, Gpa-net: No-reference point cloud quality assessment with multi-task graph convolutional network, *IEEE Transactions on Visualization and Computer Graphics* (2023).
- [308] A. Hatem, Y. Qian, Y. Wang, Point-tta: Test-time adaptation for point cloud registration using multitask meta-auxiliary learning, in: *Proceedings of the IEEE/CVF International Conference on Computer Vision*, 2023, pp. 16494–16504.
- [309] C. Zhang, H. Fan, An improved multi-task pointwise network for segmentation of building roofs in airborne laser scanning point clouds, *The Photogrammetric Record* 37 (179) (2022) 260–284.
- [310] G. Wei, L. Ma, C. Wang, C. Desrosiers, Y. Zhou, Multi-task joint learning of 3d keypoint saliency and correspondence estimation, *Computer-Aided Design* 141 (2021) 103105.
- [311] H. Zhang, S. Zhang, Y. Zhang, J. Liang, Z. Wang, Machining feature recognition based on a novel multi-task deep learning network, *Robotics and Computer-Integrated Manufacturing* 77 (2022) 102369.
- [312] M. Afham, I. Dissanayake, D. Dissanayake, A. Dharmasiri, K. Thilakarathna, R. Rodrigo, Crosspoint: Self-supervised cross-modal contrastive learning for 3d point cloud understanding, in: *Proceedings of the IEEE/CVF Conference on Computer Vision and Pattern Recognition*, 2022, pp. 9902–9912.
- [313] X. Yan, H. Zhan, C. Zheng, J. Gao, R. Zhang, S. Cui, Z. Li, Let images give you more: Point cloud cross-modal training for shape analysis, *Advances in Neural Information Processing Systems* 35 (2022) 32398–32411.
- [314] Y. Wu, J. Liu, M. Gong, P. Gong, X. Fan, A. Qin, Q. Miao, W. Ma, Self-supervised intra-modal and cross-modal contrastive learning for point cloud understanding, *IEEE Transactions on Multimedia* (2023).
- [315] J. Zhang, H. Yang, D.-J. Wu, J. Keung, X. Li, X. Zhu, Y. Ma, Cross-modal and cross-domain knowledge transfer for label-free 3d segmentation, in: *Chinese Conference on Pattern Recognition and Computer Vision (PRCV)*, Springer, 2023, pp. 465–477.
- [316] L. Jing, Y. Xue, X. Yan, C. Zheng, D. Wang, R. Zhang, Z. Wang, H. Fang, B. Zhao, Z. Li, X4d-sceneformer: Enhanced scene understanding on 4d point cloud videos through cross-modal knowledge transfer, in: *Proceedings of the AAAI Conference on Artificial Intelligence*, Vol. 38, 2024, pp. 2670–2678.
- [317] Q. Zhang, J. Hou, Y. Qian, Pointmcd: Boosting deep point cloud encoders via multi-view cross-modal distillation for 3d shape recognition, *IEEE Transactions on Multimedia* (2023).
- [318] P. Falco, S. Lu, C. Natale, S. Pirozzi, D. Lee, A transfer learning approach to cross-modal object recognition: from visual observation to robotic haptic exploration, *IEEE Transactions on Robotics* 35 (4) (2019) 987–998.
- [319] P. K. Murali, C. Wang, D. Lee, R. Dahiya, M. Kaboli, Deep active cross-modal visuo-tactile transfer learning for robotic object recognition, *IEEE Robotics and Automation Letters* 7 (4) (2022) 9557–9564.
- [320] X. Shen, I. Stamos, Simcrosstrans: A simple cross-modality transfer learning for object detection with convnets or vision transformers, *arXiv preprint arXiv:2203.10456* (2022).
- [321] L. Jing, E. Vahdani, J. Tan, Y. Tian, Cross-modal center loss for 3d cross-modal retrieval, in: *Proceedings of the IEEE/CVF Conference on Computer Vision and Pattern Recognition*, 2021, pp. 3142–3151.
- [322] Z. Zhu, L. Nan, H. Xie, H. Chen, J. Wang, M. Wei, J. Qin, Csdn: Cross-modal shape-transfer dual-refinement network for point cloud completion, *IEEE Transactions on Visualization and Computer Graphics* (2023).
- [323] M. Li, Y. Zhang, Y. Xie, Z. Gao, C. Li, Z. Zhang, Y. Qu, Cross-domain and cross-modal knowledge distillation in domain adaptation for 3d semantic segmentation, in: *Proceedings of the 30th ACM International Conference on Multimedia*, 2022, pp. 3829–3837.
- [324] D. Peng, Y. Lei, W. Li, P. Zhang, Y. Guo, Sparse-to-dense feature matching: Intra and inter domain cross-modal learning in domain adaptation for 3d semantic segmentation, in: *Proceedings of the IEEE/CVF International Conference on Computer Vision*, 2021, pp. 7108–7117.
- [325] J. Nitsch, J. Nieto, R. Siegwart, M. Schmidt, C. Cadena, Learning common and transferable feature representations for multi-modal data, in: *2020 IEEE Intelligent Vehicles Symposium (IV)*, IEEE, 2020, pp. 1601–1607.
- [326] M. Li, Y. Zhang, X. Ma, Y. Qu, Y. Fu, Bev-dg: Cross-modal learning under bird’s-eye view for domain generalization of 3d semantic segmentation, in: *Proceedings of the IEEE/CVF International Conference on Computer Vision*, 2023, pp. 11632–11642.

- [327] P. Tang, H.-M. Xu, C. Ma, Prototransfer: Cross-modal prototype transfer for point cloud segmentation, in: Proceedings of the IEEE/CVF International Conference on Computer Vision, 2023, pp. 3337–3347.
- [328] B. Xing, X. Ying, R. Wang, J. Yang, T. Chen, Cross-modal contrastive learning for domain adaptation in 3d semantic segmentation, in: Proceedings of the AAAI Conference on Artificial Intelligence, Vol. 37, 2023, pp. 2974–2982.
- [329] Z. Yuan, X. Yan, Y. Liao, Y. Guo, G. Li, S. Cui, Z. Li, X-trans2cap: Cross-modal knowledge transfer using transformer for 3d dense captioning, in: Proceedings of the IEEE/CVF Conference on Computer Vision and Pattern Recognition, 2022, pp. 8563–8573.
- [330] H. Zhou, X. Peng, Y. Luo, Z. Wu, Pointcmc: Cross-modal multi-scale correspondences learning for point cloud understanding (2023).
- [331] X. Zheng, X. Huang, G. Mei, Y. Hou, Z. Lyu, B. Dai, W. Ouyang, Y. Gong, Point cloud pre-training with diffusion models, in: Proceedings of the IEEE/CVF Conference on Computer Vision and Pattern Recognition, 2024, pp. 22935–22945.
- [332] Y. Kasten, O. Rahamim, G. Chechik, Point cloud completion with pretrained text-to-image diffusion models, Advances in Neural Information Processing Systems 36 (2024).
- [333] C. Liu, A. Jiang, Y. Tang, Y. Zhu, Q. Chen, 3d point cloud semantic segmentation based on diffusion model, in: ICASSP 2024-2024 IEEE International Conference on Acoustics, Speech and Signal Processing (ICASSP), IEEE, 2024, pp. 4375–4379.
- [334] H. Jiang, M. Salzmann, Z. Dang, J. Xie, J. Yang, Se (3) diffusion model-based point cloud registration for robust 6d object pose estimation, Advances in Neural Information Processing Systems 36 (2024).
- [335] S. Jin, I. Armeni, M. Pollefeys, D. Barath, Multiway point cloud mosaicking with diffusion and global optimization, in: Proceedings of the IEEE/CVF Conference on Computer Vision and Pattern Recognition, 2024, pp. 20838–20849.
- [336] Y. Feng, X. Shi, M. Cheng, Y. Xiong, Diffpoint: Single and multi-view point cloud reconstruction with vit based diffusion model, arXiv preprint arXiv:2402.11241 (2024).
- [337] G. Sharma, C. Gupta, A. Agarwal, L. Sharma, A. Dhall, Generating point cloud augmentations via class-conditioned diffusion model, in: Proceedings of the IEEE/CVF Winter Conference on Applications of Computer Vision, 2024, pp. 480–488.
- [338] S. Mo, E. Xie, R. Chu, L. Hong, M. Niessner, Z. Li, Dit-3d: Exploring plain diffusion transformers for 3d shape generation, Advances in Neural Information Processing Systems 36 (2024).
- [339] T. Yi, J. Fang, J. Wang, G. Wu, L. Xie, X. Zhang, W. Liu, Q. Tian, X. Wang, Gaussiandreamer: Fast generation from text to 3d gaussians by bridging 2d and 3d diffusion models, in: Proceedings of the IEEE/CVF Conference on Computer Vision and Pattern Recognition, 2024, pp. 6796–6807.
- [340] C.-J. Ho, C.-H. Tai, Y.-Y. Lin, M.-H. Yang, Y.-H. Tsai, Diffusion-ss3d: Diffusion model for semi-supervised 3d object detection, Advances in Neural Information Processing Systems 36 (2024).
- [341] M. Ohno, R. Ukyo, T. Amano, H. Rizk, H. Yamaguchi, Privacy-preserving pedestrian tracking with path image inpainting and 3d point cloud features, Pervasive and Mobile Computing 100 (2024) 101914.
- [342] X. Bi, Y. Chen, L. Li, Diffusionemis: Diffusion model for 3d electromagnetic inverse scattering, IEEE Transactions on Geoscience and Remote Sensing (2024).
- [343] N. S. Dutt, S. Muralikrishnan, N. J. Mitra, Diffusion 3d features (diff3f): Decorating untextured shapes with distilled semantic features, in: Proceedings of the IEEE/CVF Conference on Computer Vision and Pattern Recognition, 2024, pp. 4494–4504.
- [344] Z. Li, R. Mrad, R. Jiao, G. Huang, J. Shan, S. Chu, Y. Chen, Generative design of crystal structures by point cloud representations and diffusion model, arXiv preprint arXiv:2401.13192 (2024).
- [345] Y. Ze, G. Zhang, K. Zhang, C. Hu, M. Wang, H. Xu, 3d diffusion policy, arXiv preprint arXiv:2403.03954 (2024).
- [346] R. She, Q. Kang, S. Wang, W. P. Tay, K. Zhao, Y. Song, T. Geng, Y. Xu, D. N. Navarro, A. Hartmannsgruber, Pointdifformer: Robust point cloud registration with neural diffusion and transformer, IEEE Transactions on Geoscience and Remote Sensing (2024).
- [347] B. Li, X. Wei, B. Liu, W. Wang, Z.-F. He, Y.-K. Lai, 3d colored object reconstruction from a single view image through diffusion, Expert Systems with Applications 252 (2024) 124225.
- [348] Z. Chen, Y. Wang, F. Wang, Z. Wang, H. Liu, V3d: Video diffusion models are effective 3d generators, arXiv preprint arXiv:2403.06738 (2024).
- [349] J. Hu, B. Fei, B. Xu, F. Hou, W. Yang, S. Wang, N. Lei, C. Qian, Y. He, Topology-aware latent diffusion for 3d shape generation, arXiv preprint arXiv:2401.17603 (2024).
- [350] Y. Dong, Q. Zuo, X. Gu, W. Yuan, Z. Zhao, Z. Dong, L. Bo, Q. Huang, Gpld3d: Latent diffusion of 3d shape generative models by enforcing geometric and physical priors, in: Proceedings of the IEEE/CVF Conference on Computer Vision and Pattern Recognition, 2024, pp. 56–66.